Activated TAFI Promotes the Development of Chronic Thromboembolic Pulmonary Hypertension

A Possible Novel Therapeutic Target

Taijyu Satoh, Kimio Satoh, Nobuhiro Yaoita, Nobuhiro Kikuchi, Junichi Omura, Ryo Kurosawa, Kazuhiko Numano, Elias Al-Mamun, Mohammad Abdul Hai Siddique, Shinichiro Sunamura, Masamichi Nogi, Kota Suzuki, Satoshi Miyata, John Morser, Hiroaki Shimokawa

Rationale: **Pulmonary hypertension is a fatal disease; however, its pathogenesis still remains to be elucidated. Thrombin-activatable fibrinolysis inhibitor (TAFI) is synthesized by the liver and inhibits fibrinolysis. Plasma TAFI levels are significantly increased in chronic thromboembolic pulmonary hypertension (CTEPH) patients.**

Objective: **To determine the role of activated TAFI (TAFIa) in the development of CTEPH.**

Methods and Results: **Immunostaining showed that TAFI and its binding partner thrombomodulin (TM) were highly expressed in the pulmonary arteries (PAs) and thrombus in patients with CTEPH. Moreover, plasma levels of TAFIa were increased 10-fold in CTEPH patients compared with controls. In mice, chronic hypoxia caused a 25-fold increase in plasma levels of TAFIa with increased plasma levels of thrombin and TM, which led to thrombus formation in PA, vascular remodeling, and pulmonary hypertension. Consistently, plasma clot lysis time was positively correlated with plasma TAFIa levels in mice. Additionally, overexpression of TAFIa caused organized thrombus with multiple obstruction of PA flow and reduced survival rate under hypoxia in mice. Bone marrow transplantation showed that circulating plasma TAFI from the liver, not in the bone marrow, was activated locally in PA endothelial cells through interactions with thrombin and TM. Mechanistic experiments demonstrated that TAFIa increased PA endothelial permeability, smooth muscle cell proliferation, and monocyte/macrophage activation. Importantly, TAFIa inhibitor and peroxisome proliferator–activated receptor-α agonists significantly reduced TAFIa and ameliorated animal models of pulmonary hypertension in mice and rats.**

Conclusions: **These results indicate that TAFIa could be a novel biomarker and realistic therapeutic target of CTEPH. (*Circ Res*. 2017;120:1246-1262. DOI: 10.1161/CIRCRESAHA.117.310640.)**

Key Words: bone marrow ■ fibrinolysis ■ hypoxia ■ pulmonary hypertension ■ thrombus

Chronic thromboembolic pulmonary hypertension (CTEPH) is a distinct pulmonary vascular disease, categorized as group IV in the WHO classification of pulmonary hypertension (PH).[1] CTEPH still remains a serious disorder because it is associated with progressive PH, leading to severe right ventricular failure and death.[2] The main feature of CTEPH, as opposed to pulmonary arterial hypertension, is obstruction of pulmonary arteries (PA) by organized thrombi that are resistant to fibrinolysis.[2–6] Although CTEPH has long been considered to simply occur after acute pulmonary embolism,[7,8] it is frequently noted in patients without any previous clinical episodes of acute pulmonary embolism or deep vein thrombosis.[9] Moreover, most patients with CTEPH are free from the traditional risk factors for venous thromboembolism.[10] Thus, the pathogenesis of CTEPH still remains obscure. Pulmonary vascular beds are continuously exposed to circulating microthrombi and contribute to their filtration and fibrinolysis.[11] The interaction between microthrombi and PA endothelial cells (PAECs) is the initial step for thrombolysis.[12,13] Thus, there should be a key molecular factor(s) involved in the interactions between local pulmonary vascular beds and microthrombi.

We have recently demonstrated that plasma levels of thrombin-activatable fibrinolysis inhibitor (TAFI, also known as carboxypeptidase B2, encoded by *CPB2*) are significantly elevated in CTEPH patients compared with pulmonary arterial hypertension patients or controls.[14] Additionally, we demonstrated the minor allele of *CPB2* in CTEPH patients compared with the standard Asian population.[14] TAFI is a glycoprotein that is cleaved and activated by the interaction with thrombin and thrombomodulin (TM) in vascular beds.[15,16] The activated

Original received January 14, 2017; revision received March 7, 2017; accepted March 10, 2017. In February 2016, the average time from submission to first decision for all original research papers submitted to *Circulation Research* was 15.4 days.

From the Department of Cardiovascular Medicine, Tohoku University Graduate School of Medicine, Sendai, Japan (T.S., K. Satoh, N.Y., N.K., J.O., R.K., K.N., E.A.-M., M.A.H.S., S.S., M.N., K. Suzuki, S.M., H.S.); and Department of Hematology, Stanford School of Medicine, CA (J.M.).

The online-only Data Supplement is available with this article at http://circres.ahajournals.org/lookup/suppl/doi:10.1161/CIRCRESAHA.117.310640/-/DC1.

Correspondence to Hiroaki Shimokawa, Department of Cardiovascular Medicine, Tohoku University Graduate School of Medicine, 1-1 Seiryo-machi, Aoba-ku, Sendai 980-8574, Japan. E-mail shimo@cardio.med.tohoku.ac.jp

Novelty and Significance

What Is Known?

- Chronic thromboembolic pulmonary hypertension (CTEPH) is a fatal disease; however, its pathogenesis still remains to be fully elucidated.
- Thrombin-activated fibrinolysis inhibitor (TAFI) inhibits fibrinolysis.

What New Information Does This Article Contribute?

- We developed a novel mouse model of CTEPH, on systemic overexpression of TAFI and hypoxia exposure, which showed organized thrombus with multiple obstructions of pulmonary arteries and reduced survival rate.
- Activated TAFI (TAFIa) enhanced pulmonary artery endothelial permeability, smooth muscle cell proliferation, and monocyte/macrophage activation.
- TAFIa inhibitor and peroxisome proliferator–activated receptor-α agonists ameliorated the development of pulmonary hypertension and thrombus formation in the novel model of CTEPH.

This is the first study that demonstrates the pathogenic role of TAFI in CTEPH. Based on the findings of the present study, TAFIa can be regarded as a crucial molecule at the crossroad of inflammation, pulmonary artery remodeling, and thrombus formation in the pathogenesis of CTEPH. Mechanistically, increased plasma levels of TAFIa induced pulmonary artery endothelial cell dysfunction and promoted adjacent pulmonary artery smooth muscle cells proliferation. Three-dimensional computed tomography showed that TAFI-overexpressing mice had multiple pulmonary artery obstructions, which were similar to those of CTEPH patients. Finally, inhibition of TAFIa reduced thrombus formation in pulmonary arteries and improved survival of the mouse model of CTEPH. These findings implicate TAFI as a crucial molecule in the development of CTEPH and thrombus formation, supporting its role as a potential biomarker and therapeutic target.

Nonstandard Abbreviations and Acronyms

BM	bone marrow
CPI	carboxypeptidase inhibitor
CTEPH	chronic thromboembolic pulmonary hypertension
GFP	green fluorescent protein
HIF-1α	hypoxia-inducible factor-1α
IL	interleukin
PA	pulmonary artery
PAEC	pulmonary artery endothelial cell
PAI-1	plasminogen activator inhibitor-1
PASMC	pulmonary artery smooth muscle cell
PH	pulmonary hypertension
PPAR	peroxisome proliferator–activated receptor
TAFI	thrombin-activatable fibrinolysis inhibitor
TAFIa	activated thrombin-activatable fibrinolysis inhibitor
TAFI-P	TAFI-plasmid
Tg	transgenic
TM	thrombomodulin
tPA	tissue-type plasminogen activator
VE-cadherin	vascular endothelial cadherin

form of TAFI (TAFIa) reduces plasmin activity and inhibits fibrinolysis.[17] We found that plasma levels of TAFIa are negatively correlated with clot lysis time in CTEPH patients.[14] Thus, we hypothesized that TAFI is directly involved in the pathogenesis of thrombus formation in PA, promoting the development of CTEPH. To test this hypothesis, in the present study, we used 3 genetically modified mice of TAFI, including systemic knockout mice, systemic overexpressing mice, and liver-specific overexpressing mice in combination with bone marrow (BM) transplantation technique. Here, we report a line of evidence that TAFIa levels are markedly increased not only in the plasma but also in PA in CTEPH patients and that plasma TAFI is activated by TM locally in pulmonary vascular beds, inhibiting fibrinolysis and promoting thrombus formation and PH in mice. Importantly, peroxisome proliferator–activated receptor-α (PPARα) agonists significantly reduced TAFI synthesis by the liver, with a resultant amelioration of PH in mice and rats. Thus, our data suggest that TAFIa could be a novel and realistic therapeutic target of CTEPH.

Methods

An expanded Methods section is available in the Online Data Supplement.

Results

Activation of Plasma TAFI in CTEPH Patients

We have recently reported that CTEPH patients have higher plasma levels of total TAFI (TAFIa plus nonactivated TAFI) assessed by enzyme-linked immunosorbent assay (ELISA) and higher prevalence of single nucleotide polymorphisms of *CPB2* compared with controls.[14] Here, we further performed Western blotting to evaluate plasma levels of TAFIa and intact TAFI (TAFI, nonactivated TAFI), separately. Although there was no difference in plasma TAFI levels between patients with CTEPH and those without it or controls, plasma TAFIa levels showed a 10-fold increase in CTEPH patients compared with pulmonary arterial hypertension patients or controls (Figure 1A). Similarly, although there was no significant difference in plasma TAFI levels between hypoxic and normoxic mice, plasma TAFIa levels showed a 25-fold increase in hypoxic mice compared with normoxic mice (Figure 1B). Interestingly, in the liver, TAFI levels were also significantly increased in hypoxic mice compared with normoxic mice, with no change in TAFIa levels (Figure 1C). Moreover, immunostaining showed the presence of TAFI in the pulmonary thrombus of CTEPH patients (Figure 1D). Similarly, we detected the endothelial expression of TM,[17] which is a binding partner of TAFI and thrombin (Figure 1D; Online Figure II). These results suggest that TAFI is activated by TM in PAECs to promote the development of CTEPH.

TAFI Deficiency Ameliorates Hypoxia-Induced PH In Vivo

To evaluate the role of TAFI in the pathogenesis of CTEPH, we used systemic *Cpb2*$^{-/-}$ mice and littermate controls

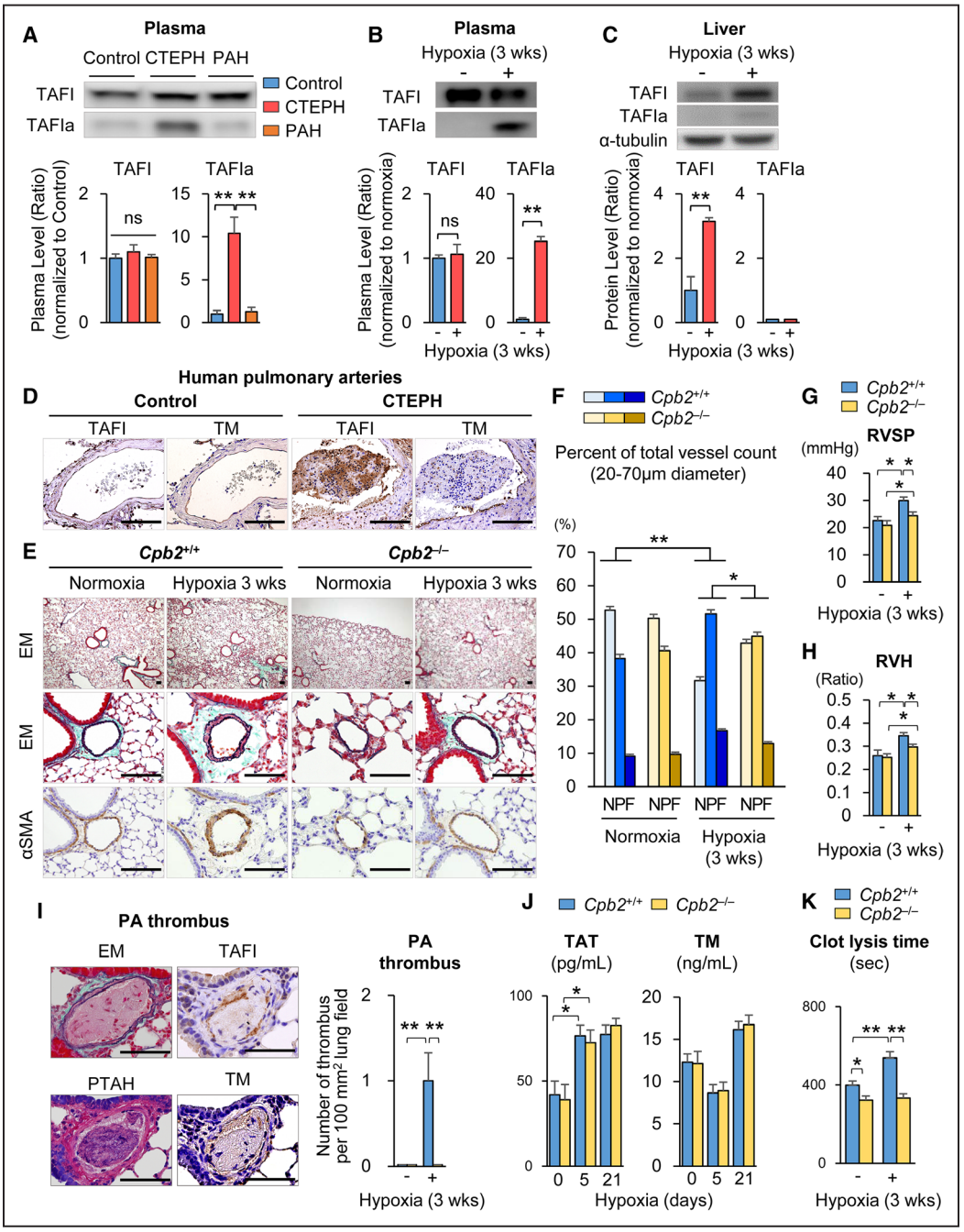

Figure 1. Increased plasma levels of activated thrombin-activatable fibrinolysis inhibitor (TAFI) in chronic thromboembolic pulmonary hypertension (CTEPH) patients. A, Representative Western blot and quantification of intact TAFI (TAFI) and activated TAFI (TAFIa) levels in the plasma from CTEPH patients (n=32) compared with pulmonary arterial hypertension (PAH) patients (n=22) and controls (n=13). **B** and **C**, Representative Western blot and quantification of TAFI and TAFIa levels in the plasma (**B**) and liver homogenates (**C**) of wild-type mice exposed to normoxia or hypoxia (10% O_2) for 3 weeks (n=6 each). **D**, Representative immunostaining for TAFI and thrombomodulin (TM) of the pulmonary arteries (PA) in CTEPH patients and controls. Scale bars, 50 μm. **E**, Representative Elastica–Masson (EM) and immunostaining for α-smooth muscle actin (αSMA) of the PAs in *Cpb2*$^{-/-}$ and control mice (*Cpb2*$^{+/+}$). Scale bars, 50 μm. **F**, Muscularization of distal PAs with a diameter of 20 to 70 μm in *Cpb2*$^{-/-}$ and *Cpb2*$^{+/+}$ mice exposed to normoxia (n=10 each) or hypoxia for 3 weeks (n=14 each). **G** and **H**, Right ventricular systolic pressure (RVSP; **G**) and right ventricular hypertrophy (RVH) assessed by the ratio of right ventricle to left ventricle plus septum weight (**H**) in *Cpb2*$^{+/+}$ and *Cpb2*$^{-/-}$ mice exposed to normoxia (n=10 each) or hypoxia (10% O_2) for 3 weeks (n=14 each). **I**, Representative EM, phosphotungstic acid-hematoxylin (PTAH), and immunostaining for TAFI and TM of the PA thrombus in *Cpb2*$^{+/+}$ mice exposed to hypoxia (10% O_2) for 3 weeks. Quantification of PA thrombi per 100 mm^2 lung field in *Cpb2*$^{+/+}$ and *Cpb2*$^{-/-}$ mice exposed to normoxia (n=10 each) or hypoxia (10% O_2) for 3 weeks (n=14 each). **J**, Quantification of plasma levels of thrombin–antithrombin complex (TAT) and TM in *Cpb2*$^{+/+}$ and *Cpb2*$^{-/-}$ mice exposed to normoxia or hypoxia (10% O_2) for 3 weeks (n=6 each). The plasma levels at each point were compared with those at day 0 by analysis of variance (ANOVA) followed by Tukey HSD test for multiple comparisons. **K**, Quantification of plasma clot lysis time in *Cpb2* $^{+/+}$ and *Cpb2*$^{-/-}$ mice exposed to normoxia (n=10 each) or hypoxia (10% O_2) for 3 weeks (n=14 each). Results are expressed as mean±SEM. **P*<0.05, ***P*<0.01. Comparisons of parameters were performed with the unpaired Student *t* test or 2-way ANOVA followed by Tukey HSD test for multiple comparisons. F indicates fully muscularized vessels; N, nonmuscularized vessels; and P, partially muscularized vessels.

(*Cpb2*$^{+/+}$ mice). Hypoxia promotes the cleavage of TAFI, increases plasma levels of TAFIa,[15] and prolongs the clot lysis time.[18,19] Thus, we used a mouse model of hypoxia-induced PH. Importantly, in wild-type mice, TM expression was high in PAECs (Online Figure III), but was low in aortic endothelial cells (Online Figure IV). Under normoxia, the morphology of PAs was similar between *Cpb2*$^{-/-}$ and control mice (Figure 1E). When exposed to hypoxia for 3 weeks, the animals exhibited increased medial thickness of PAs and muscularized distal PAs with immunoreactivity for α-smooth muscle actin, the extent of which was attenuated in *Cpb2*$^{-/-}$ mice than in *Cpb2*$^{+/+}$ mice (Figure 1E). Compared with *Cpb2*$^{+/+}$ mice, *Cpb2*$^{-/-}$ mice exhibited fewer muscularized distal PAs after hypoxic exposure (Figure 1F). Consistent with these morphological changes, *Cpb2*$^{+/+}$ mice exhibited increased right ventricular systolic pressure, which was significantly attenuated in *Cpb2*$^{-/-}$ mice (Figure 1G). The increased ratio of the right ventricle to the left ventricle plus the septum weight [RV/(LV+Sep)] was also attenuated in *Cpb2*$^{-/-}$ mice (Figure 1H), suggesting a crucial role of TAFI in hypoxia-induced PH. Importantly, chronic hypoxia significantly increased the number of PAs with thrombus in *Cpb2*$^{+/+}$ mice, which was significantly less in *Cpb2*$^{-/-}$ mice (Figure 1I). Moreover, chronic hypoxia increased plasma thrombin–antithrombin complex in both *Cpb2*$^{+/+}$ and *Cpb2*$^{-/-}$ mice (Figure 1J). Additionally, hypoxia transiently reduced soluble TM followed by recovery after 21 days (Figure 1J), indicating increased binding partners for TAFI activation. Consistently, hypoxia significantly prolonged plasma clot lysis time in *Cpb2*$^{+/+}$ mice, which was significantly lower in *Cpb2*$^{-/-}$ mice (Figure 1K). These results suggest that TAFI is crucial for enhancing pulmonary thrombus formation, vascular remodeling, and development of hypoxia-induced PH.

TAFI Overexpression Aggravates Hypoxia-Induced PH In Vivo.

To further evaluate the role of TAFI in the pathogenesis of PH, we developed systemic TAFI-overexpressing mice (TAFI-Tg). TAFI-Tg and control mice showed normal growth under physiological conditions and no significant difference in systolic blood pressure or laboratory data (Online Table II). After 3-week exposure to hypoxia, 38% of the TAFI-Tg mice died, whereas only 4% of the control mice did (Figure 2A). Hypoxia significantly increased plasma levels of TAFI and TAFIa in both TAFI-Tg and control mice to a greater extent in TAFI-Tg mice than in controls (Figure 2B). Under normoxia, the morphology of the PAs was similar between control and TAFI-Tg mice (Figure 2C). In contrast, after hypoxia for 3 weeks, alive TAFI-Tg mice exhibited increased muscularization of distal PAs compared with control mice (Figure 2D). Consistent with these morphological changes, TAFI-Tg mice exhibited increased right ventricular systolic pressure and right ventricular hypertrophy compared with control mice (Figure 2E). These changes in male mice were comparable in female mice (Online Figure V). Moreover, TAFI-Tg mice, as compared with controls, had an increased number of PA thrombi (Figure 2F) and plasma levels of D-dimer (Figure 2G). Hypoxia significantly increased plasma levels of thrombin–antithrombin complex and tended to increase those of TM (Figure 2G), contributing to TAFI activation as binding partners. Indeed, plasma clot lysis time was significantly prolonged in TAFI-Tg mice compared with control mice (Figure 2H). Treatment with carboxypeptidase inhibitor (CPI; TAFIa inhibitor)[20] significantly shortened plasma clot lysis time in TAFI-Tg mice (Figure 2I). In contrast, additional human TAFI significantly prolonged plasma clot lysis time in control mice (Figure 2J), which was again shortened by CPI. Moreover, plasma clot lysis time was significantly prolonged in TAFI-Tg PAECs compared with control PAECs in situ (Online Figure VIA and VIB). Likewise, plasma clot lysis time was significantly prolonged in human PAECs transfected with human TAFI compared with those transfected with control plasmid in situ (Online Figure VIC through VIE). Finally, 3-dimensional computed tomography showed that TAFI-Tg mice had multiple obstructions of PAs after 3 weeks of hypoxia, which was not observed in control mice (Figure 2K). These results suggest that TAFI promotes thrombus formation, pulmonary vascular remodeling, and development of hypoxia-induced PH.

TAFI Augments Pulmonary Vascular Inflammation

Pulmonary vascular inflammation is a trigger for thrombus formation and the development of CTEPH.[21,22] TAFI overexpression augmented hypoxia-induced perivascular inflammation in TAFI-Tg mice (Online Figure VII), in which we found increased accumulation of perivascular F4/80^{+} macrophages (Online Figure VIII). Consistently, TAFI overexpression increased cytokines/chemokines and growth factors in the lung and the serum after hypoxic exposure (Online Figures VIIC and IX). Importantly, TAFI-Tg mice showed a significant increase in platelet-derived growth factor-BB as compared with controls (Online Figure VIIC). It is widely known that BM-derived cells are involved in the pathogenesis of PH.[23,24] Thus, we considered that TAFI overexpression in BM cells could promote hypoxia-induced PH in TAFI-Tg mice. To address this issue, green fluorescent protein (GFP)–positive BM cells were transplanted into irradiated control and TAFI-Tg mice (Figure 3A). After reconstitution of the BM, chimeric mice were exposed to normoxia or hypoxia for 3 weeks. Under normoxia, GFP expression in the whole lung of the chimeric mice was comparable between control and TAFI-Tg mice (Online Figure X). However, hypoxia enhanced GFP expression and the number of GFP^{+} cells in the PAs of the chimeric mice, the extents of which were greater in TAFI-Tg than in control mice (Figure 3B and 3C; Online Figure X). Indeed, as shown in the 3D images of distal PAs, abundant GFP^{+} cells adhered to the adventitia in TAFI-Tg recipient mice (Figure 3D). To further elucidate the cell phenotypes in the adventitia, we used flow cytometry for analyzing lung cell suspensions from TAFI-Tg and control chimeric mice (Figure 3E and 3F).[25] The percentages of CD45^{+} leukocytes in lungs were significantly increased in TAFI-Tg chimeric mice compared with control chimeric mice (Figure 3E). Moreover, the percentages of CD45^{+}CD11b^{+}Ly6G^{-} monocytes/macrophages in lungs were significantly increased in TAFI-Tg chimeric mice compared with control chimeric mice (Figure 3F), suggesting a crucial role of monocytes/macrophages in TAFI-mediated PA inflammation. Consistently, the secretions of cytokines/chemokines

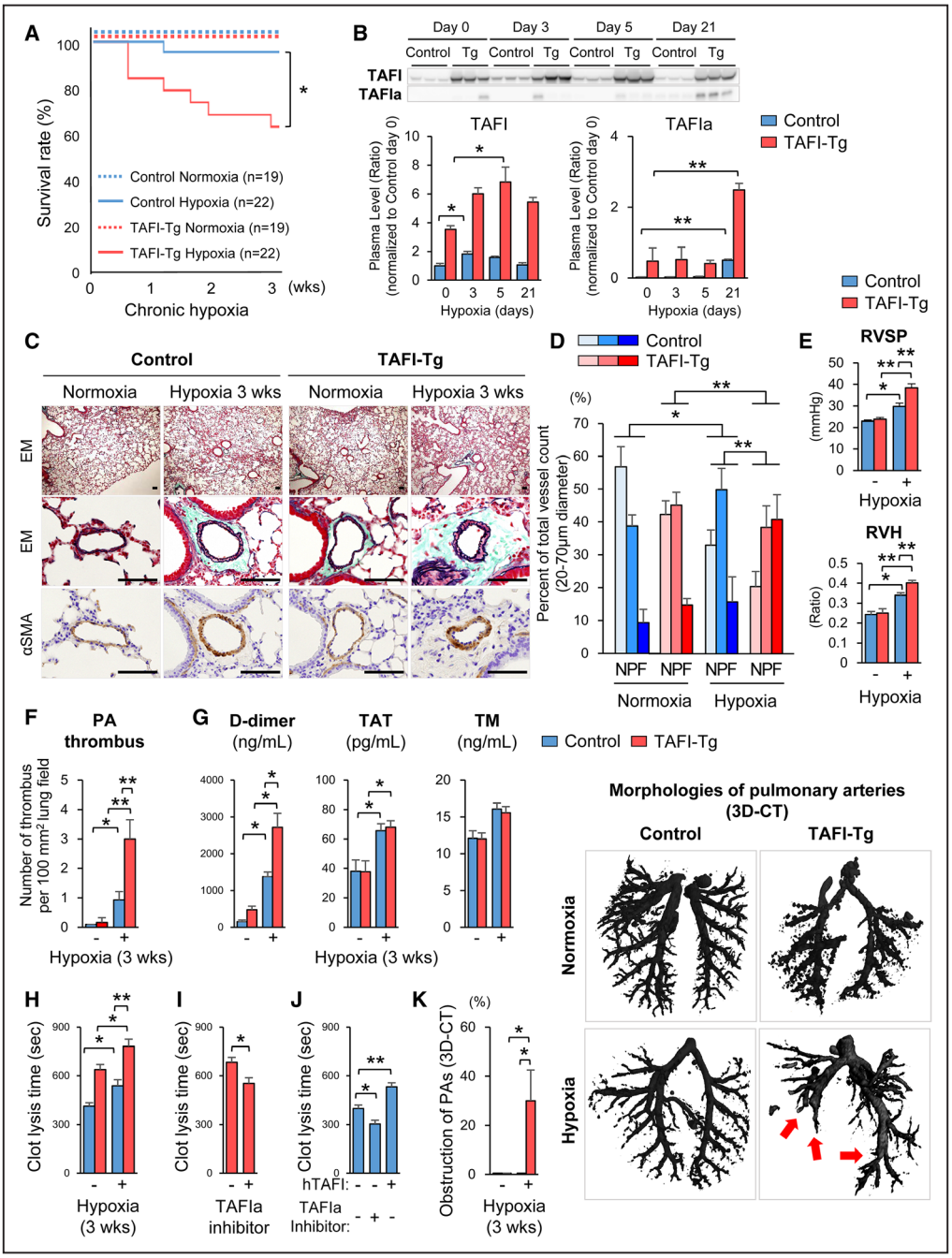

Figure 2. Thrombin-activatable fibrinolysis inhibitor (TAFI) overexpression promotes hypoxia-induced pulmonary hypertension (PH) in mice. A, Survival rate of systemic TAFI-overexpressing mice (TAFI-Tg) and control mice exposed to normoxia (n=19 each) or hypoxia (10% O_2) for 3 weeks (n=22 each). Results are expressed as log-rank test. **B**, Representative Western blot and quantification of TAFI and activated TAFI (TAFIa) expression in the plasma from TAFI-Tg and control mice exposed to normoxia or hypoxia (10% O_2; n=3 each). Each plasma level was compared with that at day 0 by unpaired Student *t* test. **C**, Representative Elastica–Masson (EM) and immunostaining for α-smooth muscle actin (αSMA) of the distal pulmonary arteries (PA) in TAFI-Tg and control mice exposed to normoxia or hypoxia (10% O_2) for 3 weeks. Scale bars, 50 μm. **D**, Muscularization of distal PAs in TAFI-Tg and control mice exposed to normoxia (n=19 each) or hypoxia (10% O_2) for 3 weeks (TAFI-Tg, n=14; controls, n=21). **E**, Right ventricular systolic pressure (RVSP) and right ventricular hypertrophy (RVH) in TAFI-Tg and control mice exposed to normoxia (n=19 each) or hypoxia (10% O_2) for 3 weeks (TAFI-Tg, n=14; controls, n=21). **F**, Quantification of number of PA thrombus per 100 mm^2 lung field in TAFI-Tg and control mice exposed to normoxia (n=19 each) or hypoxia (10% O_2) for 3 weeks (TAFI-Tg, n=14; controls, n=21). **G**, Plasma levels of D-dimer, thrombin–antithrombin complex (TAT), and thrombomodulin (TM) in TAFI-Tg and control mice exposed to normoxia or hypoxia (10% O_2) for 3 weeks (n=8 each). **H**, Measurement of plasma clot lysis time (CLT) in TAFI-Tg and control mice exposed to normoxia (n=19 each) or hypoxia (10% O_2) for 3 weeks (TAFI-Tg, n=14; controls, n=21). **I**, Measurement of plasma CLT in TAFI-Tg mice. The plasma was mixed with a TAFIa inhibitor (25 μg/mL) or vehicle (n=19 each). **J**, Measurement of plasma CLT in control mice. The plasma was mixed with human TAFI (hTAFI; 1 nmol/L), TAFIa inhibitor (25 μg/mL), or vehicle (n=19 each). **K**, Representative images of 3-dimensional computed tomography (3D-CT) of PAs in TAFI-Tg and control mice. Quantification of frequency of obstruction in large PAs detected by 3D-CT (n=12 each). Results are expressed as mean±SEM. **P*<0.05, ***P*<0.01. Comparisons of parameters were performed with the unpaired Student *t* test or 2-way analysis of variance (ANOVA) followed by Tukey HSD test for multiple comparisons. F indicates fully muscularized vessels; N, nonmuscularized vessels; and P, partially muscularized vessels.

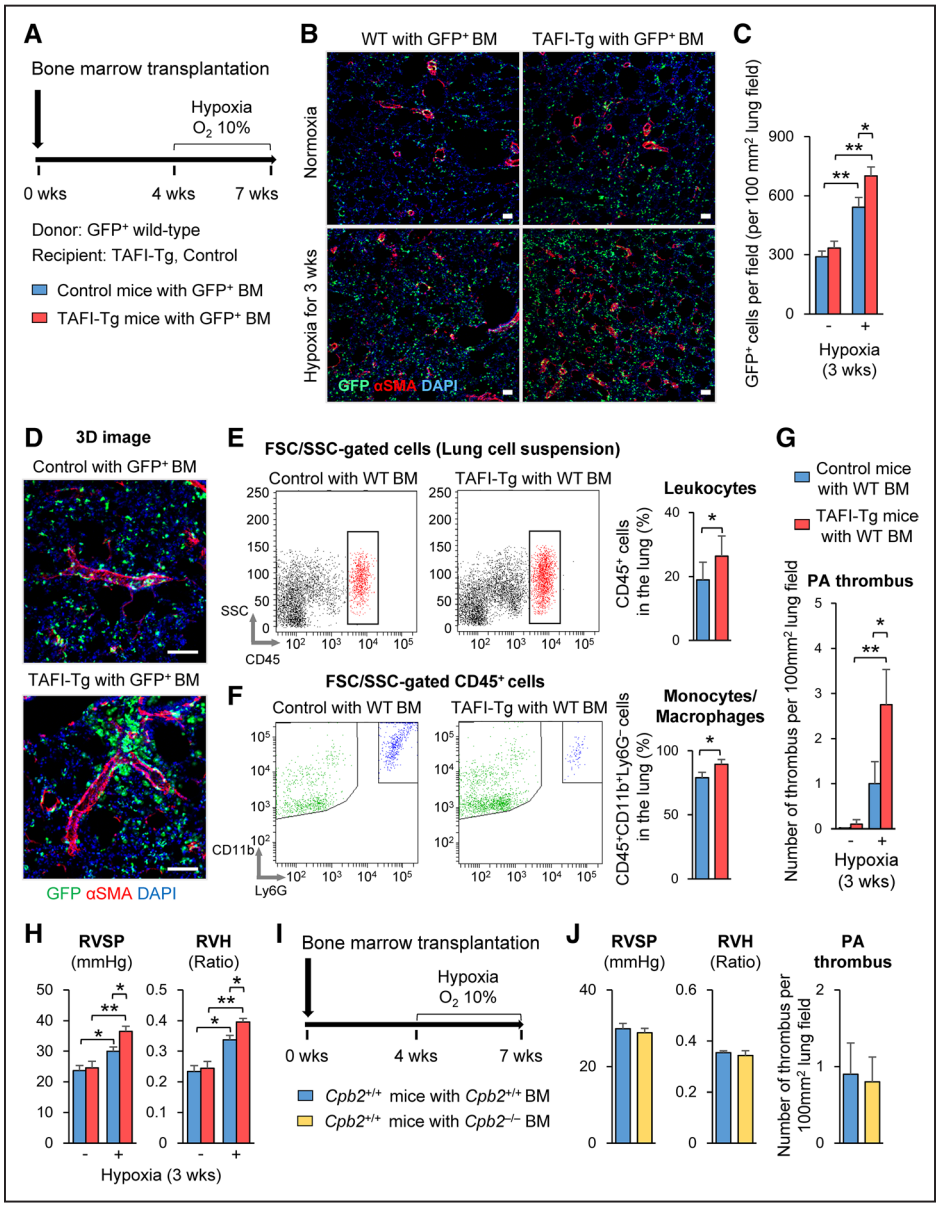

Figure 3. Thrombin-activatable fibrinolysis inhibitor (TAFI) recruits bone marrow–derived cells. A, Bone marrow transplantation (BMT) protocol. Bone marrow (BM) cells (GFP⁺) were transplanted into irradiated TAFI-overexpressing mice (TAFI-Tg) or control mice. After reconstitution of the BM, the chimeric mice were exposed to hypoxia (10% O_2) for 3 weeks. **B**, Representative immunostaining for green fluorescent protein (GFP; green), α-smooth muscle actin (αSMA; Cy3, red), and DAPI (blue) of lung sections from TAFI-Tg and wild-type (WT) recipient mice with GFP⁺ BM exposed to normoxia or hypoxia (10% O_2) for 3 weeks. Scale bars, 50 μm. **C**, Quantification of GFP⁺ cells per 100 mm^2 lung field in TAFI-Tg and WT recipient mice with GFP⁺ BM in normoxia (n=10 each) or hypoxia (10% O_2) for 3 weeks (n=12 each). **D**, Representative 3-dimensional (3D) images of immunostaining for GFP (green), αSMA (Cy3, red), and DAPI (blue) of the distal pulmonary arteries (PAs) in TAFI-Tg and WT recipient mice with GFP⁺ BM exposed to normoxia or hypoxia (10% O_2) for 3 weeks. Scale bars, 50 μm. **E**, Lung cell suspensions within the forward scatter (FSC)/side scatter (SSC) gate were analyzed for CD45⁺ positivity (red) against SSC. Quantification of CD45⁺ cells in WT and TAFI-Tg mice (n=10 each). **F**, Quantification of populations of $CD45^+$ $CD11b^+$ $Ly6G^-$ monocytes/macrophages (green) and $CD45^+CD11b^+Ly6G^+$ neutrophils (blue; n=10 each). **G**, Quantification of the number of PA thrombi per 100 mm^2 lung field in TAFI-Tg and WT recipient mice with GFP⁺ BM exposed to normoxia (n=10 each) or hypoxia (10% O_2) for 3 weeks (n=12 each). **H**, Right ventricular systolic pressure (RVSP) and right ventricular hypertrophy (RVH) in TAFI-Tg and WT recipient mice with GFP⁺ BM exposed to normoxia (n=10 each) or hypoxia (10% O_2) for 3 weeks (n=12 each). **I**, $Cpb2^{+/+}$ and $Cpb2^{-/-}$ BM were transplanted into irradiated 8-week-old $Cpb2^{+/+}$ mice. After reconstitution of the BM, chimeric mice were exposed to hypoxia (10% O_2) for 3 weeks. **J**, RVSP, RVH, and the number of PA thrombi in $Cpb2^{+/+}$ recipient mice with $Cpb2^{+/+}$ or $Cpb2^{-/-}$ BM exposed to hypoxia (10% O_2) for 3 weeks (n=14 each). Results are expressed as mean±SEM. **P*<0.05, ***P*<0.01. Comparisons of parameters were performed with the unpaired Student *t* test or 2-way analysis of variance (ANOVA) followed by Tukey HSD test for multiple comparisons.

and growth factors were significantly increased in PA smooth muscle cells (PASMCs) harvested from the distal PAs of TAFI-Tg mice compared with controls (Online Figure XIA). Thus, contrary to our original notion, these results indicate that enhanced PA inflammation in TAFI-Tg mice is because of upregulated TAFI in the recipient lung. Again, PA thrombus formation was consistently increased in TAFI-Tg mice compared with controls (Figure 3G). Similarly, the extent of

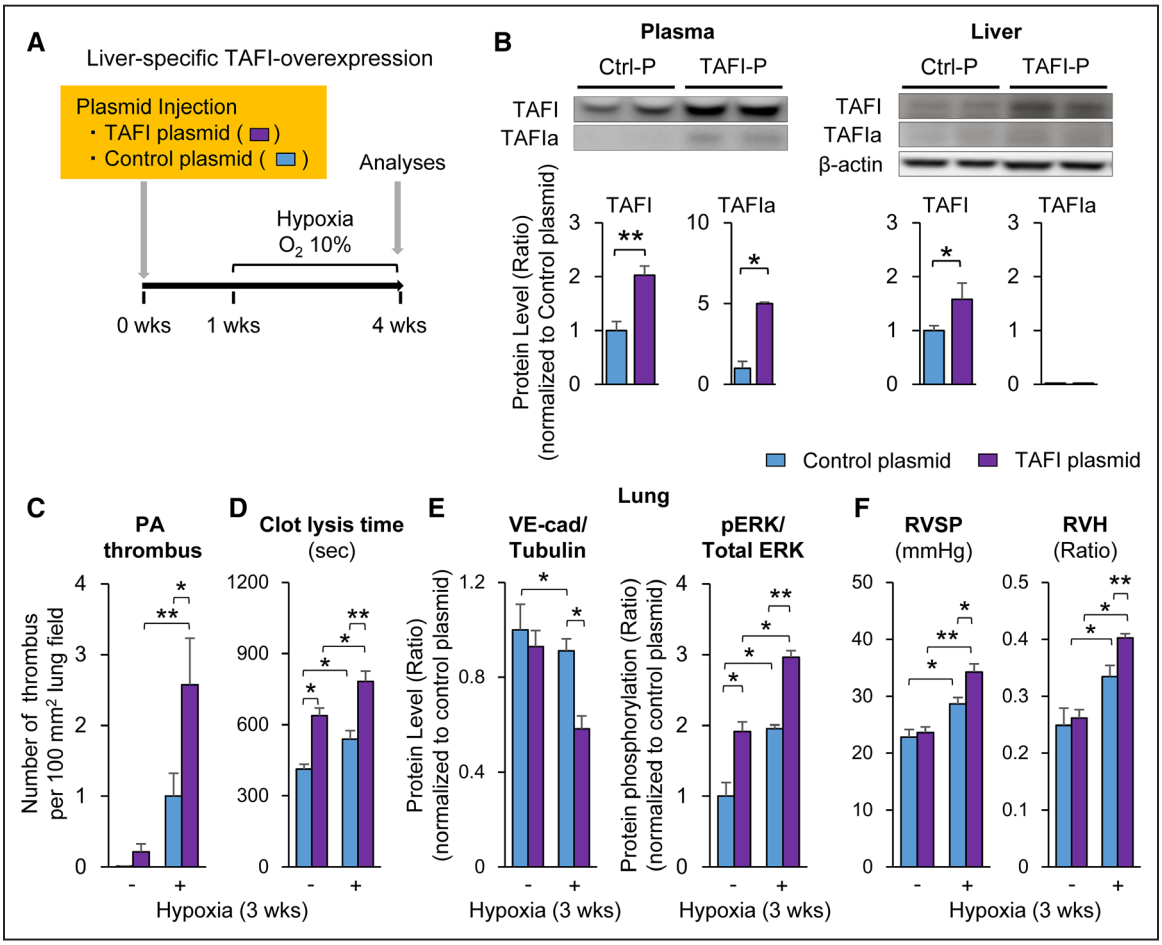

Figure 4. Plasma thrombin-activatable fibrinolysis inhibitor (TAFI) promotes hypoxia-induced thrombus formation and pulmonary hypertension (PH). A, Recombinant plasmid protocol to develop liver-specific TAFI-overexpressing mice. Liver-specific TAFI-overexpressing plasmid is human TAFI plasmid cloned into pLIVE (plasmid for liver in vivo expression) vector. The recombinant plasmid and control plasmid were injected through the tail vein of wild-type (WT) mice. After 1 week, WT mice treated with recombinant plasmid (TAFI-P) and control plasmid (Ctrl-P) were exposed to hypoxia (10% O_2) for 3 weeks. **B**, Representative Western blot and quantification of TAFI, activated (TAFIa), and β actin expression in the plasma and liver homogenates of TAFI-P and Ctrl-P mice exposed to normoxia for 3 weeks (n=6 each). **C**, Quantification of the number of pulmonary artery (PA) thrombus in TAFI-P and Ctrl-P mice exposed to normoxia (n=10 each) or hypoxia (10% O_2) for 3 weeks (n=14 each). **D**, Quantification of plasma clot lysis time in TAFI-P and Ctrl-P mice exposed to normoxia (n=10 each) or hypoxia (10% O_2) for 3 weeks (n=14 each). **E**, Western blot assessments of vascular endothelial cadherin (VE-cadherin)/α-tubulin and phosphorylated/total extracellular signal–regulated kinase (ERK)1/2 in lung homogenates of TAFI-P and Ctrl-P mice exposed to normoxia (n=6 each) or hypoxia (10% O_2) for 3 weeks (n=6 each). **F**, Right ventricular systolic pressure (RVSP) and right ventricular hypertrophy (RVH) in TAFI-P and Ctrl-P mice exposed to normoxia (n=10 each) or hypoxia (10% O_2) for 3 weeks (n=14 each). Results are expressed as mean±SEM. *P<0.05, **P<0.01. Comparisons of parameters were performed with the unpaired Student t test or 2-way analysis of variance (ANOVA) followed by Tukey HSD test for multiple comparisons.

PH was still severe in TAFI-Tg mice compared with controls even after BM reconstitution (Figure 3H). To further confirm the role of TAFI in BM-derived cells, *Cpb2*$^{+/+}$ and *Cpb2*$^{-/-}$ BM cells were transplanted into irradiated *Cpb2*$^{+/+}$ mice (Figure 3I). Complete blood count was comparable between the chimeric mice (Online Table III). Again, there was no significant difference in right ventricular systolic pressure, right ventricular hypertrophy, or thrombus formation between the chimeric mice (Figure 3J), indicating that TAFI in the lung, but not in the BM, causes PA inflammation and PH.

Plasma TAFI Promotes Hypoxia-Induced Thrombus Formation and PH

Although immunostaining showed the presence of TAFI in the lung of CTEPH patients (Figure 1D), TAFI is known to be synthesized mainly by the liver and is released into the plasma.[17] Here, to further examine the role of TAFI in the plasma, we overexpressed TAFI in the liver by using an albumin promoter-driven recombinant plasmid (pLIVE [plasmid for liver in vivo expression]-human TAFI). Then, the liver-specific TAFI-overexpressing mice (TAFI-P) and mice with control plasmid were exposed to hypoxia for 3 weeks (Figure 4A). Western blotting showed that both the plasma and the liver levels of TAFI were significantly increased in TAFI-P mice compared with mice with control plasmid (Figure 4B). After 3 weeks of exposure to hypoxia, the number of PA thrombi was significantly increased in TAFI-P mice compared with mice with control plasmid (Figure 4C). Consistently, plasma clot lysis time was significantly prolonged in TAFI-P mice compared with mice with control plasmid (Figure 4D). Additionally, increased plasma TAFI reduced vascular endothelial cadherin (VE-cadherin) expression and increased

extracellular signal–regulated kinase 1/2 signaling in the lung (Figure 4E). Finally, TAFI-P mice showed severe PH (Figure 4F), suggesting that plasma TAFI directly promotes the development of thrombus formation and PH.

Plasma TAFI Enhances PAEC Permeability and PASMC Proliferation

Considering the importance of increased plasma levels of TAFI in CTEPH, we considered that plasma TAFI may directly affect PAECs to induce endothelial dysfunction. Indeed, TAFI was also expressed in PAECs of CTEPH patients (Online Figure II), implicating the adhesion of plasma TAFI to PAECs. To address this issue, we treated PAECs with human TAFI and examined the changes in multiple genes that regulate endothelial function. Interestingly, human TAFI significantly increased mRNA level of vascular cell adhesion molecule-1 and reduced that of VE-cadherin and tPA (tissue-type plasminogen activator; Figure 5A). Additionally, human TAFI significantly reduced VE-cadherin protein level (Figure 5B) and staining (Figure 5C). Moreover, tube formation assay demonstrated that human TAFI significantly reduced angiogenesis in PAECs (Online Figure XIIA). TM is highly expressed in PAECs[26] and binds TAFI for its activation through interaction with thrombin.[27,28] Thus, we considered that TM is crucial for TAFI-mediated VE-cadherin downregulation in PAECs. Interestingly, TM siRNA significantly attenuated TAFI-mediated VE-cadherin downregulation (Figure 5B). Moreover, TM siRNA reduced TAFIa in conditioned medium, a consistent finding with the previous reports that TM in PAECs contributes to TAFI activation (Figure 5B).[27,28] In contrast, in human aortic endothelial cells, TAFI-mediated VE-cadherin downregulation (Online Figure XIIB) and TM expression (Figure 5D) were significantly less compared with PAECs. Interestingly, treatment with human TAFI significantly reduced oxygen consumption rate and increased extracellular acidification rate in PAECs compared with vehicle, suggesting that TAFI dysregulates the metabolic homeostasis and function of PAECs (Figure 5E and 5F). These results suggest that TM is crucial for TAFI activation and endothelial dysfunction, which is a plausible mechanism for the pulmonary vasculature-selective occurrence of vascular lesions in CTEPH patients.

VE-cadherin regulates endothelial permeability,[29,30] which is important in the pathogenesis of PH.[31] Thus, we next examined PAEC permeability after human TAFI treatment. Interestingly, human TAFI significantly increased PAEC permeability (Figure 5G), whereas it had no effects in aortic endothelial cells. Additionally, knockdown of TM or VE-cadherin significantly reduced TAFI-mediated increase in PAEC permeability (Figure 5H). Here, we performed permeability assay after treatment with CTEPH plasma. Compared with control plasma, CTEPH plasma significantly increased PAEC permeability, which was partially attenuated by a TAFIa inhibitor (Figure 5I). Consistently, CTEPH plasma significantly downregulated VE-cadherin in PAECs, which was again attenuated by a TAFIa inhibitor (Online Figure XIIC). Finally, plasma levels of TAFIa positively correlated with PAEC permeability (Figure 5J), suggesting that plasma TAFIa promotes PAEC permeability through TM in CTEPH patients.

Increased endothelial permeability will expose PASMCs to plasma TAFIa, which may promote cell proliferation. To address this issue, we examined PASMC apoptosis and proliferation after treatment with human TAFI. Human TAFI activated extracellular signal–regulated kinase 1/2 (Figure 6A), reduced caspase-3 expression (Figure 6B), and increased PASMC proliferation (Figure 6C). Consistently, proliferation of PASMCs harvested from the distal PAs of TAFI-Tg mice was significantly increased compared with control mice (Online Figure XIB). To further confirm the role of increased plasma TAFIa in CTEPH patients, we performed cell proliferation assays with PASMCs after treatment with CTEPH plasma. Treatment with CTEPH plasma significantly increased extracellular signal–regulated kinase 1/2 activity (Figure 6D) and cell proliferation in PASMCs (Figure 6E) as compared with control plasma. This proliferative effect was attenuated by a TAFIa inhibitor (Figure 6E). Finally, plasma levels of TAFIa positively correlated with PASMC proliferation (Figure 6F), suggesting that TAFIa promotes PASMC proliferation in CTEPH patients (Figure 6G).

TAFIa Inhibition Ameliorates Hypoxia-Induced PH

To evaluate the effects of TAFIa inhibition in hypoxia-induced PH in mice, we first performed in silico screening using the Life Science Knowledge Bank software (http://www.lskb.w-fusionus.com/) and found several TAFIa inhibitors in the database (Online Data Set). Among the TAFIa inhibitors, we chose CPI (IC_{50}=2.1 nmol/L) to perform in vivo experiments. After 3-week exposure to hypoxia, 25% of the TAFI-Tg mice with vehicle died, whereas only 6% of the TAFI-Tg mice with CPI treatment did (Figure 7A). CPI treatment significantly reduced plasma levels of TAFIa (Figure 7B), reduced clot lysis time and clot formation (Figure 7C), and ameliorated hypoxia-induced PH in both TAFI-Tg and control mice (Figure 7D), demonstrating the beneficial effects of the TAFIa inhibitor for the treatment of PH.

PPARα Agonists Ameliorate Animal Models of PH

We further examined TAFI inhibitors that are currently used in clinical settings and found PPARα agonists. Consistent with the hypoxia-induced increase in TAFI in the liver (Figure 1C), hypoxia significantly increased TAFI synthesis by hepatocytes ($HepG_2$ cell lines; Online Figure XIIIA). We examined the possible therapeutic effects of the PPARα agonists as they have been reported to suppress TAFI synthesis by hepatocytes.[32] Importantly, hypoxia-induced synthesis and secretion of TAFI were significantly attenuated by a selective PPARα agonist, WY14643, in a concentration-dependent manner (Online Figure XIIIA). We further confirmed that partial PPARα agonists (WY14643, fenofibrate, bezafibrate, and clofibrate) and a PPARγ agonist (GW1929) inhibit TAFI mRNA, whereas a high-affinity PPARδ agonist (GW0742) had no effects (Online Figure XIIIB). Additionally, Western blotting showed that PPARα agonists, especially WY14643 and fenofibrate, inhibited TAFI protein levels in both cell lysates and conditioned medium (Figure 7E; Online Figure XIIIC). Moreover, hypoxia-inducible factor-1α (HIF-1α) knockdown by siRNA significantly reduced the secretion of TAFI (Figure 7E), suggesting an involvement of HIF-1α in

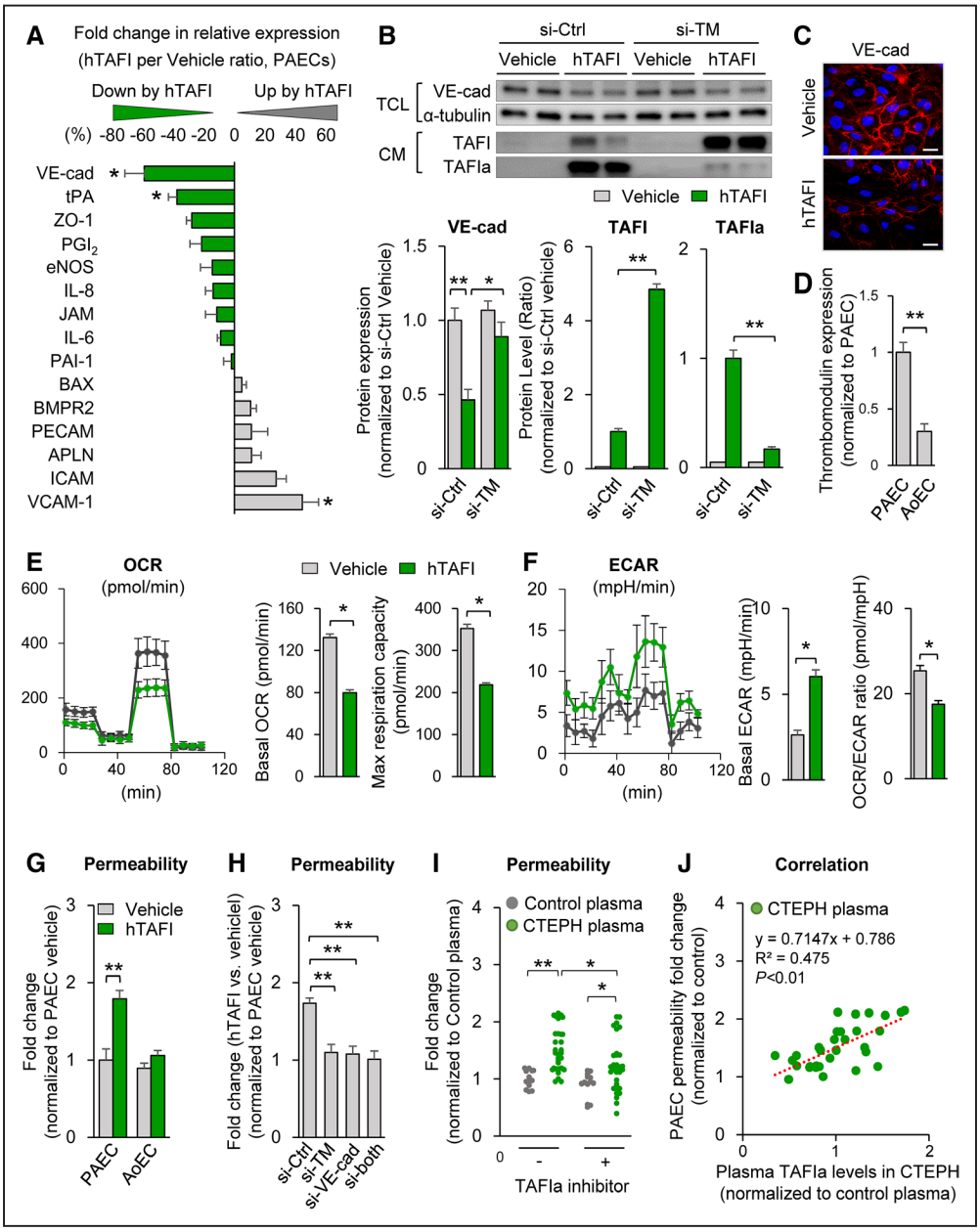

Figure 5. Thrombin-activatable fibrinolysis inhibitor (TAFI) induces pulmonary artery endothelial cell (PAEC) dysfunction and permeability. A, Quantification of mRNA expression of vascular endothelial cadherin (VE-cadherin; VE-cad), tPA (tissue-type plasminogen activator), zona occludens protein-1 (ZO-1), prostaglandin I_2 (PGI_2), endothelial NOS (eNOS), interleukin (IL)-8, junctional adhesion molecules (JAM), IL-6, plasminogen activator inhibitor-1 (PAI-1), BCL2-associated X protein (BAX), bone morphogenetic protein receptor type II (BMPR2), platelet endothelial cell adhesion molecule-1 (PECAM), apelin (APLN), intercellular adhesion molecule (ICAM)-1, and vascular cell adhesion molecule (VCAM)-1 in human pulmonary artery endothelial cells (PAECs) treated with human TAFI (hTAFI, 300 nmol/L) for 24 h (n=4 samples per group). For the statistical analyses, unpaired Student *t* test was used. **B**, Representative Western blot and quantification of VE-cad, TAFI, TAFIa, and α-tubulin expression in total cell lysates (TCL) and conditioned medium (CM) of human PAECs treated with hTAFI (300 nmol/L) for 24 h after transfection with thrombomodulin siRNA (si-TM) or control siRNA (si-Ctrl; n=4 samples per group). **C**, Representative immunostaining for VE-cadherin (red) and DAPI (blue) of human PAECs treated with hTAFI (300 nmol/L) for 24 h. **D**, Quantification of mRNA expression of TM in human PAECs and aortic endothelial cells (AoECs). **E**, Quantification of basal oxygen consumption rate (OCR) and max respiration capacity in human PAECs treated with TAFI protein (300 nmol/L) for 24 h (n=5 samples per group). **F**, Basal extracellular acidification rate (ECAR) and OCR/ECAR ratio in human PAECs treated with TAFI protein (300 nmol/L) for 24 h (n=5 samples per group). **G**, Quantification of the permeability in the cell layer of human pulmonary PAECs and AoECs treated with hTAFI (300 nmol/L) for 24 h (n=10 samples per group). **H**, Quantification of the permeability in PAEC layer treated with hTAFI (300 nmol/L) for 24 h after transfection with si-TM, si-VE-cad, both siRNA (si-both), and si-Ctrl (n=10 samples per group). **I**, Quantification of the permeability in PAEC layer treated with the plasma from chronic thromboembolic pulmonary hypertension (CTEPH) patients (n=32) and controls (n=13) for 24 h. The plasma was mixed with a TAFIa inhibitor (25 μg/mL) or vehicle. **J**, Correlation between PAECs permeability and plasma levels of activated TAFI (TAFIa) in CTEPH patients (n=32). Results were analyzed with Pearson rank correlation coefficient. Results are expressed as mean±SEM. **P*<0.05, ***P*<0.01. Comparisons of parameters were performed with the unpaired Student *t* test or 2-way ANOVA followed by Tukey HSD test for multiple comparisons.

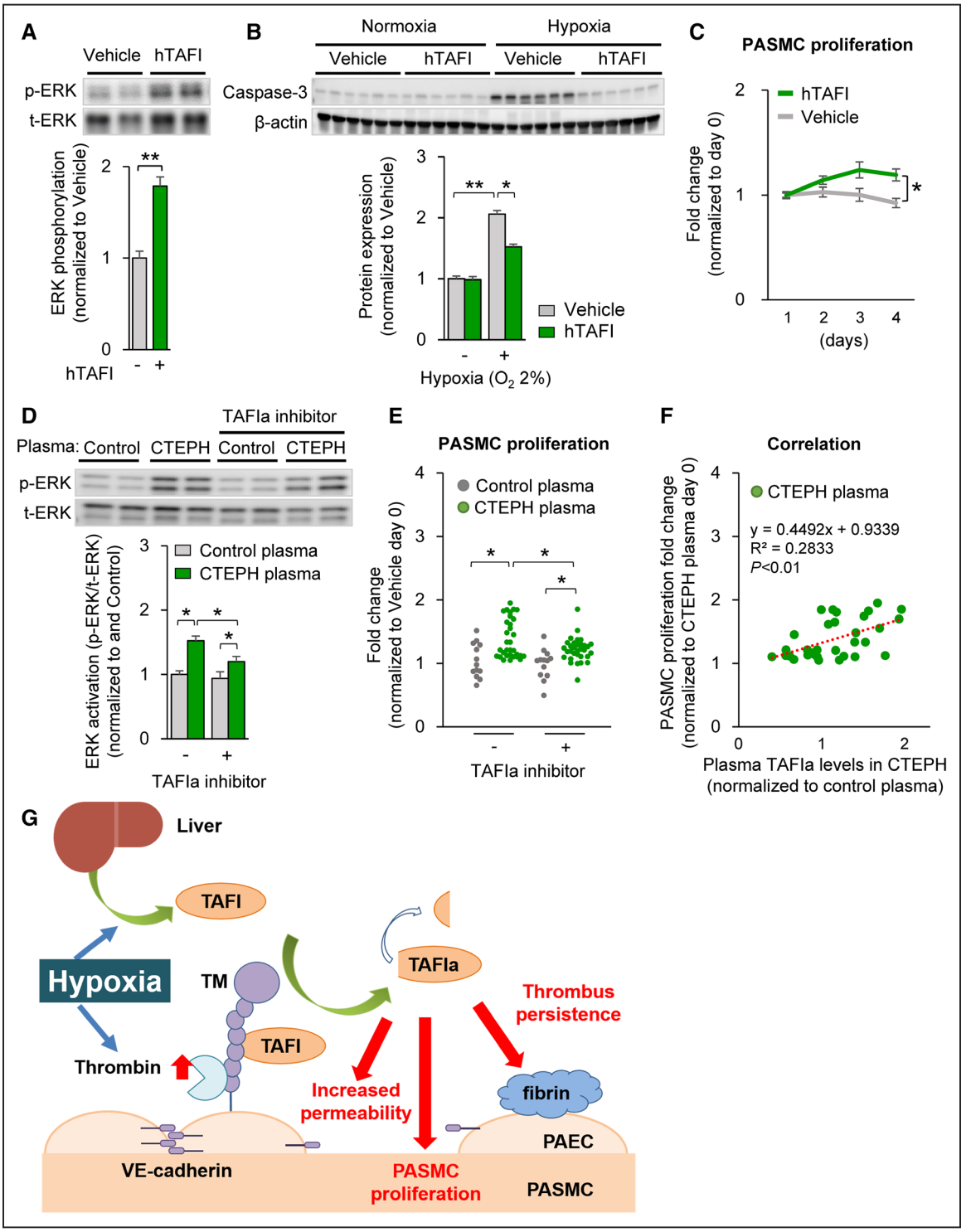

Figure 6. Thrombin-activatable fibrinolysis inhibitor (TAFI) promotes proliferation in pulmonary artery smooth muscle cells. **A**, Representative Western blot and quantification of extracellular signal–regulated kinase (ERK)1/2 activity in human pulmonary artery smooth muscle cells (PASMCs) treated with TAFI purified from human plasma (hTAFI; 300 nmol/L) or vehicle for 24 h (n=6 samples per group). **B**, Representative Western blot and quantification of caspase-3 and β-actin in human PASMCs exposed to hypoxia (O_2 2%) with human TAFI (300 μM) or vehicle for 24 h (n=6 samples per group). **C**, Proliferation (Cell Titer 96 MTT assay) of human PASMCs treated with hTAFI (300 nmol/L) or vehicle for 4 days (n=8 samples per group). **D**, Representative Western blot and quantification of ERK1/2 activity in human PASMCs treated with plasma from patients with chronic thromboembolic pulmonary hypertension (CTEPH) or controls mixed with a TAFIa inhibitor (25 μg/mL) or vehicle (n=6 each). **E**, Proliferation of human PASMCs treated with the plasma from CTEPH patients (n=32) or controls (n=13) mixed with a TAFIa inhibitor (25 μg/mL) for 4 days. **F,** Correlation between human PASMC proliferation and plasma levels of activated TAFI (TAFIa) in patients with CTEPH (n=32). Results were analyzed with Pearson rank correlation coefficient. **G**, Schematic representation of the molecular mechanisms underlying hypoxia-mediated TAFI activation, thrombus formation, PAEC permeability, and PASMC proliferation. Results are expressed as mean±SEM. *P<0.05, **P<0.01. Comparisons of parameters were performed with the unpaired Student t test or 2-way analysis of variance (ANOVA) followed by Tukey HSD test for multiple comparisons.

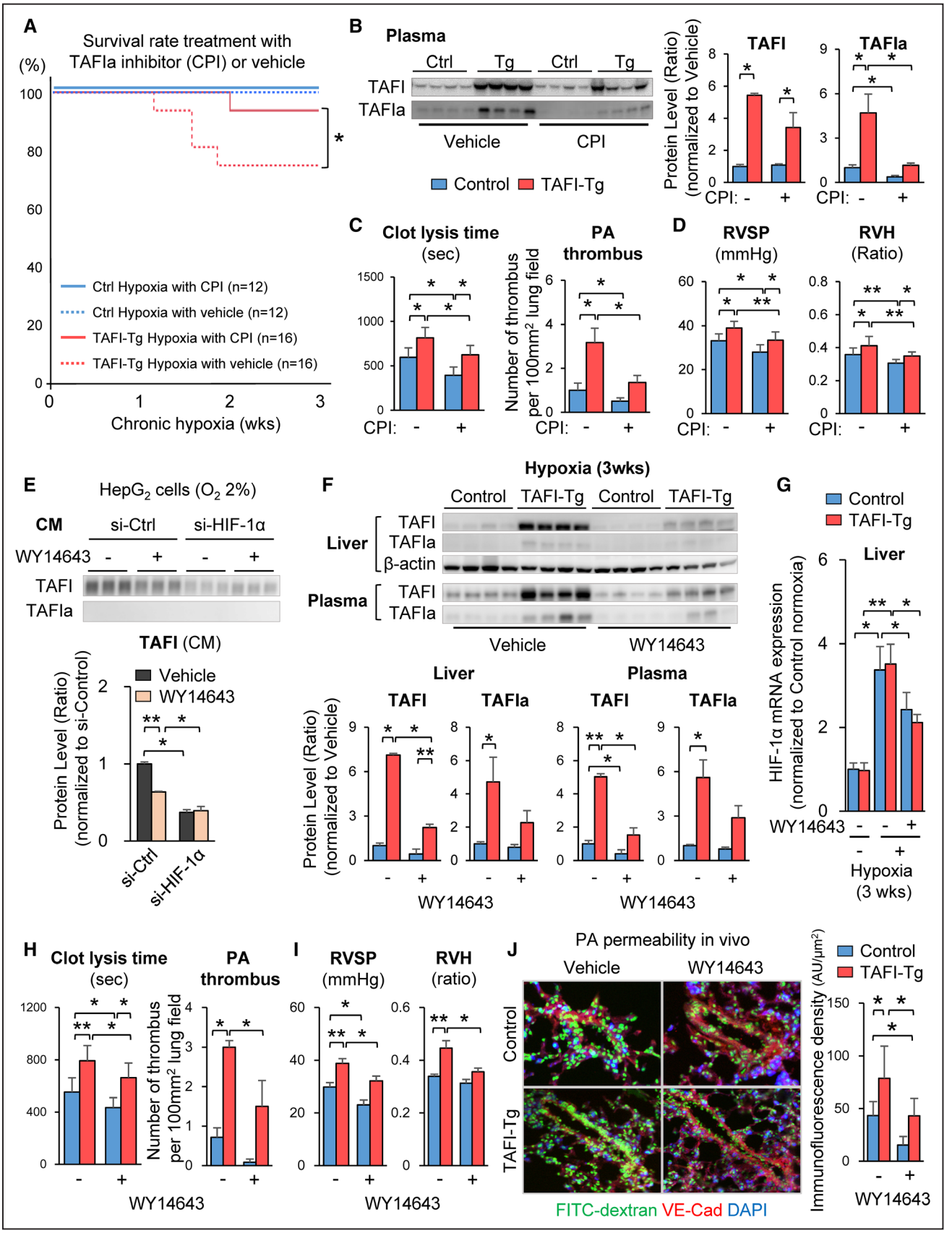

Figure 7. Activated thrombin-activatable fibrinolysis inhibitor (TAFIa) inhibitors ameliorate pulmonary hypertension (PH) in mice. A, Survival rate of TAFI-overexpressing mice (TAFI-Tg) and control mice exposed to hypoxia (10% O_2) treatment with a TAFIa inhibitor (carboxypeptidase inhibitor [CPI]; 5 mg/kg/d) or vehicle for 3 weeks. Results are expressed as long-rank test. **B**, (*Continued*)

Figure 7 Continued. Representative Western blot and quantification of TAFI and TAFIa in the plasma from TAFI-Tg and control mice exposed to hypoxia for 3 weeks with CPI (5 mg/kg/d) or vehicle (n=4 each). **C**, Clot lysis time and the number of pulmonary artery (PA) thrombi in TAFI-Tg and control mice exposed to hypoxia for 3 weeks with CPI (5 mg/kg/d) or vehicle (n=12 each). **D**, Right ventricular systolic pressure (RVSP) and right ventricular hypertrophy (RVH) in TAFI-Tg and control mice exposed to hypoxia for 3 weeks with CPI (5 mg/kg/d) or vehicle (n=12 each). **E**, Representative Western blot and quantification of TAFI and TAFIa in conditioned medium (CM) of $HepG_2$ cells treated with WY14643 (10 μM) for 24 h after transfection with hypoxia-inducible factor-1α (HIF-1α) si-RNA (si-HIF-1α) or control siRNA (si-Ctrl; n=3 each). **F**, Representative Western blot and quantification of TAFI, TAFIa, and β-actin in the liver and the plasma of TAFI-Tg and control mice exposed to hypoxia for 3 weeks with WY14643 (3 mg/kg/d) or vehicle (n=4 each). **G**, HIF-1α mRNA expression in the liver from TAFI-Tg and control mice exposed to hypoxia with WY14643 (n=10 each) or vehicle (n=12 each). **H**, Clot lysis time and the number of PA thrombi in TAFI-Tg and control mice exposed to hypoxia with WY14643 (3 mg/kg/d; n=12 each) or vehicle (n=30 each) for 3 weeks. **I,** RVSP and RVH in TAFI-Tg and control mice exposed to hypoxia for 3 weeks with WY14643 (3 mg/kg/d; n=12 each) or vehicle (n=30 each). **J**, Representative confocal images of immunostaining for FITC-dextran (green), vascular endothelial cadherin (VE-cadherin; red), and DAPI (blue) and quantification of PA permeability in TAFI-Tg and control mice exposed to hypoxia for 3 weeks with WY14643 (3 mg/kg/d) or vehicle (n=8 each). Results are expressed as mean±SEM. **P*<0.05, ***P*<0.01. Comparisons of parameters were performed with the unpaired Student *t* test or 2-way analysis of variance (ANOVA) followed by Tukey HSD test for multiple comparisons.

the regulation of TAFI synthesis. To further evaluate the role of WY14643 and fenofibrate, we treated TAFI-Tg and control mice with oral administration of the drugs during hypoxic exposure for 3 weeks. Importantly, both PPARα agonists significantly improved the survival of TAFI-Tg mice compared with vehicle control (Online Figure XIIID and XIIIF). WY14643 reduced TAFI levels in the liver and the plasma in hypoxic TAFI-Tg and control mice (Figure 7F). After 3-week exposure to hypoxia, HIF-1α expressions in the liver were significantly upregulated in both TAFI-Tg and control mice, which were again downregulated by WY14643 treatment (Figure 7G). Additionally, WY14643 downregulated HIF-1α expression in hepatocytes (HepG2; Online Figure XIV). Moreover, WY14643 significantly reduced plasma D-dimer (Online Figure XIIIE), clot lysis time, and PA thrombus formation in both TAFI-Tg and control mice (Figure 7H), resulting in the amelioration of PH in both TAFI-Tg and control mice (Figure 7I; Online Figure XIIIG). Interestingly, WY14643 treatment significantly reduced pulmonary vascular permeability in both TAFI-Tg and control mice (Figure 7J). Consistently, serum levels of inflammatory cytokines and growth factors (eg, interleukin [IL]-1β, IL-6, GM-CSF [granulocyte macrophage colony-stimulating factor], interferon-γ, and tumor necrosis factor-α) were significantly reduced, especially in TAFI-Tg mice by WY14643 treatment (Online Figure XV). Finally, to further confirm the role of PPARα agonists, we used additional 2 rat models of PH; monocrotaline-induced PH and Sugen/hypoxia-induced PH (Figure 8A and 8E). Plasma levels of TAFIa were significantly increased in both models, which were significantly reduced by WY14643 treatment (Figure 8B and 8F). Moreover, we found significantly increased clot lysis time and PA thrombus formation in the lungs of both models, which were reduced by WY14643 (Figure 8C and 8G). Consistently, WY14643 treatment significantly ameliorated PH in both rat models (Figure 8D and 8H).

Discussion

Considerable efforts have been devoted to understand the pathogenesis of CTEPH, which is caused by residual thromboemboli with flaps and meshwork formation in the PAs.[33] However, the molecular pathogenesis of CTEPH has long been elusive.[34,35] To the best of our knowledge, this is the first study that demonstrates the pathogenic role of TAFI in CTEPH. The major findings of the present study are that (1) plasma levels of TAFIa were markedly increased in CTEPH patients and hypoxic mice, (2) TAFI knockdown attenuated the development of hypoxia-induced PH, (3) TAFI overexpression promoted the development of hypoxia-induced PH and thrombus formation, (4) 3-dimensional computed tomography showed multiple obstruction of PAs in TAFI-overexpressing mice, (5) the plasma from CTEPH patients enhanced PAEC permeability and PASMC proliferation, and (6) TAFIa inhibitor and PPARα agonists reduced plasma TAFI and ameliorated the development of PH in mice and rats. Based on these findings, we propose the crucial role of plasma TAFIa in the development of PH and thrombus formation in PAs.

TM-Mediated TAFI Activation in PAECs

Hypoxia increases plasma TAFIa[15] and promotes the development of PH.[1] Consistently, we detected a 25-fold increase in plasma TAFIa in hypoxic mice. In accordance with the increase in plasma TAFIa, hypoxic mice showed enhanced thrombus formation in PAs. PAECs highly express TM,[26] a binding partner of thrombin and TAFI, by which TAFI is cleaved and activated.[17] Importantly, TM expression in PAECs was enhanced in patients with CTEPH compared with controls. Likewise, TM expression in PAECs was enhanced in hypoxic mice compared with normoxic mice. Additionally, hypoxia significantly increased plasma levels of thrombin–antithrombin complex, which is an indicator of plasma levels of thrombin. Thus, it is possible that chronic hypoxia will increase the TM–thrombin–TAFI complex on the surface of PAECs, promoting cleavage and activation of plasma TAFI in pulmonary vascular beds. Conversely, TM knockdown in PAECs reduced cleavage and activation of human TAFI in the culture medium, supporting the TM-mediated TAFI activation.[27,28] Moreover, TM knockdown attenuated TAFI-mediated VE-cadherin downregulation and permeability in PAECs. However, these TAFI-mediated changes were absent in aortic endothelial cells, which express lower levels of TM compared with PAECs. Thus, TM-mediated TAFI activation and endothelial permeability is one of the plausible mechanisms for the pulmonary vasculature-selective occurrence of vascular lesions in patients.

Mechanisms for TAFI Activation in CTEPH Patients

Based on the present results and the previous reports, the increased plasma levels of TAFIa in CTEPH patients can be explained in part by the increased TM in PAECs and thrombin in the plasma. However, it remains unclear why TAFI is

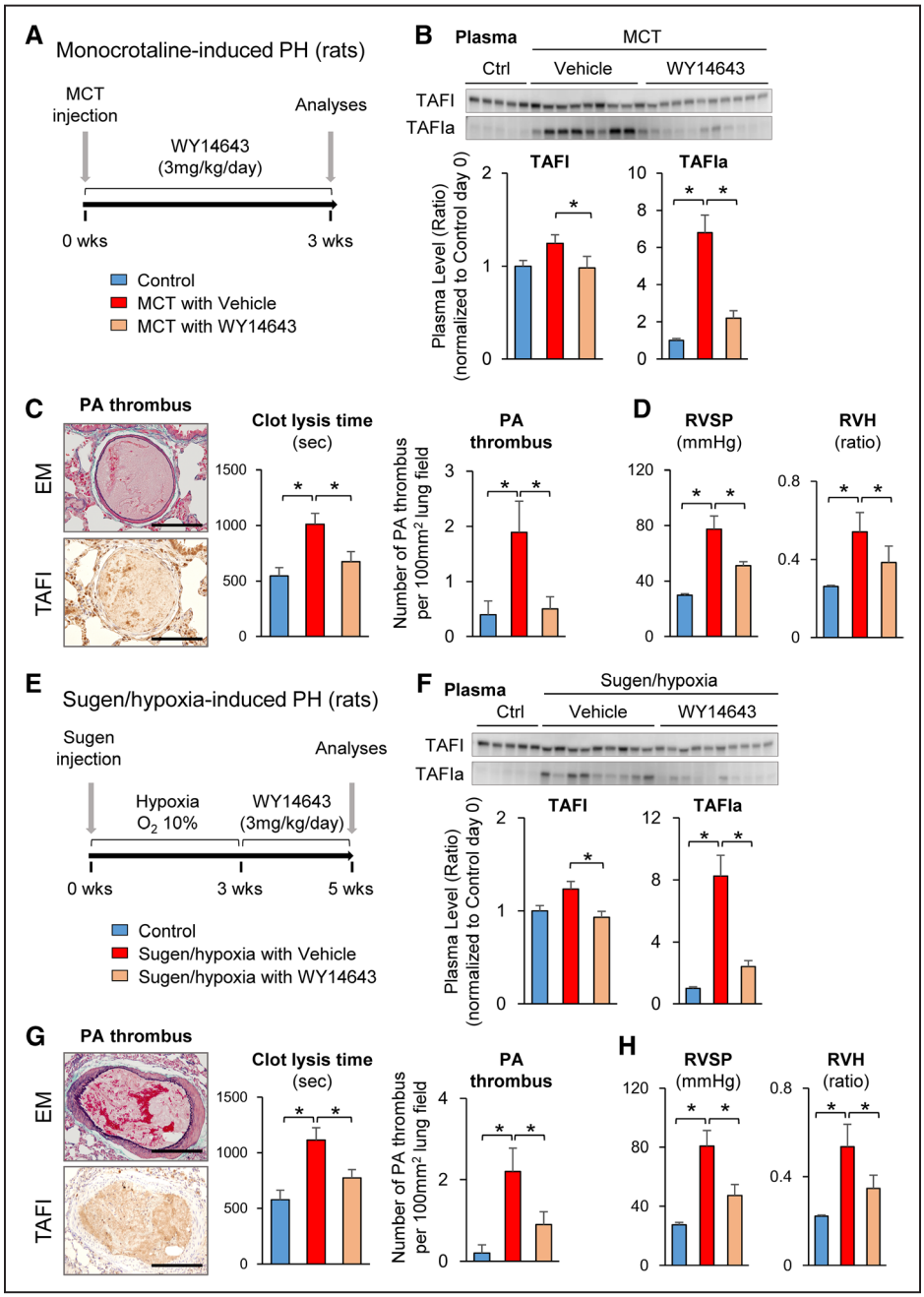

Figure 8. Peroxisome proliferator–activated receptor (PPAR)α agonists ameliorate Pulmonary Hypertension in Rats. A, Protocol for monocrotaline (MCT)-induced pulmonary hypertension (PH) with WY14643 (3 mg/kg/d) or vehicle in rats. **B**, Representative Western blot of thrombin-activatable fibrinolysis inhibitor (TAFI) and activated TAFI (TAFIa) in the plasma after treatment with WY14643 (3 mg/kg/d) or vehicle for 3 weeks (Control [Ctrl], n=5; MCT with vehicle, n=9; MCT with WY14643, n=10). **C**, Representative Elastica–Masson (EM) and TAFI staining of the pulmonary artery (PA) thrombus. Scale bars, 50 μm. Clot lysis time and PA thrombus formation after treatment with WY14643 (3 mg/kg/d) or vehicle for 3 weeks (Control [Ctrl], n=5; MCT with vehicle, n=9; MCT with WY14643, n=10). **D**, Right ventricular systolic pressure (RVSP) and right ventricular hypertrophy (RVH) assessed by the ratio of right ventricle to left ventricle plus septum weight after 3 weeks of treatment with WY14643 (3 mg/kg/d) or vehicle (control [Ctrl], n=5; MCT with vehicle, n=9; MCT with WY14643, n=10). **E**, Protocol for Sugen/hypoxia-induced PH with WY14643 (3 mg/kg/d) or vehicle in rats. **F**, Representative Western blot of TAFI and TAFIa in the plasma after treatment with WY14643 or vehicle for 2 weeks (Ctrl, n=5; Sugen/hypoxia with vehicle, n=10; Sugen/hypoxia with WY14643, n=10). **G**, Clot lysis time and PA thrombus formation after treatment with WY14643 or vehicle for 2 weeks (Ctrl, n=5; Sugen/hypoxia with vehicle, n=10; Sugen/hypoxia with WY14643, n=10). **H**, Right ventricular systolic pressure (RVSP) and right ventricular hypertrophy (RVH) after treatment with WY14643 or vehicle for 2 weeks (Ctrl, n=5; Sugen/hypoxia with vehicle, n=10; Sugen/hypoxia with WY14643, n=10). Results are expressed as mean±SEM. *P<0.05. Comparisons of parameters were performed with the unpaired Student t test or analysis of variance (ANOVA) followed by Tukey HSD test for multiple comparisons.

10-fold more activated in CTEPH patients compared with controls. One of the possible mechanisms is the difference in the genetic background of CTEPH patients. As we have recently reported, there is a prevalence of the minor allele of *CPB2* in CTEPH patients compared with the standard population.[14] Indeed, it has been reported that the single nucleotide

polymorphisms of *CPB2* (eg, −1120 G/T; rs799916836 and −1583 A/T; rs108737) were related to the elevation of plasma TAFI levels.[36–38] Importantly, it has been reported that Thr325/Ile (rs192644738) is associated with differences in TAFIa stability.[38] Among those single nucleotide polymorphisms, we detected the minor allele of rs7999168 in 24% of patients, that of rs1926447 in 24%, and that of rs1087 in 35%.[14] The prevalence of the minor allele of *CPB2* in CTEPH patients is higher compared with the that in standard Asian population in the HapMap.[39] However, we need to increase the number of CTEPH patients to elucidate the role of single nucleotide polymorphisms in the pathogenesis of CTEPH. Additionally, there may be other minor allele of *THBD* (TM gene), *F2* (thrombin gene), and *F2Rs* (thrombin receptor family genes), all of which may play crucial roles in the activation of TAFI in the plasma. Specifically, we can speculate that some minor alleles may increase the binding affinity of TAFI for TM or strengthen the interaction with thrombin. However, further rigorous analyses, especially targeting TM, thrombin, and other coagulation factors, are needed to explain the increase in TAFIa levels in CTEPH patients. For this purpose, we have recently started the registration of CTEPH patients and analyses of whole-genome sequencing. Further studies into the specific mechanism of TAFI cleavage and activation would provide important additional insights into the pathogenesis of CTEPH.

In addition to these genetic backgrounds, additional environmental factors (eg, infection, inflammation, residence, air pollutions, smoking, and especially hypoxia) would result in complex interactions and trigger the activation of TAFI in CTEPH patients. Plasma levels of TAFIa were significantly increased in mice by hypoxia. Consistently, plasma levels of TAFIa were significantly increased in CTEPH patients. Synthesis and secretion of TAFI were regulated by HIF-1α signaling that mediates hypoxia-induced increases in multiple inflammatory cytokines/chemokines and growth factors. In contrast, expressions of HIF-1α mRNA in the liver were equally upregulated by hypoxia in both control and TAFI-Tg mice, which were significantly downregulated by WY14643 treatment. Additionally, WY14643 treatment downregulated HIF-1α expression in hepatocytes in vitro. However, these WY14643-mediated HIF-1α downregulations in vivo and in vitro were potentially the consequences of indirect effects of suppression of inflammatory cytokines. Indeed, WY14643 significantly reduced serum levels of cytokines/chemokines and growth factors in TAFI-Tg mice. Moreover, it has been demonstrated that inflammatory cytokines (eg, IL-1β, IL-6, and IL-18) activate intracellular signaling and transcription factors that are recruited to the hypoxia-responsive element in the HIF-1α promoter.[40–43] Thus, WY14643-mediated reductions in circulating inflammatory cytokines may have downregulated HIF-1α activity in the liver. Importantly, the levels of HIF-1α activity in the liver were comparable between the control and TAFI-Tg mice, suggesting that TAFI protein itself would not affect HIF-1α activity. In contrast, in mice treated with vehicle in hypoxia for 3 weeks, serum levels of cytokines/chemokines and growth factors (eg, IL-1β, IL-6, G-CSF [granulocyte colony-stimulating factor], RANTES [regulated on activation, normal T-cell expressed and secreted], tumor necrosis factor-α, and platelet-derived growth factor-BB) were significantly higher in TAFI-Tg mice compared with control mice. Additionally, in vitro experiments with mouse PASMCs and secretion of inflammatory cytokines (eg, IL-1β and IL-6) were significantly increased in TAFI-Tg PASMCs compared with control PASMCs. Moreover, PASMC proliferation in response to 10% FBS was significantly higher in TAFI-Tg PASMCs compared with control PASMCs. These results suggest that TAFI protein itself may have proinflammatory effects and promotes secretion of inflammatory cytokines and growth factors. On the other hand, WY14643-mediated reductions of circulating inflammatory cytokines should have beneficial effects on pulmonary vasculature, including an improvement of PAEC function, reduced adhesion molecule expression, reduced PASMC proliferation, and deactivation of inflammatory cells. Thus, PPARα agonists may have multiple effects on the pulmonary vasculature in addition to the downregulation of HIF-1α-mediated TAFI synthesis. Altogether, we could offer some mechanistic explanations for the WY14643-mediated amelioration of PH, which were associated with the inhibitory effects on TAFI synthesis and the anti-inflammatory effects on pulmonary vasculature.

TAFI-Mediated Pulmonary Vascular Inflammation

Increased endothelial permeability is one of the important features of PH because it promotes the translocation of inflammatory factors across the vascular wall.[31,44] Recent studies clearly demonstrated the role of VE-cadherin for endothelial permeability.[29,45] In the present study, treatment with human TAFI reduced VE-cadherin expression and increased PAEC permeability. In vivo, it is possible that the increased endothelial permeability exposes PASMCs to plasma TAFI and other circulating growth factors. Indeed, in the present study, treatment with human TAFI significantly increased extracellular signal–regulated kinase 1/2 phosphorylation and PASMCs proliferation. Moreover, the secretions of cytokines/chemokines and growth factors were significantly increased in PASMCs harvested from the distal PAs of TAFI-Tg mice, supporting the autocrine/paracrine effects of TAFI for PASMC activation and proliferation. Consistently, TAFI overexpression increased cytokines/chemokines and growth factors in the lung after hypoxic exposure, suggesting the crucial role of TAFI in hypoxia-induced pulmonary vascular inflammation. This is consistent with the previous report that TAFI promotes lung inflammation in a mouse model of sepsis.[46] Because inflammation plays a crucial role for the development of PH,[47,48] TAFI-mediated enhancement of perivascular inflammation substantially contributes to the development of pulmonary vascular remodeling and PH. Based on these results and the previous reports, TAFI promotes pulmonary vascular remodeling and PH through increasing PAEC permeability, PASMC proliferation, and augmented inflammation. However, we still do not know the precise mechanisms underlying the TAFI-induced VE-cadherin downregulation and PASMC proliferation. Indeed, the receptors for TAFI in PAECs or PASMCs remain unidentified. Further studies into the specific mechanism of TAFI-mediated intracellular signaling in PAECs and PASMCs would provide important additional insights into the pathogenesis of PH.

Study Limitations

Several limitations should be mentioned for the present study. First, we showed that TAFI in BM cells did not contribute to the development of PH or thrombus formation. However, BM-derived cells are the source of several types of cells including platelets. In the present BM experiments, we were unable to distinguish the roles of TAFI in each cell component. Indeed, we already reported that platelets in CTEPH patients are highly activated[6] and release TAFI into the plasma.[14] Thus, BM-derived TAFI, especially from platelets, may play a crucial role in the development of PH. Next, the beneficial effects of PPARα agonists may involve factors other than reducing plasma TAFIa. Indeed, PPARα agonists regulate lipid metabolism and blood pressure, oxidative stress, and inflammation.[49,50] Moreover, PPARα agonists have been reported to reduce plasma levels of fibrinogen.[51] Thus, PPARα agonists may ameliorate PH by reducing plasma TAFIa and by other mechanisms.

Clinical Implication and Conclusions

Patients with CTEPH show no typical signs or symptoms at the onset of the disease and have no typical risk factors.[52] Although pulmonary embolism is considered as one of the predictive factors for the development of CTEPH, the incidence was not so high (<10%) in the international prospective registry.[7,8] Thus, it is difficult to diagnose CTEPH and predict the risk in clinical practice. Additionally, most of the established diagnostic techniques are invasive, including cardiac catheterization. In the present study, we demonstrated that CTEPH patients have a 10-fold increase in plasma TAFIa compared with controls, suggesting the usefulness of plasma TAFIa as a novel biomarker for CTEPH. Plasma levels of TAFIa can be easily measured in outpatient clinics and, thus, could be widely used for clinical application. Further accumulation of evidence with clinical studies will establish the importance of plasma TAFIa as a novel biomarker in CTEPH patients.

Next, we showed that PPARα agonists reduced plasma TAFIa levels and thrombus formation, which has the potential to cure CTEPH patients. PPARs are members of the nuclear hormone receptor superfamily of ligand-activated transcription factors, which are mainly related to lipid metabolism, insulin sensitivity, and glucose homeostasis.[44] Several studies indicated that PPAR agonists suppress inflammation in endothelial cells and smooth muscle cells.[53,54] Moreover, PPARγ agonists attenuate the development of hypoxia-induced PH in mice and monocrotaline-induced PH in rats.[55] In contrast, the role of PPARα agonists in PH remained to be elucidated. Importantly, it has also been reported that PPARα agonists regulate fibrinolysis[56] and suppress TAFI synthesis in hepatocytes.[32] Indeed, in the present study, PPARα agonists significantly reduced plasma TAFIa, ameliorated hypoxia-induced PH, and improved survival in TAFI-overexpressing mice. Moreover, these findings were also found in both monocrotaline-induced PH and Sugen/hypoxia-induced PH models in rats. Based on the present results and the previous reports, PPARα agonists may have a potential to be a useful therapeutic option in PH patients. Recently, we and others demonstrated that balloon pulmonary angioplasty improves the prognosis of CTEPH patients.[4,33,57] Additionally, we can use vasodilators such as Riociguat for CTEPH patients.[52] However, CTEPH patients still need anticoagulants for the rest of their life, which could cause fatal bleeding and life-threatening events at a higher rate (2%–3%/year).[52] Here, based on the pathogenic role of TAFI in PH, we may consider the use of anticoagulants without the risk of bleeding, such as PPARα agonists or TAFIa-specific inhibitors.

In conclusion, TAFI is a crucial molecule in the development of PH and thrombus formation in PAs and is useful as a novel biomarker and a therapeutic target of CTEPH.

Acknowledgments

We are grateful to the laboratory members in the Department of Cardiovascular Medicine at Tohoku University for valuable technical assistance, especially Yumi Watanabe, Ai Nishihara, and Hiromi Yamashita.

Sources of Funding

This work was supported in part by the grants-in-aid for Scientific Research (15H02535, 15H04816, and 15K15046), all of which are from the Ministry of Education, Culture, Sports, Science and Technology, Tokyo, Japan, the grants-in-aid for Scientific Research from the Ministry of Health, Labor, and Welfare, Tokyo, Japan (10102895), and the grants-in-aid for Scientific Research from the Japan Agency for Medical Research and Development, Tokyo, Japan (15ak0101035h0001 and 16ek0109176h0001).

Disclosures

None.

References

1. Simonneau G, Gatzoulis MA, Adatia I, Celermajer D, Denton C, Ghofrani A, Gomez Sanchez MA, Krishna Kumar R, Landzberg M, Machado RF, Olschewski H, Robbins IM, Souza R. Updated clinical classification of pulmonary hypertension. *J Am Coll Cardiol*. 2013;62:D34–D41. doi: 10.1016/j.jacc.2013.10.029.
2. Pengo V, Lensing AW, Prins MH, Marchiori A, Davidson BL, Tiozzo F, Albanese P, Biasiolo A, Pegoraro C, Iliceto S, Prandoni P; Thromboembolic Pulmonary Hypertension Study Group. Incidence of chronic thromboembolic pulmonary hypertension after pulmonary embolism. *N Engl J Med*. 2004;350:2257–2264. doi: 10.1056/NEJMoa032274.
3. Galiè N, Hoeper MM, Humbert M, *et al*.; ESC Committee for Practice Guidelines (CPG). Guidelines for the diagnosis and treatment of pulmonary hypertension: the Task Force for the Diagnosis and Treatment of Pulmonary Hypertension of the European Society of Cardiology (ESC) and the European Respiratory Society (ERS), endorsed by the International Society of Heart and Lung Transplantation (ISHLT). *Eur Heart J*. 2009;30:2493–2537. doi: 10.1093/eurheartj/ehp297.
4. Tatebe S, Fukumoto Y, Sugimura K, Nakano M, Miyamichi S, Satoh K, Oikawa M, Shimokawa H. Optical coherence tomography as a novel diagnostic tool for distal type chronic thromboembolic pulmonary hypertension. *Circ J*. 2010;74:1742–1744.
5. Morris TA, Marsh JJ, Chiles PG, Auger WR, Fedullo PF, Woods VL Jr. Fibrin derived from patients with chronic thromboembolic pulmonary hypertension is resistant to lysis. *Am J Respir Crit Care Med*. 2006;173:1270–1275. doi: 10.1164/rccm.200506-916OC.
6. Yaoita N, Shirakawa R, Fukumoto Y, Sugimura K, Miyata S, Miura Y, Nochioka K, Miura M, Tatebe S, Aoki T, Yamamoto S, Satoh K, Kimura T, Shimokawa H, Horiuchi H. Platelets are highly activated in patients of chronic thromboembolic pulmonary hypertension. *Arterioscler Thromb Vasc Biol*. 2014;34:2486–2494. doi: 10.1161/ATVBAHA.114.304404.
7. Pepke-Zaba J, Delcroix M, Lang I, *et al*. Chronic thromboembolic pulmonary hypertension (CTEPH): results from an international prospective registry. *Circulation*. 2011;124:1973–1981. doi: 10.1161/CIRCULATIONAHA.110.015008.
8. Morris TA, Marsh JJ, Chiles PG, Pedersen CA, Konopka RG, Gamst AC, Loza O. Embolization itself stimulates thrombus propagation in pulmonary embolism. *Am J Physiol Heart Circ Physiol*. 2004;287:H818–H822. doi: 10.1152/ajpheart.01197.2003.

9. Shigeta A, Tanabe N, Shimizu H, Hoshino S, Maruoka M, Sakao S, Tada Y, Kasahara Y, Takiguchi Y, Tatsumi K, Masuda M, Kuriyama T. Gender differences in chronic thromboembolic pulmonary hypertension in Japan. *Circ J*. 2008;72:2069–2074.
10. Lang IM, Pesavento R, Bonderman D, Yuan JX. Risk factors and basic mechanisms of chronic thromboembolic pulmonary hypertension: a current understanding. *Eur Respir J*. 2013;41:462–468. doi: 10.1183/09031936.00049312.
11. Alias S, Lang IM. Coagulation and the vessel wall in pulmonary embolism. *Pulm Circ*. 2013;3:728–738. doi: 10.1086/674768.
12. Speidl WS, Zeiner A, Nikfardjam M, Geppert A, Jordanova N, Niessner A, Zorn G, Maurer G, Schreiber W, Wojta J, Huber K. An increase of C-reactive protein is associated with enhanced activation of endogenous fibrinolysis at baseline but an impaired endothelial fibrinolytic response after venous occlusion. *J Am Coll Cardiol*. 2005;45:30–34. doi: 10.1016/j.jacc.2004.09.052.
13. Larsson P, Ulfhammer E, Karlsson L, Bokarewa M, Wåhlander K, Jern S. Effects of IL-1beta and IL-6 on tissue-type plasminogen activator expression in vascular endothelial cells. *Thromb Res*. 2008;123:342–351. doi: 10.1016/j.thromres.2008.03.013.
14. Yaoita N, Satoh K, Satoh T, Sugimura K, Tatebe S, Yamamoto S, Aoki T, Miura M, Miyata S, Kawamura T, Horiuchi H, Fukumoto Y, Shimokawa H. Thrombin-activatable fibrinolysis inhibitor in chronic thromboembolic pulmonary hypertension. *Arterioscler Thromb Vasc Biol*. 2016;36:1293–1301. doi: 10.1161/ATVBAHA.115.306845.
15. Gursoy T, Tekinalp G, Yigit S, Kirazli S, Korkmaz A, Gurgey A. Thrombin activatable fibrinolysis inhibitor activity (TAFIa) levels in neonates with meconium-stained amniotic fluid. *J Matern Fetal Neonatal Med*. 2008;21:123–128. doi: 10.1080/14767050801891135.
16. Bajzar L, Nesheim M, Morser J, Tracy PB. Both cellular and soluble forms of thrombomodulin inhibit fibrinolysis by potentiating the activation of thrombin-activable fibrinolysis inhibitor. *J Biol Chem*. 1998;273:2792–2798.
17. Bouma BN, Meijers JC. Thrombin-activatable fibrinolysis inhibitor (TAFI, plasma procarboxypeptidase B, procarboxypeptidase R, procarboxypeptidase U). *J Thromb Haemost*. 2003;1:1566–1574.
18. Nagashima M, Yin ZF, Zhao L, White K, Zhu Y, Lasky N, Halks-Miller M, Broze GJ Jr, Fay WP, Morser J. Thrombin-activatable fibrinolysis inhibitor (TAFI) deficiency is compatible with murine life. *J Clin Invest*. 2002;109:101–110. doi: 10.1172/JCI12119.
19. Morser J, Gabazza EC, Myles T, Leung LL. What has been learnt from the thrombin-activatable fibrinolysis inhibitor-deficient mouse? *J Thromb Haemost*. 2010;8:868–876. doi: 10.1111/j.1538-7836.2010.03787.x.
20. Mutch NJ, Moore NR, Wang E, Booth NA. Thrombus lysis by uPA, scuPA and tPA is regulated by plasma TAFI. *J Thromb Haemost*. 2003;1:2000–2007.
21. Wynants M, Vengethasamy L, Ronisz A, Meyns B, Delcroix M, Quarck R. NF-κB pathway is involved in CRP-induced effects on pulmonary arterial endothelial cells in chronic thromboembolic pulmonary hypertension. *Am J Physiol Lung Cell Mol Physiol*. 2013;305:L934–L942. doi: 10.1152/ajplung.00034.2013.
22. Quarck R, Delcroix M. Is inflammation a potential therapeutic target in chronic thromboembolic pulmonary hypertension? *Eur Respir J*. 2014;44:842–845. doi: 10.1183/09031936.00120014.
23. Satoh K, Kagaya Y, Nakano M, et al. Important role of endogenous erythropoietin system in recruitment of endothelial progenitor cells in hypoxia-induced pulmonary hypertension in mice. *Circulation*. 2006;113:1442–1450. doi: 10.1161/CIRCULATIONAHA.105.583732.
24. Satoh K, Fukumoto Y, Nakano M, Sugimura K, Nawata J, Demachi J, Karibe A, Kagaya Y, Ishii N, Sugamura K, Shimokawa H. Statin ameliorates hypoxia-induced pulmonary hypertension associated with down-regulated stromal cell-derived factor-1. *Cardiovasc Res*. 2009;81:226–234. doi: 10.1093/cvr/cvn244.
25. Pugliese SC, Poth JM, Fini MA, Olschewski A, El Kasmi KC, Stenmark KR. The role of inflammation in hypoxic pulmonary hypertension: from cellular mechanisms to clinical phenotypes. *Am J Physiol Lung Cell Mol Physiol*. 2015;308:L229–L252. doi: 10.1152/ajplung.00238.2014.
26. Ishii H, Salem HH, Bell CE, Laposata EA, Majerus PW. Thrombomodulin, an endothelial anticoagulant protein, is absent from the human brain. *Blood*. 1986;67:362–365.
27. Wu C, Kim PY, Manuel R, Seto M, Whitlow M, Nagashima M, Morser J, Gils A, Declerck P, Nesheim ME. The roles of selected arginine and lysine residues of TAFI (Pro-CPU) in its activation to TAFIa by the thrombin–thrombomodulin complex. *J Biol Chem*. 2009;284:7059–7067. doi: 10.1074/jbc.M804745200.
28. Bajzar L, Morser J, Nesheim M. TAFI, or plasma procarboxypeptidase B, couples the coagulation and fibrinolytic cascades through the thrombin-thrombomodulin complex. *J Biol Chem*. 1996;271:16603–16608.
29. Orsenigo F, Giampietro C, Ferrari A, et al. Phosphorylation of VE-cadherin is modulated by haemodynamic forces and contributes to the regulation of vascular permeability in vivo. *Nat Commun*. 2012;3:1208. doi: 10.1038/ncomms2199.
30. Vandenbroucke St Amant E, Tauseef M, Vogel SM, Gao XP, Mehta D, Komarova YA, Malik AB. PKC α activation of p120-catenin serine 879 phospho-switch disassembles VE-cadherin junctions and disrupts vascular integrity. *Circ Res*. 2012;111:739–749.
31. Long L, Ormiston ML, Yang X, et al. Selective enhancement of endothelial BMPR-II with BMP9 reverses pulmonary arterial hypertension. *Nat Med*. 2015;21:777–785. doi: 10.1038/nm.3877.
32. Masuda Y, Saotome D, Takada K, Sugimoto K, Sasaki T, Ishii H. Peroxisome proliferator-activated receptor-alpha agonists repress expression of thrombin-activatable fibrinolysis inhibitor by decreasing transcript stability. *Thromb Haemost*. 2012;108:74–85. doi: 10.1160/TH12-02-0101.
33. Sugimura K, Fukumoto Y, Miura Y, Nochioka K, Miura M, Tatebe S, Aoki T, Satoh K, Yamamoto S, Yaoita N, Shimokawa H. Three-dimensional-optical coherence tomography imaging of chronic thromboembolic pulmonary hypertension. *Eur Heart J*. 2013;34:2121. doi: 10.1093/eurheartj/eht203.
34. Alias S, Redwan B, Panzenböck A, et al. Defective angiogenesis delays thrombus resolution: a potential pathogenetic mechanism underlying chronic thromboembolic pulmonary hypertension. *Arterioscler Thromb Vasc Biol*. 2014;34:810–819. doi: 10.1161/ATVBAHA.113.302991.
35. Mercier O, Fadel E. Chronic thromboembolic pulmonary hypertension: animal models. *Eur Respir J*. 2013;41:1200–1206. doi: 10.1183/09031936.00101612.
36. Franco RF, Fagundes MG, Meijers JC, Reitsma PH, Lourenço D, Morelli V, Maffei FH, Ferrari IC, Piccinato CE, Silva WA Jr, Zago MA. Identification of polymorphisms in the 5'-untranslated region of the TAFI gene: relationship with plasma TAFI levels and risk of venous thrombosis. *Haematologica*. 2001;86:510–517.
37. Morange PE, Aillaud MF, Nicaud V, Henry M, Juhan-Vague I. Ala147Thr and C+1542G polymorphisms in the TAFI gene are not asssociated with a higher risk of venous thrombosis in FV Leiden carriers. *Thromb Haemost*. 2001;86:1583–1584.
38. Schneider M, Boffa M, Stewart R, Rahman M, Koschinsky M, Nesheim M. Two naturally occurring variants of TAFI (Thr-325 and Ile-325) differ substantially with respect to thermal stability and antifibrinolytic activity of the enzyme. *J Biol Chem*. 2002;277:1021–1030. doi: 10.1074/jbc.M104444200.
39. International HapMap Consortium. The international HapMap project. *Nature*. 2003;426:789–796. doi: 10.1038/nature02168.
40. Sharma V, Dixit D, Koul N, Mehta VS, Sen E. Ras regulates interleukin-1β-induced HIF-1α transcriptional activity in glioblastoma. *J Mol Med (Berl)*. 2011;89:123–136. doi: 10.1007/s00109-010-0683-5.
41. Sartori-Cintra AR, Mara CS, Argolo DL, Coimbra IB. Regulation of hypoxia-inducible factor-1α (HIF-1α) expression by interleukin-1β (IL-1 β), insulin-like growth factors I (IGF-I) and II (IGF-II) in human osteoarthritic chondrocytes. *Clinics (Sao Paulo)*. 2012;67:35–40.
42. Zhang F, Duan S, Tsai Y, Keng PC, Chen Y, Lee SO, Chen Y. Cisplatin treatment increases stemness through upregulation of hypoxia-inducible factors by interleukin-6 in non-small cell lung cancer. *Cancer Sci*. 2016;107:746–754. doi: 10.1111/cas.12937.
43. Kim J, Shao Y, Kim SY, Kim S, Song HK, Jeon JH, Suh HW, Chung JW, Yoon SR, Kim YS, Choi I. Hypoxia-induced IL-18 increases hypoxia-inducible factor-1alpha expression through a Rac1-dependent NF-kappaB pathway. *Mol Biol Cell*. 2008;19:433–444. doi: 10.1091/mbc.E07-02-0182.
44. Koo SH, Satoh H, Herzig S, Lee CH, Hedrick S, Kulkarni R, Evans RM, Olefsky J, Montminy M. PGC-1 promotes insulin resistance in liver through PPAR-alpha-dependent induction of TRB-3. *Nat Med*. 2004;10:530–534. doi: 10.1038/nm1044.
45. Benn A, Bredow C, Casanova I, Vukičević S, Knaus P. VE-cadherin facilitates BMP-induced endothelial cell permeability and signaling. *J Cell Sci*. 2016;129:206–218. doi: 10.1242/jcs.179960.
46. Muto Y, Suzuki K, Iida H, Sakakibara S, Kato E, Itoh F, Kakui N, Ishii H. EF6265, a novel inhibitor of activated thrombin-activatable fibrinolysis inhibitor, protects against sepsis-induced organ dysfunction in rats. *Crit Care Med*. 2009;37:1744–1749. doi: 10.1097/CCM.0b013e31819ffc14.
47. Satoh K, Satoh T, Kikuchi N, *et al*. Basigin mediates pulmonary hypertension by promoting inflammation and vascular smooth

muscle cell proliferation. *Circ Res*. 2014;115:738–750. doi: 10.1161/CIRCRESAHA.115.304563.
48. Shimokawa H, Sunamura S, Satoh K. RhoA/Rho-kinase in the cardiovascular system. *Circ Res*. 2016;118:352–366. doi: 10.1161/CIRCRESAHA.115.306532.
49. Duncan JG, Bharadwaj KG, Fong JL, Mitra R, Sambandam N, Courtois MR, Lavine KJ, Goldberg IJ, Kelly DP. Rescue of cardiomyopathy in peroxisome proliferator-activated receptor-alpha transgenic mice by deletion of lipoprotein lipase identifies sources of cardiac lipids and peroxisome proliferator-activated receptor-alpha activators. *Circulation*. 2010;121:426–435. doi: 10.1161/CIRCULATIONAHA.109.888735.
50. Martin OJ, Lai L, Soundarapandian MM, Leone TC, Zorzano A, Keller MP, Attie AD, Muoio DM, Kelly DP. A role for peroxisome proliferator-activated receptor γ coactivator-1 in the control of mitochondrial dynamics during postnatal cardiac growth. *Circ Res*. 2014;114:626–636. doi: 10.1161/CIRCRESAHA.114.302562.
51. Gervois P, Vu-Dac N, Kleemann R, Kockx M, Dubois G, Laine B, Kosykh V, Fruchart JC, Kooistra T, Staels B. Negative regulation of human fibrinogen gene expression by peroxisome proliferator-activated receptor alpha agonists via inhibition of CCAAT box/enhancer-binding protein beta. *J Biol Chem*. 2001;276:33471–33477. doi: 10.1074/jbc.M102839200.
52. Kim NH, Delcroix M, Jenkins DP, Channick R, Dartevelle P, Jansa P, Lang I, Madani MM, Ogino H, Pengo V, Mayer E. Chronic thromboembolic pulmonary hypertension. *J Am Coll Cardiol*. 2013;62:D92–D99. doi: 10.1016/j.jacc.2013.10.024.
53. Wang S, Liu J, Wu DI, Pang X, Zhao J, Zhang X. Pro-inflammatory effect of fibrinogen on vascular smooth muscle cells by regulating the expression of PPARα, PPARγ and MMP-9. *Biomed Rep*. 2015;3:513–518. doi: 10.3892/br.2015.459.
54. Kang BY, Kleinhenz JM, Murphy TC, Hart CM. The PPARγ ligand rosiglitazone attenuates hypoxia-induced endothelin signaling in vitro and in vivo. *Am J Physiol Lung Cell Mol Physiol*. 2011;301:L881–L891. doi: 10.1152/ajplung.00195.2011.
55. Wang Y, Lu W, Yang K, Wang Y, Zhang J, Jia J, Yun X, Tian L, Chen Y, Jiang Q, Zhang B, Chen X, Wang J. Peroxisome proliferator-activated receptor γ inhibits pulmonary hypertension targeting store-operated calcium entry. *J Mol Med (Berl)*. 2015;93:327–342. doi: 10.1007/s00109-014-1216-4.
56. Ali FY, Armstrong PC, Dhanji AR, Tucker AT, Paul-Clark MJ, Mitchell JA, Warner TD. Antiplatelet actions of statins and fibrates are mediated by PPARs. *Arterioscler Thromb Vasc Biol*. 2009;29:706–711. doi: 10.1161/ATVBAHA.108.183160.
57. Sato H, Ota H, Sugimura K, Aoki T, Tatebe S, Miura M, Yamamoto S, Yaoita N, Suzuki H, Satoh K, Takase K, Shimokawa H. Balloon pulmonary angioplasty improves biventricular functions and pulmonary flow in chronic thromboembolic pulmonary hypertension. *Circ J*. 2016;80:1470–1477. doi: 10.1253/circj.CJ-15-1187.

Circulation Research
JOURNAL OF THE AMERICAN HEART ASSOCIATION

Activated TAFI Promotes the Development of Chronic Thromboembolic Pulmonary Hypertension: A Possible Novel Therapeutic Target

Taijyu Satoh, Kimio Satoh, Nobuhiro Yaoita, Nobuhiro Kikuchi, Junichi Omura, Ryo Kurosawa, Kazuhiko Numano, Elias Al-Mamun, Mohammad Abdul Hai Siddique, Shinichiro Sunamura, Masamichi Nogi, Kota Suzuki, Satoshi Miyata, John Morser and Hiroaki Shimokawa

Circ Res. 2017;120:1246-1262; originally published online March 13, 2017;
doi: 10.1161/CIRCRESAHA.117.310640
Circulation Research is published by the American Heart Association, 7272 Greenville Avenue, Dallas, TX 75231

Print ISSN: 0009-7330. Online ISSN: 1524-4571

Supplementary Materials

Activated TAFI Promotes the Development of Chronic Thromboembolic Pulmonary Hypertension - A Possible Novel Therapeutic Target -

Taijyu Satoh, MD[1]; Kimio Satoh, MD, PhD[1]; Nobuhiro Yaoita, MD, PhD[1]; Nobuhiro Kikuchi, MD[1]; Junichi Omura, MD[1]; Ryo Kurosawa, MD[1]; Kazuhiko Numano MD[1], Md. Elias-Al-Mamun, PhD[1]; Mohammad Abdul Hai Siddique, PhD[1]; Shinichiro Sunamura, MD[1]; Masamichi Nogi, MD[1]; Kota Suzuki, MD, PhD[1]; Satoshi Miyata, PhD[1]; John Morser, PhD[2],
Hiroaki Shimokawa, MD, PhD[1]

[1]Department of Cardiovascular Medicine, Tohoku University Graduate School of Medicine, Sendai, Japan, and [2]Department of Hematology, Stanford School of Medicine, Stanford, California, USA.

Supplementary Detailed Methods

Supplement References

Supplementary Tables I-III

Supplementary Figures I-XV

Supplementary Figure Legends I-XV

Supplementary Detailed Methods

Diagnosis of CTEPH

The diagnosis of patients with CTEPH was made according to the European Society of Cardiology (ESC)/European Respiratory Society (ERS) guideline.[1] PH was defined as mean pulmonary artery pressure (mPAP) >25 mmHg at rest. CTEPH was diagnosed by ventilation-perfusion scintigraphy, computed tomography (CT), optimal coherence tomography (OCT) and pulmonary angiography after the treatment with anticoagulants more than 6 months. Pulmonary function tests, arterial blood gases, chest X-ray, and CT scan were also used for the diagnosis.

Clinical Data

We collected clinical data and blood samples from patients with symptoms and/or signs of CTEPH or PAH who were referred to Tohoku University Hospital for right heart catheter examination from August 2011 to June 2013. All protocols using human specimens were approved by the Institutional Review Board of Tohoku University, Sendai Japan (No. 2011-197). CTEPH patients (*n*=32) and PAH patients (*n*=22) were enrolled and those with cancer were excluded. As non-PH controls, we collected blood samples from volunteers (*n*=13). All patients provided written consent for the use of their plasma for the present study.

Clinical Information

Clinical characteristics of the controls and the patients with PAH and CTEPH are shown in **Supplementary Table I**. There was no significant difference in complete blood count among the groups. Mean pulmonary arterial (PA) pressure and pulmonary vascular resistance (PVR) were significantly higher in PAH and CTEPH patients compared with controls. Cardiac index was significantly lower in PAH and CTEPH patients compared with controls. Bioplex cytokine array analyses showed significant increases in serum levels of cytokines/chemokines and growth factors in CTEPH patients compared with controls (**Supplementary Figure I**).

Human Lung Samples

All protocols using human specimens were approved by the Institutional Review Board of Tohoku University, Sendai Japan (No. 2013-1-160). Lung tissues were obtained from CTEPH patients at the time of autopsy and controls at the time of thoracic surgery for lung cancer at a site far from the tumor margins as previously described.[2] All patients and families provided written consent for the use of their lung tissues for the present study. Primary human pulmonary artery smooth muscle cells (PASMCs), primary human PAECs, and human aortic endothelial cells (AoECs) were purchased from Lonza (Basel, Switzerland). PASMCs were cultured in Dulbecco's Modified Eagle Medium (DMEM) containing 10%

fetal bovine serum (FBS) at 37°C in a humidified atmosphere of 5% CO_2 and 95% air. PASMCs of passage 4 to 7 at 70–80% confluence were used for experiments. PAECs and AoECs were grown in **Endothelial Basal M**edium (EBM)-2 basal medium supplemented with Endothelial Growth Basal Medium (EGM)-2 (Lonza). Endothelial cells of passages 3 to 5 at 70–80% confluence were used for experiments.

Generation and Genotyping of *CPB2*$^{-/-}$ Mice and TAFI-Tg Mice

CPB2$^{-/-}$ mice (C57BL/6 background) were obtained from Dr. Morser at the Stanford University (California, United States).[3] The genotype of mice was confirmed by polymerase chain reaction using primers specific for the *CPB2* gene, which were one annealing to the 5′ end of TAFI cDNA (5′-CAAGTCACTGTTGGGATGAAGC-3′) and the second one annealing to the 3′ end of TAFI cDNA (5′-ATTAACTGTTCCTGATGACATGCC-3′).[3] We newly developed systemic TAFI-overexpressing mice (TAFI-Tg) (Balb/c background). Briefly, CAG promoter was inserted into the 5′ site of the mouse TAFI cDNA, which was inserted into the pCAGGS vector. The targeting construct was linearized and injected into pronuclei of fertilized zygotes from Balb/c mice and transferred to pseudo-pregnant females. Offspring were screened for genomic integration by PCR of tail DNA using the CAG-TAFI specific primers. Mice were generated by breeding F1 heterozygous transgenic males to wild-type females. All mice were backcrossed to the Balb/c strain for at least 6 generations and were genotyped by PCR amplification of tail clip samples. Genotyping primers were as follows: 5′-CCTACAGCTCCTGGGCAACGT GCTGGTT-3′ and 5′-AGAGGGAAAAAGA- TCTCAGTGGTAT-3′. All mice were genotyped by PCR amplification of tail clip samples, and the levels of TAFI were confirmed with immunoblotting or immunofluorescence staining using an anti-TAFI monoclonal antibody (Abcam, Cambridge, UK). All experiments *in vivo* were performed with male mice using littermate as wild-type (WT) controls (12-15 weeks of age). Female mice were used only when we evaluated the survival rate and the development of PH in supplements. Animals were housed under a 12-h light and 12-h dark regimen and placed on a normal chow diet as previously descrived.[2]

Preparation of Human TAFI Plasmids and Liver-specific TAFI Overexpression in Mice

The human TAFI-overexpressing plasmids were obtained from Takara Bio Inc. The human TAFI gene was cloned into the pLIVE vector, and control plasmid DNA was also produced. Plasmid was injected into the tail vein of mice. The 55 μg of human TAFI pDNA or control pDNA in 1.8 ml of phosphate-buffered saline (pH 7.4, $CaCl_2^-$, $MgCl_2^-$) were injected within 10 sec into the tail of male C57BL/6J mice weighing 25 g each using a 26 G needle. Two days after injection, TAFI expression in the liver and plasma of mice was quantified by Western blotting.[4]

Animal Experiments

All animal experiments were performed in accordance with the protocols approved by the Tohoku University Animal Care and Use Committee (No. 2015-Kodo-006) based on the ARRIVE guideline. In all animal experiments, we used littermate as controls. Hypoxia-induced PH models were used to assess the development of PH in mice.[2] Eight-week-old male WT mice on a normal chow diet were exposed to hypoxia (10% O_2) or normoxia for 3 weeks as previously described.[5,6] Briefly, hypoxic mice were housed in an acrylic chamber with a non-recirculating gas mixture of 10% O_2 and 90% N_2 by adsorption-type oxygen concentrator to utilized exhaust air (Teijin, Tokyo, Japan), while normoxic mice were housed in room air (21% O_2) under a 12 h light and dark cycle. After 3 weeks of exposure to hypoxia (10% O_2) or normoxia, mice were anesthetized with isoflurane (1.0%). To examine the development of PH, we measured right ventricular systolic pressure (RVSP), right ventricular hypertrophy (RVH), and pulmonary vascular remodeling.[2,5,6] For right heart catheterization, a 1.2-F pressure catheter (SciSense Inc., Ontario, Canada) was inserted in the right jugular vein and advanced into the right ventricle to measure RVSP.[7] All data were analyzed using the Power Lab data acquisition system (AD Instruments, Bella Vista, Australia) and were averaged over 10 sequential beats.[2,5,6]

Assessment of Right Ventricular Hypertrophy

Formaldehyde-fixed dry hearts were dissected and the right ventricular wall was removed from the left ventricle and septum. The ratio of the right ventricle to the left ventricle plus septum weight [RV/(LV+S)] was calculated to determine the extent of RVH.[2]

Histological Analysis

After hemodynamic measurements, the heart, lungs, and aorta were rigorously and completely perfused with cold phosphate-buffered saline (PBS) at physiological pressure until the colors of the heart and lungs clearly showed white, and thereafter, perfusion-fixed with 10% formaldehyde solution. Then, they were fixed in 10% formaldehyde solution for 24 h on a shaker at room temperature. After the serial steps of washing and dehydration, the whole heart, lungs, and aorta were embedded in paraffin, and cross sections (3 μm) were prepared. Paraffin sections were stained with Elastica-Masson (EM), phosphotungstic acid hematoxylin (PTAH) staining (Muto Pure Chemicals) for the detection of chronic PA thrombus formation, or used for immunostaining. Antibodies used were as follows; α-smooth muscle actin (αSMA, Sigma-Aldrich, 1:400), thrombomodulin (TM, R&D systems, 1:400), CD31 (PECAM-1, BD Pharmingen, 1:400), CD45 (clone Ly-5, BD Pharmingen, 1:100), Mac-3 (CD107b, BD Pharmingen, 1:400), F4/80 (Biolegend, 1:400), and CD3 (NICHIREI, 1:400). Pulmonary arteries adjacent to an airway distal to the respiratory bronchiole were evaluated as previously reported.[2] Briefly, arteries were considered fully muscularized when they had a distinct double elastic lamina visible throughout the diameter of the vessel cross section. The arteries were considered partially muscularized when they had a distinct double elastic lamina visible for at least half the diameter. The percentage of vessels with double elastic lamina was calculated as the

number of muscularized vessels per total number of vessels counted. In each section, a total of 60–80 vessels were examined by use of a computer-assisted imaging system (BX51, Olympus, Tokyo, Japan). This analysis was performed for the small vessels with external diameters of 20–70 μm.

Baseline Measurements

Plasma samples were collected using citrate acid from the inferior vena cava in mice under anesthesia and then centrifuged for 15 min at 1,000 g within 30 min; aliquots were immediately stored at -80°C. Thrombin-antithrombin complex (TAT) and D-dimer were quantified by commercially available ELISA kits (USCN Life Science). TM was quantified by commercially available ELISA kits (R&D systems). Each experiment was performed in duplicate.

Plasma Clot Lysis Assay

The plasma clot lysis assay was performed in a 96-well microtiter plate, using a modification of the previous methods.[8,9] Briefly, 50 μL of mouse plasma from each mouse was mixed with 30 μL assay buffer (100 mmol/L NaCl, 20 mmol/L Tris-HCl, pH 7.4, 0.8 mmol/L CHAPS) at room temperature. Plasma samples were pre-incubated with 25 μg/mL of carboxypeptidase inhibitor (CPI; TAFIa inhibitor) for 5 min prior to incubation with assay buffer. Then, 500 ng/ml monteplase, 10 mmol/L $CaCl_2$ and 2.5 U/mL human thrombin (Sigma Aldrich, St. Louis, MO) were mixed and clot formation and lysis were monitored at 405 nm every 1 min at 37ºC, using SpectraMAX M2e microplate spectrophotometer (Molecular Devices Corporation, Sunnyvale, CA). The clot lysis time was defined as the time from peak to the half of the peak and bottom.[10]

Pulmonary Artery Visualization Using Micro-CT

After 3 weeks of exposure to hypoxia (10% O_2) or normoxia, mice were anesthetized with isoflurane (1.0%). A 25G needle was placed into the right ventricle of mice, and heparin (10 mg/kg body weight) was administered. Microfil (Flowtech) was used as a high-density vascular contrast agent, which was delivered via the needle placed in the right ventricle. The femoral artery was severed to allow drainage of the perfusate.[11] The lungs were removed from the mice and then fixed with 10% phosphate-buffered formalin for 24 h. The isolated lungs were then preserved with 70–100% concentration raised ethanol for 4 days. After dehydration by ethanol, the lungs were preserved with methyl salicylate for 24 h and were then left in open air for 24 h. The specimens were scanned by a micro-CT system (24–48 μm voxel size) (LCT200; Hitachi-Aloka, Tokyo, Japan). 3D micro-CT images were reconstructed by VG Studio MAX (Volume Graphics GmbH, Heidelberg, Germany).[12] The deficit of large pulmonary arteries detected by 3D-CT was considered as ‘obstruction of PA’.

Measurement of Cytokines/Chemokines and Growth Factors by Bioplex System

Cytokines/chemokines and growth factors secretion from PASMCs or whole lungs were measured with a Bioplex system (Bio-Rad, Tokyo, Japan) according to the manufacturer's instructions. We measured cytokines in conditioned medium from PASMCs (100-mm dish, 10 mL DMEM). To analyze the levels of cytokines/chemokines in lung tissues, pulmonary arteries were perfused with PBS and the circulating blood was completely removed. Lung tissues were homogenized with tissue protein extraction reagent (Pierce, Rockford, America) and centrifuged (4°C, 2,500g, 20 min), and thereafter, clear supernatants were standardized for total protein content using the BCA Protein Assay kit (Pierce, Rockford, America).[13] Plasma samples were collected using citrate acid from the inferior vena cava in mice under anesthesia, and then centrifuged (4°C, 1,000g, 15 min) and aliquots were immediately stored at -80°C. Mouse cytokines/chemokines and growth factors were measured with commercially available kits (Bio-Rad, 9-Plex, MD0-00000EL and 23-Plex, M60-009RDPD). Serum levels of cytokines/chemokines and growth factors in human samples were measured with commercially available kits (Bio-Rad, 27-Plex, #M50-0KCAF0Y and 21-Plex, #MF0-005KMII). Each experiment was performed in duplicate.

Bone Marrow Transplantation

Bone marrow (BM) transplantation was performed as previously described.[5,6,14,15] Briefly, recipient mice were lethally irradiated and received an intravenous injection of 5×10^6 donor GFP^+ BM cells suspended in 100 μL calcium- and magnesium-free PBS with 2% FBS. After transplantation, the mice were placed on a regular chow diet for 4 weeks followed by hypoxic exposure (10% O_2) for 3 weeks. Transgenic mice ubiquitously expressing GFP were obtained from Jackson Laboratory.

BM-Derived Cell Recruitment Assays

Whole lung imaging was performed 3 weeks after exposure to hypoxia (10% O_2) or normoxia. Animals were anesthetized with isoflurane (1.0%) and pulmonary arteries were perfused with PBS and perfusion-fixed with 4% phosphate-buffered paraformaldehyde at physiological pressure for 5 min. Whole lungs were viewed with an entity fluorescence microscope (Leica, MZ16FA) equipped with a digital camera. The whole heart and lungs were harvested, fixed for 6 h, embedded in OCT (Tissue-Tek; Miles Inc., Elkhart, Illinois, USA) and snap-frozen, and cross-sections (20 μm) were prepared. Migrating GFP^+ cells and pulmonary microvasculature were analyzed by labeling with a primary monoclonal antibody against αSMA and confocal microscopy (Zeiss, LSM780).

Primary Culture of Mouse PAECs

Mouse PAECs were isolated by digesting minced lung tissues with collagenase type 2 (GIBCO) for 45 min at 37 °C. Cells were suspended in 2 mL of cold PBS plus 0.1% bovine serum albumin, and incubated with CD31 microbeads (Miltenyi Biotec, Bergisch Gladbach, Germany). $CD31^+$ PAECs were selected by the Magnetic Cell Sorting System (Miltenyi Biotec, Bergisch Gladbach, Germany) according

to the manufacturer's instructions. PAECs of passage 4 to 5 at 80–90% confluence were used for experiments.

Human TAFI Plasmid

Human TAFI gene was cloned into the pBApo-CMV vector. Human PAECs were seeded in 24 well plate (10,000 cells/well) and were transfected with human TAFI DNA in OptiMEM™ medium and P3000™ regent. Two days after the transfection, TAFI expression in PAECs was quantified by Western blotting.[4]

RNA Isolation and Real-time PCR

Isolation of total RNA from human PAECs, human AoECs, and the liver of mice were performed using the RNeasy Plus Mini Kit (Qiagen) according to the manufacturer's protocol. Total RNA was converted to cDNA using PrimeScript RT Master Mix (Takara Bio Inc., Kusatsu). Primers for human *CPB2* (Primer Set ID: Hs00255533_m1), *CDH5* (Primer Set ID: HS00901465_m1), *PECAM1* (Primer Set ID: Hs01065282_m1), *F11R* (Primer Set ID: Hs00170991_m1), *TJP1* (Primer Set ID: HS01551861_m1), *VCAM1* (Primer Set ID: HS0100372_m1), *ICAM1* (Primer Set ID: HS00164932_m1), *NOS3* (Primer Set ID: Hs01574665_m1), *PTGIS* (Primer Set ID: Hs00919949_m1), *SERPINE1* (Primer Set ID: Hs01126606_m1), *PLAT* (Primer Set ID: Hs00263492_m1), *BMPR2* (Primer Set ID: Hs00176148_m1), *BAX* (Primer Set ID: Hs00180269_m1), *APLN* (Hs00936329_m1), *IL6* (Primer Set ID: Hs00985639_m1), *IL8* (Primer Set ID: Hs00174103_m1), *THBD* (Primer Set ID: HS00264920_s1), *HIF1A* (Primer Set ID: Hs00153153_m1), and *Hif1a* (Primer Set ID: Mm00468869_m1) were purchased from Life Technologies (TaqMan assays, Applied Biosystems, US). After reverse transcription, quantitative real-time PCR on the CFX 96 Real-Time PCR Detection System (Bio-Rad) was performed using either SsoFast Probes Supermix (Bio-Rad) for TaqMan probes. The Ct value determined by CFX Manager Software (version2.0, Bio-Rad) for all samples was normalized to housekeeping gene *Gapdh* and the relative fold change was computed by the ΔΔCt method.[16]

Western Blotting Analysis

Human PASMCs and $HepG_2$ cells were seeded in 100-mm dishes in DMEM with 10% FBS. PASMCs and $HepG_2$ were allowed to adhere for 24 h, washed two times and starved in serum-free medium for 24 h. Human PAECs were seeded in 6-well plates in EBM-2. PAECs were allowed to adhere for 24 h. PASMCs and PAECs were then stimulated with human TAFI protein (300 nM) (Haematologic technologies Inc.), vehicle, 5% plasma from CTEPH patients, or 5% plasma from controls for 24 h. The concentration of human TAFI protein was based on our previous paper demonstrating that plasma levels in CTEPH patients were around 300 nM.[17] $HepG_2$ were then exposed to normoxia or hypoxia (O_2 2%) with PPARα agonists, WY14643 (10-200 μM), GW0742 (10 μM), GW1927 (10 μM), fenofibrate (10 μM),

bezafibrate (10μM), clofibrate (10μM), or vehicle for 24 h. These cells were washed with cold PBS and lysed with cell lysis buffer (Cell Signaling) and protease inhibitor cocktail (Sigma-Aldrich) after the incubation period. Total cell lysates from lung and liver homogenates, human PASMCs, PAECs, and $HepG_2$ cells were loaded on the sodium dodecyl sulfate-polyacrylamide gel electrophoresis (SDS-PAGE) and transferred to polyvinylidene difluoride (PVDF) membranes (GE Healthcare), following blocking for 1 hour at room temperature in 5% bovine serum albumin in tris-buffered saline with Tween 20 (TBST).[16] The primary antibodies were as follows; α-tubulin (2000:1, Sigma), TAFI (1000:1, Abcam), VE-cadherin (1000:1, Cell Signaling Technology), phosphorylated-ERK1/2 (1000:1, Cell Signaling), total-ERK1/2 (1000:1, Cell Signaling), and caspase-3 (1000:1, Cell Signaling). The regions containing proteins were visualized by the enhanced chemiluminescence system (ECL Prime Western Blotting Detection Reagent, GE Healthcare, Buckinghamshire, UK). Densitometric analysis was performed by the Image J Software (NIH, Bethesda, USA).

Preparation of Conditioned Medium

Conditioned medium from PAECs treated with human TAFI protein (300 nM) (Haematologic technologies Inc.) or vehicle in EBM-2 were collected and filtered to remove cell debris. Likewise, conditioned medium was collected from PASMCs of TAFI-Tg mice and control mice exposed to normoxia or hypoxia (2% O_2) for 24 h, and from $HepG_2$ cells treated with WY14643 (10-200 μM), GW0742 (10 μM), GW1927 (10 μM), fenofibrate (10 μM), bezafibrate (10 μM), clofibrate (10 μM), or vehicle exposed to normoxia or hypoxia (2% O_2) in DMEM. Collected medium was concentrated 100-fold with an Amicon ultra filter (Millipore Corporation) to yield concentrated conditioned medium.[18,19]

Immunofluorescence Staining

Human PAECs were seeded in glass bottom dish (15,000 cells/well) in EBM-2 (Lonza). The next day, PAECs were stimulated with human TAFI protein (300 nM) (Haematologic Technologies Inc.) for 24 h and were then fixed with 4% phosphate-buffered paraformaldehyde. The antibody to VE-cadherin (Cell Signaling Technology, 1:500) was used for immunostaining. Slides were viewed with a fluorescence microscopy (LSM 780, Carl Zeiss, Oberkochen, Germany).

Seahorse Analyses

Human PAECs (25,000-50,000 cells per well) were plated in 24-well Seahorse XFe24 cell culture microplates and were incubated at 37ºC for 24 h. After substituting growth media with assay media (XF modified DMEM supplemented with 25 mM glucose and 1 mM sodium pyruvate for mitochondrial flux, XF minimal DMEM supplemented with 2 mM glutamine for glycolytic flux), cells were incubated in a CO_2-free incubator for equilibration prior to analyses. Oxygen consumption and extracellular acidification rates were measured using a Seahorse XFe24 Extracellular Flux Analyzer (Seahorse

Bioscience/Agilent Technologies, North Billerica, MA). For mitochondrial flux, three cycles of baseline measurements were performed, followed by three 8-minute cycles each after the addition of 2 μM oligomycin (inhibitor of ATP synthase), 2 μM FCCP (proton ionophore), and 2 μM antimycin A plus rotenone (mitochondrial complex III and complex I inhibitors, respectively). All data were normalized to total protein per well, and were expressed as mean pmol O_2 or mpH/minute/μg protein ± SEM.

Permeability Assay

Human PAECs and human AoECs monolayer permeability were examined using an *in vitro* vascular permeability 96-well assay kit (Merck Millipore) according to the manufacturer's instructions. PAECs were seeded and transfected with thrombomodulin, VE-cadherin, or control siRNA (10 nmol/l) (QIAGEN, Germany) for 72 h. PAECs were then stimulated with TAFI protein purified from human plasma (300 nM) (Haematologic Technologies Inc.), vehicle, plasma from CTEPH patients or controls for 24 h. Monolayer permeability was determined by addition of a high molecular weight FITC-dextran (Merck Millipore) and subsequent measurement of fluorescence intensity using SpectraMAX M2e microplate spectrophotometer (Molecular Devices Corporation, Sunnyvale, CA). Fluorescence intensity was measured in duplicate per condition and was normalized to untreated control cells.

Pulmonary Vascular Permeability

To evaluate pulmonary vascular permeability *in vivo*, we injected FITC-conjugated dextran (Sigma-Aldrich) through the inferior vena cava 2 h before the fixation of the whole lungs as previously described.[20] The lungs were removed and fixed with 4% phosphate-buffered paraformaldehyde for 6 h, embedded in OCT (Tissue-Tek; Miles Inc., Elkhart, Illinois, USA), snap-frozen, and cross-sections (20 μm) were prepared. Perivascular leak of FITC-conjugated dextran, which reflects vascular permeability, was detected by immunostaining for VE-cadherin with a confocal microscopy (Zeiss, LSM780). The fluorescence intensity was evaluated by Image J.

Harvest of Mouse PASMCs

Mouse PASMCs were cultured from each group of 23–26 g male mice and maintained in DMEM containing 10% FBS at 37°C in a humidified atmosphere of 5% CO2 and 95% air as previously described.[2] Passage 4 to 7 PASMCs at 70–80% confluence was used for experiments.

Cell Proliferation Assay

Human PASMCs were purchased from Lonza (Basel, Switzerland). Mouse PASMCs were harvested from TAFI-Tg and littermate control mice. PASMCs were seeded in 96-well plates (5,000 cells/well) in DMEM with 10% FBS. On the next day, PASMCs were starved for 24 h. Then, human PASMCs were stimulated with TAFI protein purified from human plasma (300 nM) (Haematologic Technologies Inc.),

vehicle, 5% plasma from CTEPH patients or controls for up to 4 days. Mouse PASMCs were cultured with 10% FBS for up to 4 days. Cell proliferation was measured by the Cell-Titer 96 AQueous One Solution Cell Proliferation Assay kit (Promega, Madison, USA).[21]

Tube Formation Assay

Sterile 96-well plates coated with Matrigel were incubated at 37°C for 30 min to form gels. After polymerization of the gels, human PAECs obtained from Lonza (Basel, Switzerland) were seeded in each well (50,000 cells/well) and incubated with EBM-2 basal medium containing 1% FBS and TAFI (300 nM) for 12 h. Six different fields in each well were randomly selected for the analyses with Image J Software.

Flow Cytometry

After 3 weeks of hypoxia, lungs were perfused with cold PBS to remove blood in the circulation and were sliced into small pieces in digestion buffer containing 0.1% collagenase II (GIBCO), which were incubated at 37°C for 20 min. After the incubation, lung tissues were further divided into smaller pieces by pipetting. Then, lung cell suspensions were filtered through a 70 μm filter and washed twice in stain buffer (BD Pharmingen) prior to staining for analysis using a BS Cantos II flow cytometer (BD Biosciences). Lung cell suspensions were pelleted and suspended in stain buffer containing rat anti-mouse CD16/CD32 (BD Pharmingen), PE-conjugated rat anti-mouse CD11b (BD Pharmingen), APC-conjugated rat anti-mouse Ly-6G IgG2a (BD Pharmingen), FITC-conjugated rat anti-mouse CD45 (BD Pharmingen), PE-conjugated rat monoclonal IgG2b (BD Pharmingen), APC-conjugated rat monoclonal IgG2a (BD Pharmingen), and FITC-conjugated rat monoclonal IgG2b (BD Pharmingen) for 20 min at 4°C. Cell suspensions were washed prior to resuspension for FACS analysis. For all flow cytometry studies, data were collected and visualized using FACSDiva software (BD Biosciences).

Treatment with a TAFIa Inhibitor and PPARα Agonists

Eight-week-old male TAFI-Tg and control mice were randomized to be treated with either WY14643 (3 mg/kg/day), fenofibrate (50 mg/kg/day), or vehicle in feed and were exposed to hypoxia (10% O_2) for 3 weeks. CPI (TAFIa inhibitor) was purchased from the Sigma and infused through the tail vein (5 mg/kg/day) as previously described.[22] After 3 weeks of hypoxia, RVSP, RVH, and thrombus formation were measured as previously described.[23,24]

Rat Models

Male Sprague-Dawley rats (250–350g) (strain 400, Charles River) were used. All the hemodynamic measurements were performed blinded to the condition. For the Sugen/hypoxia model, rats were injected with SU5416 (Sigma, 20 mg/kg) and exposed to hypoxia (10% O_2) for 3 weeks. For the

monocrotaline-induced PH model, rats were subcutaneously injected with monocrotaline (Sigma, 60 mg/kg) as previously described.[25] All rats underwent hemodynamic measurements with SciScence catheters to measure RVSP as previously described.[25] In both models, rats were treated with WY14643 (3 mg/kg/day) or vehicle by mixed feed.

Statistical Analyses

All results are shown as mean±SEM. Comparisons of means between 2 groups were performed by unpaired Student's *t*-test. Comparisons of mean responses associated with the two main effects of the different genotypes and the severity of pulmonary vascular remodeling were performed by two-way analysis of variance (ANOVA) with interaction terms, followed by Tukey's HSD (honestly significant difference) for multiple comparisons. The relation between plasma TAFIa levels and endothelial permeability or PASMC proliferation were analyzed with Pearson's rank correlation coefficient. The survival rates of TAFI-Tg and control mice during hypoxic exposure were analyzed with the log-rank test. Statistical significance was evaluated with JMP 12 (SAS Institute Inc., Cary, America) or R version 3.3.2 (http://www.R-project.org/). The time-dependent data were analyzed by repeated-measures linear mixed-effect model with lmer 1.1-12 and lmerTest 2.0-33 packages of R. The ratio of fully muscularized vessels was analyzed by the Poisson regression with the offset equals to the sum of total vessels with multcomp 1.4-6 package or R. All reported P values are 2-tailed, with a P value of less than 0.05 indicating statistical significance.[2,7]

Supplementary References

1. Galie N, Humbert M, Vachiery JL, Gibbs S, Lang I, Torbicki A, Simonneau G, Peacock A, Vonk Noordegraaf A, Beghetti M, Ghofrani A, Gomez Sanchez MA, Hansmann G, Klepetko W, Lancellotti P, Matucci M, McDonagh T, Pierard LA, Trindade PT, Zompatori M, Hoeper M, Aboyans V, Vaz Carneiro A, Achenbach S, Agewall S, Allanore Y, Asteggiano R, Paolo Badano L, Albert Barbera J, Bouvaist H, Bueno H, Byrne RA, Carerj S, Castro G, Erol C, Falk V, Funck-Brentano C, Gorenflo M, Granton J, Iung B, Kiely DG, Kirchhof P, Kjellstrom B, Landmesser U, Lekakis J, Lionis C, Lip GY, Orfanos SE, Park MH, Piepoli MF, Ponikowski P, Revel MP, Rigau D, Rosenkranz S, Voller H, Luis Zamorano J. 2015 ESC/ERS Guidelines for the diagnosis and treatment of pulmonary hypertension: The Joint Task Force for the Diagnosis and Treatment of Pulmonary Hypertension of the European Society of Cardiology (ESC) and the European Respiratory Society (ERS): Endorsed by: Association for European Paediatric and Congenital Cardiology (AEPC), International Society for Heart and Lung Transplantation (ISHLT). *Eur Heart J*. 2016;37:67-119.
2. Satoh K, Satoh T, Kikuchi N, Omura J, Kurosawa R, Suzuki K, Sugimura K, Aoki T, Nochioka K, Tatebe S, Miyamichi-Yamamoto S, Miura M, Shimizu T, Ikeda S, Yaoita N, Fukumoto Y, Minami T, Miyata S, Nakamura K, Ito H, Kadomatsu K, Shimokawa H. Basigin mediates pulmonary hypertension by promoting inflammation and vascular smooth muscle cell proliferation. *Circ Res*. 2014;115:738-750.
3. Nagashima M, Yin ZF, Zhao L, White K, Zhu YH, Lasky N, Halks-Miller M, Broze GJ, Fay WP, Morser J. Thrombin-activatable fibrinolysis inhibitor (TAFI) deficiency is compatible with murine life. *J Clin Invest*. 2002;109:101-110.
4. Ishikura K, Misu H, Kumazaki M, Takayama H, Matsuzawa-Nagata N, Tajima N, Chikamoto K, Lan F, Ando H, Ota T, Sakurai M, Takeshita Y, Kato K, Fujimura A, Miyamoto K, Saito Y, Kameo S, Okamoto Y, Takuwa Y, Takahashi K, Kidoya H, Takakura N, Kaneko S, Takamura T. Selenoprotein P as a diabetes-associated hepatokine that impairs angiogenesis by inducing VEGF resistance in vascular endothelial cells. *Diabetologia*. 2014;57:1968-1976.
5. Satoh K, Fukumoto Y, Nakano M, Sugimura K, Nawata J, Demachi J, Karibe A, Kagaya Y, Ishii N, Sugamura K, Shimokawa H. Statin ameliorates hypoxia-induced pulmonary hypertension associated with down-regulated stromal cell-derived factor-1. *Cardiovasc Res*. 2009;81:226-234.
6. Satoh K, Kagaya Y, Nakano M, Ito Y, Ohta J, Tada H, Karibe A, Minegishi N, Suzuki N, Yamamoto M, Ono M, Watanabe J, Shirato K, Ishii N, Sugamura K, Shimokawa H. Important role of endogenous erythropoietin system in recruitment of endothelial progenitor cells in hypoxia-induced pulmonary hypertension in mice. *Circulation*. 2006;113:1442-1450.
7. Shimizu T, Fukumoto Y, Tanaka S, Satoh K, Ikeda S, Shimokawa H. Crucial role of ROCK2 in

vascular smooth muscle cells for hypoxia-induced pulmonary hypertension in mice. *Arterioscler Thromb Vasc Biol*. 2013;33:2780-2791.

8. Hijazi N, Abu Fanne R, Abramovitch R, Yarovoi S, Higazi M, Abdeen S, Basheer M, Maraga E, Cines DB, Higazi AA. Endogenous plasminogen activators mediate progressive intracerebral hemorrhage after traumatic brain injury in mice. *Blood*. 2015;125:2558-2567.
9. Zhao L, Buckman B, Seto M, Morser J, Nagashima M. Mutations in the substrate binding site of thrombin-activatable fibrinolysis inhibitor (TAFI) alter its substrate specificity. *J Biol Chem*. 2003;278:32359-32366.
10. Carrieri C, Galasso R, Semeraro F, Ammollo CT, Semeraro N, Colucci M. The role of thrombin activatable fibrinolysis inhibitor and factor XI in platelet-mediated fibrinolysis resistance: a thromboelastographic study in whole blood. *J Thromb Haemost*. 2011;9:154-162.
11. Counter WB, Wang IQ, Farncombe TH, Labiris NR. Airway and pulmonary vascular measurements using contrast-enhanced micro-CT in rodents. *Am J Physiol Lung Cell Mol Physiol*. 2013;304:L831-843.
12. Nishimiya K, Matsumoto Y, Shindo T, Hanawa K, Hasebe Y, Tsuburaya R, Shiroto T, Takahashi J, Ito K, Ishibashi-Ueda H, Yasuda S, Shimokawa H. Association of adventitial vasa vasorum and inflammation with coronary hyperconstriction after drug-eluting stent implantation in pigs in vivo. *Circ J*. 2015;79:1787-1798.
13. Nakano M, Satoh K, Fukumoto Y, Ito Y, Kagaya Y, Ishii N, Sugamura K, Shimokawa H. Important role of erythropoietin receptor to promote VEGF expression and angiogenesis in peripheral ischemia in mice. *Circ Res*. 2007;100:662-669.
14. Nigro P, Satoh K, O'Dell MR, Soe NN, Cui Z, Mohan A, Abe J, Alexis JD, Sparks JD, Berk BC. Cyclophilin A is an inflammatory mediator that promotes atherosclerosis in apolipoprotein E-deficient mice. *J Exp Med*. 2011;208:53-66.
15. Satoh K, Nigro P, Matoba T, O'Dell MR, Cui Z, Shi X, Mohan A, Yan C, Abe J, Illig KA, Berk BC. Cyclophilin A enhances vascular oxidative stress and the development of angiotensin II-induced aortic aneurysms. *Nat Med*. 2009;15:649-656.
16. Ikeda S, Satoh K, Kikuchi N, Miyata S, Suzuki K, Omura J, Shimizu T, Kobayashi K, Kobayashi K, Fukumoto Y, Sakata Y, Shimokawa H. Crucial role of Rho-kinase in pressure overload-induced right ventricular hypertrophy and dysfunction in mice. *Arterioscler Thromb Vasc Biol*. 2014;34:1260-1271.
17. Yaoita N, Satoh K, Satoh T, Sugimura K, Tatebe S, Yamamoto S, Aoki T, Miura M, Miyata S, Kawamura T, Horiuchi H, Fukumoto Y, Shimokawa H. Thrombin-activatable fibrinolysis inhibitor in chronic thromboembolic pulmonary hypertension. *Arterioscler Thromb Vasc Biol*. 2016;36:1293-1301.
18. Satoh K, Matoba T, Suzuki J, O'Dell MR, Nigro P, Cui Z, Mohan A, Pan S, Li L, Jin ZG, Yan C,

Abe J, Berk BC. Cyclophilin A mediates vascular remodeling by promoting inflammation and vascular smooth muscle cell proliferation. *Circulation*. 2008;117:3088-3098.

19. Suzuki J, Jin ZG, Meoli DF, Matoba T, Berk BC. Cyclophilin A is secreted by a vesicular pathway in vascular smooth muscle cells. *Circ Res*. 2006;98:811-817.
20. Yang B, Cai B, Deng P, Wu X, Guan Y, Zhang B, Cai W, Schaper J, Schaper W. Nitric oxide increases arterial endotheial permeability through mediating VE-cadherin expression during arteriogenesis. *PLoS One*. 2015;10:e0127931.
21. Suzuki K, Satoh K, Ikeda S, Sunamura S, Otsuki T, Satoh T, Kikuchi N, Omura J, Kurosawa R, Nogi M, Numano K, Sugimura K, Aoki T, Tatebe S, Miyata S, Mukherjee R, Spinale FG, Kadomatsu K, Shimokawa H. Basigin promotes cardiac fibrosis and failure in response to chronic pressure overload in mice. *Arterioscler Thromb Vasc Biol*. 2016;36:636-646.
22. Wang X, Smith PL, Hsu MY, Tamasi JA, Bird E, Schumacher WA. Deficiency in thrombin-activatable fibrinolysis inhibitor (TAFI) protected mice from ferric chloride-induced vena cava thrombosis. *J Thromb Thrombolysis*. 2007;23:41-49.
23. Barbosa-da-Silva S, Souza-Mello V, Magliano DC, Marinho Tde S, Aguila MB, Mandarim-de-Lacerda CA. Singular effects of PPAR agonists on nonalcoholic fatty liver disease of diet-induced obese mice. *Life Sci*. 2015;127:73-81.
24. Lebeck J, Cheema MU, Skowronski MT, Nielsen S, Praetorius J. Hepatic AQP9 expression in male rats is reduced in response to PPARα agonist treatment. *Am J Physiol Gastrointest Liver Physiol*. 2015;308:G198-205.
25. Meloche J, Pflieger A, Vaillancourt M, Paulin R, Potus F, Zervopoulos S, Graydon C, Courboulin A, Breuils-Bonnet S, Tremblay E, Couture C, Michelakis ED, Provencher S, Bonnet S. Role for DNA damage signaling in pulmonary arterial hypertension. *Circulation*. 2014;129:786-797.

Supplementary Table I. Clinical Information

	Control (*n*=13)	PAH (*n*=22)	CTEPH (*n*=32)
Clinical characteristics			
Age (years-old)	59.6±3.2	41.0±4.3	56.9±1.4
Male sex, n (%)	3 (23.1)	3 (13.6)	4 (12.5)
White blood cell, $\times10^4/\mu L$	7.2±0.5	6.2±0.4	6.1±0.4
Red blood cell, $\times10^4/\mu L$	427±11	452±11	428±10
Hemoglobin, g/dL	13.1±0.4	13.3±0.3	13.1±0.3
Platelet, $\times10^3/\mu L$	242±13	298±9	235±12
D-dimer, μg/mL	0.8±0.1	0.6±0.1	1.0±0.2
BNP, pg/mL	17±3	87±22*	75±34*
NYHA class, n (%)			
I	–	5 (22.7)	7 (21.9)
II	–	12 (54.5)	21 (65.7)
III	–	5 (22.7)	3 (9.4)
IV	–	0	1 (6.2)
Medication			
Epoprostenol, n (%)	–	5 (22.7)	2 (6.3)
Oral PGI_2 analogue, n (%)	–	8 (36.3)	17 (53.1)
Endothelin receptor antagonist, n (%)	–	11 (50.0)	9 (28.1)
PDE5 inhibitor, n (%)	–	12 (54.5)	15 (46.9)
Warfarin, n (%)	–	12 (54.5)	29 (90.6)†
Hemodynamic data			
Mean RAP, mmHg	4.7±1.0	6.9±0.6	5.1±0.3
Mean PAP, mmHg	18.1±1.0	41.4±2.5*	49.4±1.1*
PCWP, mmHg	7.8±0.7	9.0±0.6	8.9±0.3
Mean BP, mmHg	99±5.0	106±2.9	82±1.4
PVR, $dyn\times s/cm^5$	191±7	548±77*	464±23*
SVR, $dyn\times s/cm^5$	1388±171	1290±87	1452±44
CI, $L/min/m^2$	3.6±0.2	2.8±0.1*	2.7±0.1*

Results are expressed as mean ±SEM. *P<0.05 compared with non-PH, †P<0.05 compared with PAH. BNP, brain natriuretic peptide; BP, blood pressure; CI, cardiac index; NYHA, New York heart association; PAP, pulmonary artery pressure; PCWP, pulmonary capillary wedge pressure; PDE, phosphodiesterase; PGI_2, prostaglandin I_2; PVR, pulmonary vascular resistance; RAP, right atrial pressure; SVR, systemic vascular resistance.

Supplementary Table II. Baseline Characteristics of TAFI Overexpressing (TAFI-Tg) Mice

	Control (*n*=6)	TAFI-Tg (*n*=6)	P value
Blood test			
White blood cell ($\times 10^4/\mu L$)	4.6±1.5	5.1±0.9	n.s.
Red blood cell ($\times 10^4/\mu L$)	9.7±0.1	9.8±0.1	n.s.
Hemoglobin (g/dL)	15.5±0.1	15.8±0.3	n.s.
Hematocrit	43.9±0.3	44.9±0.6	n.s.
Platelet ($\times 10^3/\mu L$)	321±61	353±35	n.s.
Fibrinogen (mg/dL)	209±35	247±66	n.s.
aPTT (sec)	27.3±1.2	28.4±1.6	n.s.
PT (sec)	8.5±0.3	8.4±0.2	n.s.
Blood pressure (mmHg)	102±9.0	108±11.7	n.s.
Bleeding test			
bleeding time (sec)	91.2±8.3	92.7±9.3	n.s.
bleeding volume (mg)	5.9±0.7	6.0±2.3	n.s.
Body weight (g)	22.3±0.4	21.4±0.6	n.s.
Organ weight/ BW (mg/g)			
Lung/BW	7.5±0.3	7.2±0.5	n.s.
Heart/BW	7.8±0.4	7.6±0.5	n.s.
Liver/BW	47.7±2.1	45.0±1.5	n.s.
Spleen/BW	4.6±0.1	4.6±0.2	n.s.
Kidney/BW	14.6±0.7	13.6±0.5	n.s.

Results are expressed as mean±SEM. Tg, transgenic; aPTT, activated partial thromboplastin time; PT, prothrombin time; BW, body weight; n.s., not significant.

Supplementary Table III. Complete Blood Count of the Chimeric Mice

	Cpb2$^{+/+}$ with *Cpb2*$^{+/+}$ BM (*n*=14)	*Cpb2*$^{+/+}$ with *Cpb2*$^{-/-}$ BM (*n*=14)	P value
Blood test			
White blood cell ($\times 10^4/\mu L$)	6.3±0.5	6.4±0.5	n.s.
Red blood cell ($\times 10^4/\mu L$)	9.2±0.2	9.1±0.1	n.s.
Hemoglobin (g/dL)	13.6±0.3	13.0±0.3	n.s.
Hematocrit (%)	42.2±0.9	43.0±1.2	n.s.
Platelet ($\times 10^3/\mu L$)	383±52	363.5±52	n.s.

Results are expressed as mean±SEM. BM, bone marrow; n.s., not significant.

Supplementary Figure I

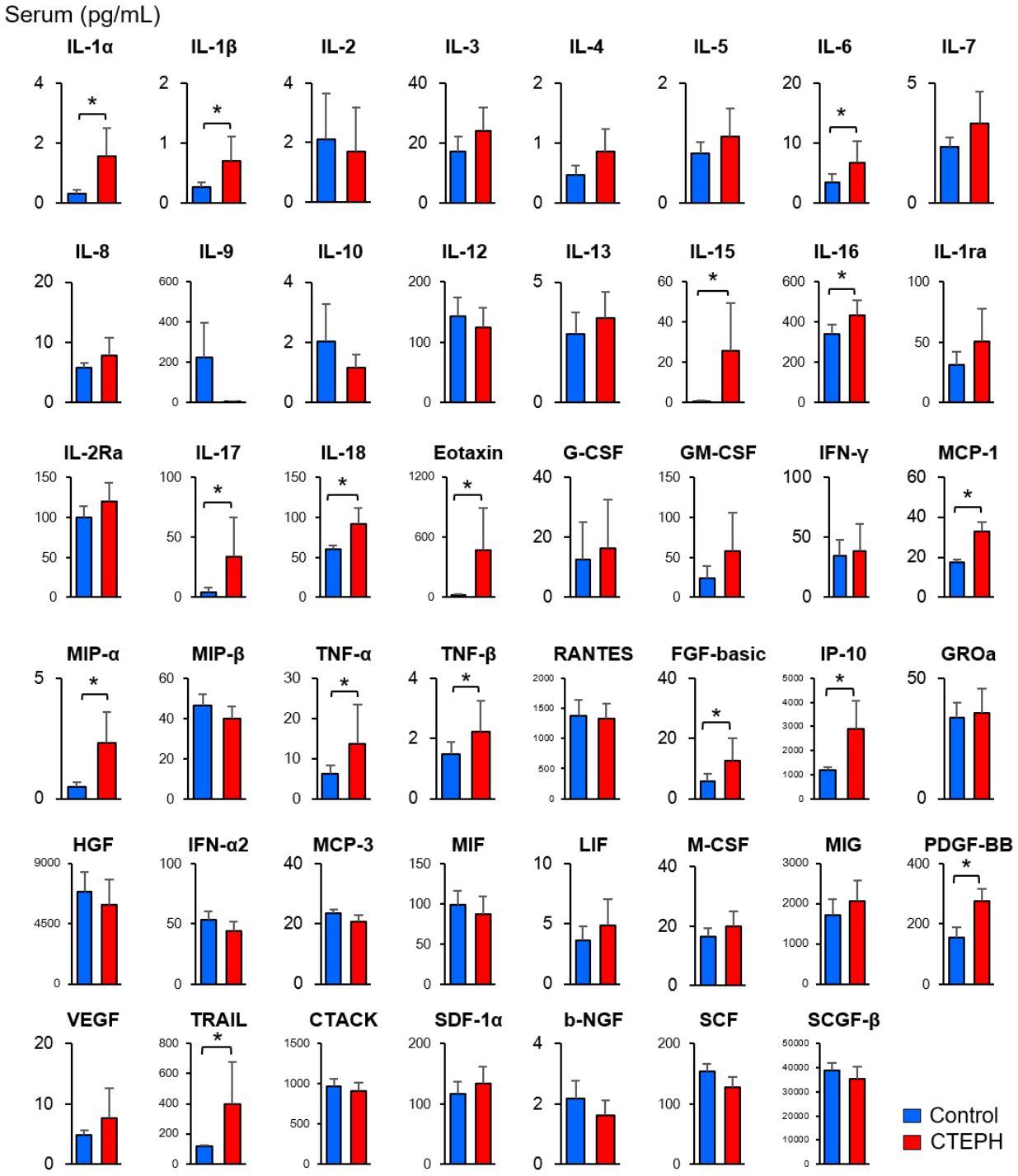

Supplementary Figure I. Serum Levels of Cytokines/Chemokines and Growth Factors in CTEPH Patients. Serum levels of cytokines/chemokines and growth factors in CTEPH patients (n=32) and controls (n=13). Results are expressed as mean±SEM. *P<0.05.

Supplementary Figure II

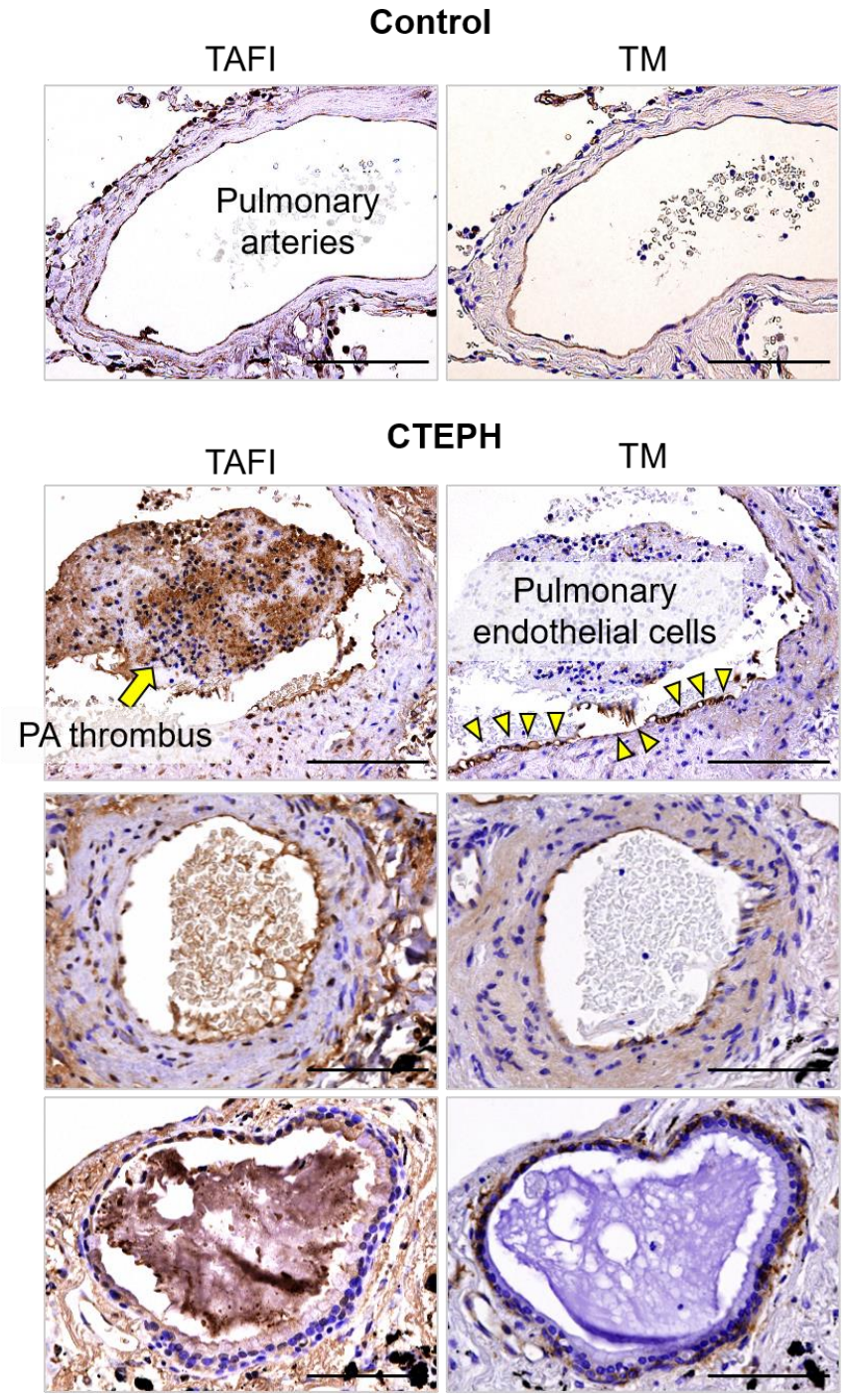

Supplementary Figure II. Higher Expression of TAFI and Thrombomodulin in Distal Pulmonary Arteries in CTEPH Patients.

Representative immunostaining of lung sections for thrombin-activatable fibrinolysis inhibitor (TAFI) and thrombomodulin (TM) in CTEPH patients and controls. Scale bars, 50 μm.

Supplementary Figure III

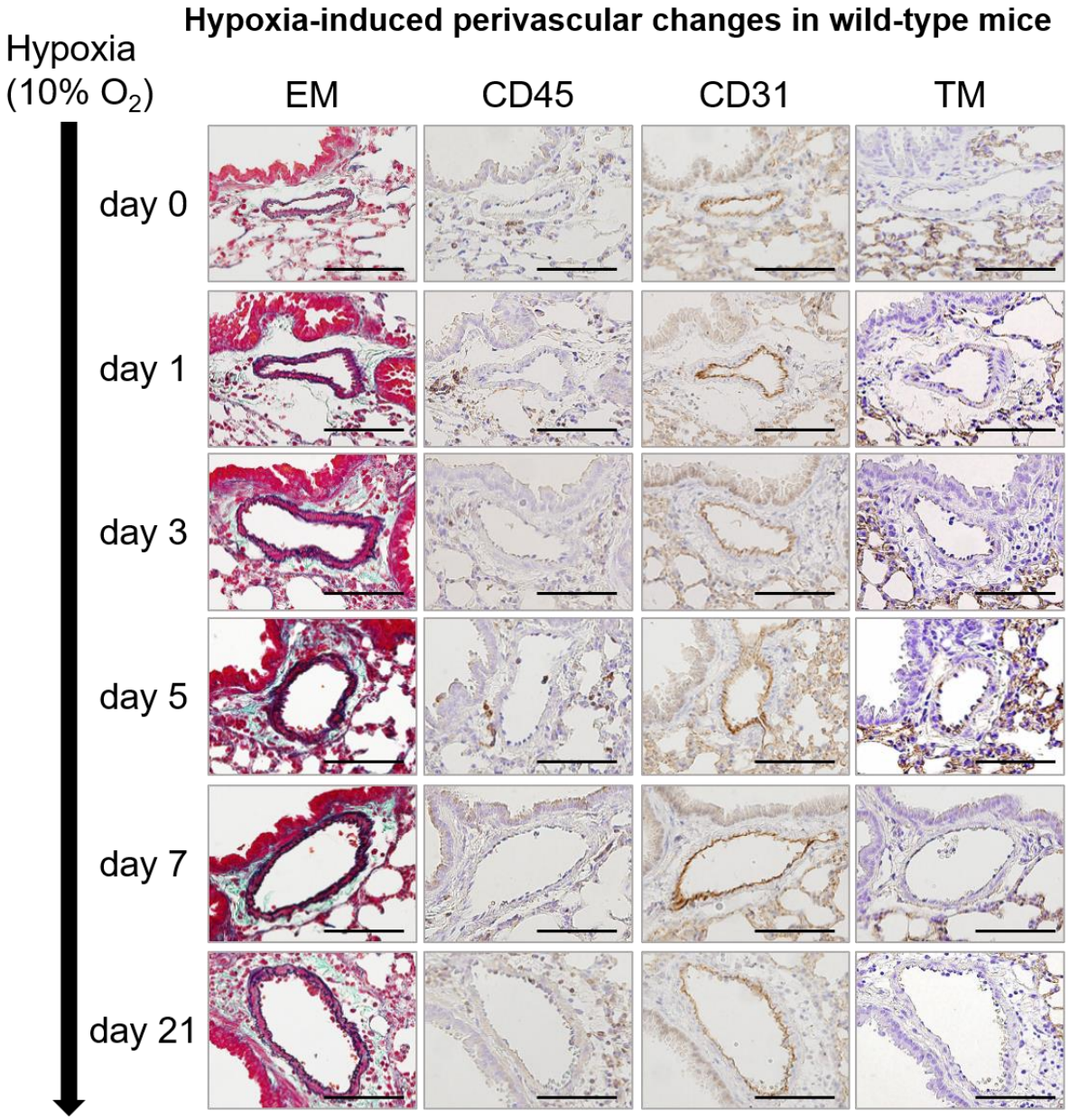

Supplementary Figure III. Higher Expression of Thrombomodulin in Distal Pulmonary Arteries in Hypoxic Mice.

Representative staining of lung sections for Elastica-Masson (EM), CD45, CD31, and thrombomodulin (TM) after hypoxic exposure (10% O_2) of wild-type mice for 0, 1, 3, 5, 7, and 21 days. EM, Elastica-masson staining; TM, Thrombomodulin. Scale bars, 50 μm.

Supplementary Figure IV

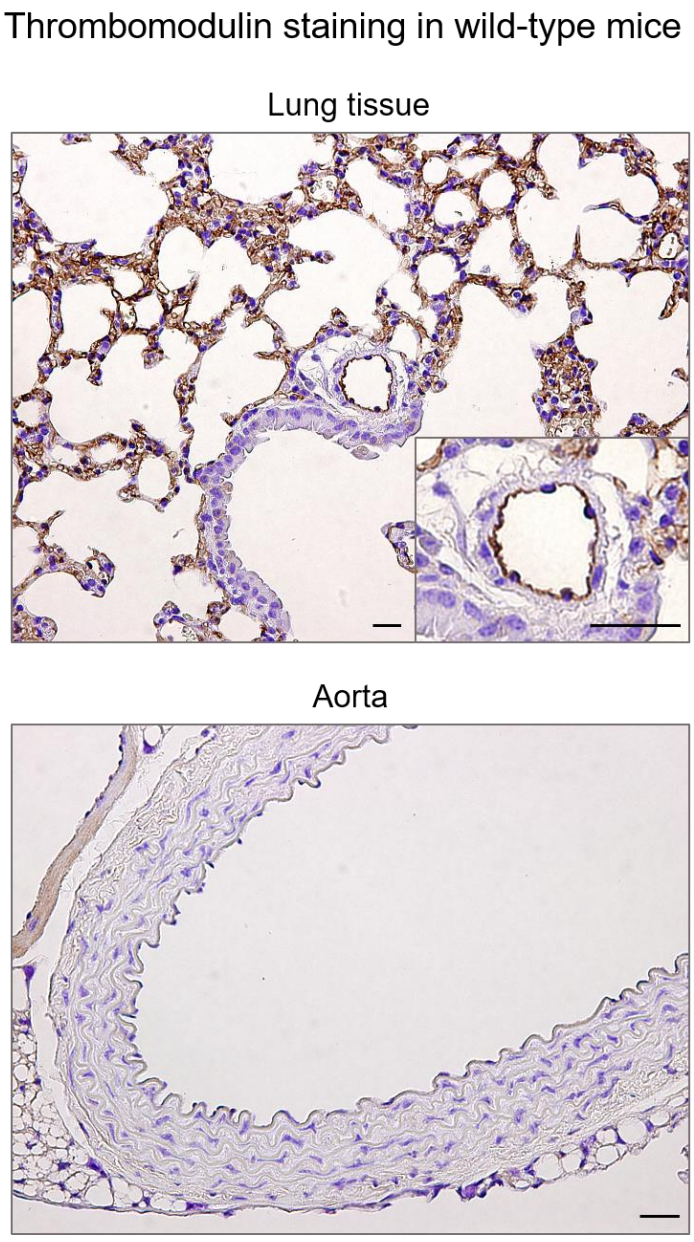

Supplementary Figure IV. Thrombomodulin Expression in Distal Pulmonary Artery and Aorta in Mice.

Representative thrombomodulin (TM) staining of the lung and the aorta in wild-type mice. Scale bars, 50 μm.

Supplementary Figure V

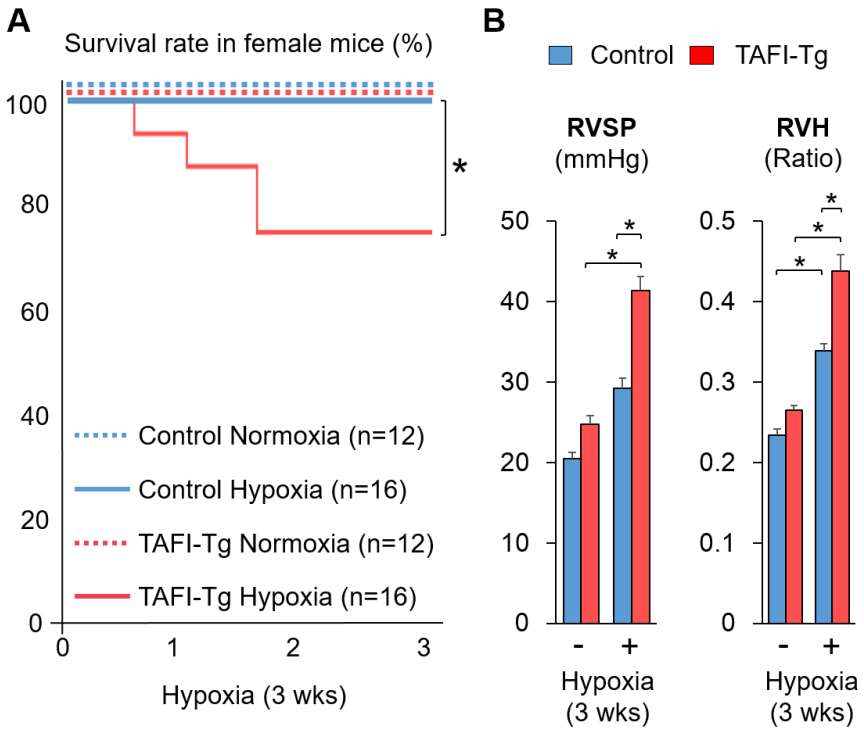

Supplementary Figure V. TAFI Overexpression Promotes Hypoxia-induced PH in Female Mice. (**A**) Survival rate of systemic TAFI-overexpressing female mice (TAFI-Tg) and control female mice exposed to normoxia (*n*=12 each) or hypoxia (10% O_2) for 3 weeks (*n*=16 each). Results are expressed as log-rank test. (**B**) Right ventricular systolic pressure (RVSP) and right ventricular hypertrophy (RVH) in TAFI-Tg female mice and control female mice exposed to normoxia (*n*=12 each) or hypoxia (10% O_2) for 3 weeks (*n*=12 each). Results are expressed as mean±SEM. **P*<0.05, ***P*<0.01.

Supplementary Figure VI

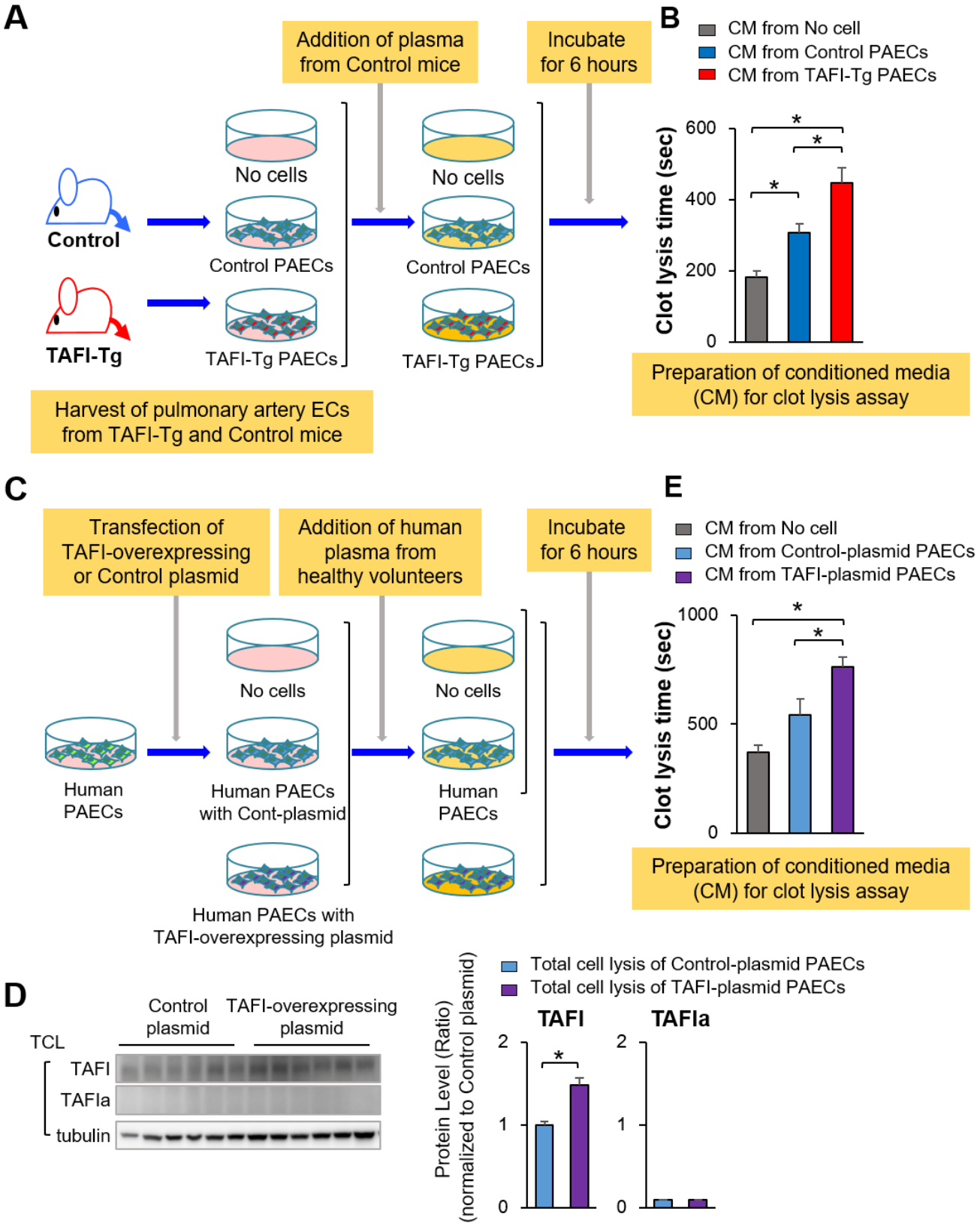

Supplementary Figure VI. ***In Situ*** **Plasma Clot Lysis Assay.**

(**A**) Protocol for plasma clot lysis assay using primary cultured mouse pulmonary artery endothelial cells (PAECs) from TAFI-Tg and control mice. (**B**) Quantification of plasma clot lysis time in TAFI-Tg PAECs, control PAECs, and controls (no cells) (*n*=6 each). (**C**) Protocol for plasma clot lysis assay using human PAECs transfected with human TAFI or control. (**D**) Representative Western blot and quantification of TAFI and TAFIa in PAECs transfected with TAFI or control (*n*=6 samples per group). (**E**) Quantification of plasma clot lysis time in PAECs transfected with TAFI or control (*n*=6 each). Results are expressed as mean±SEM. **P*<0.05.

Supplementary Figure VII

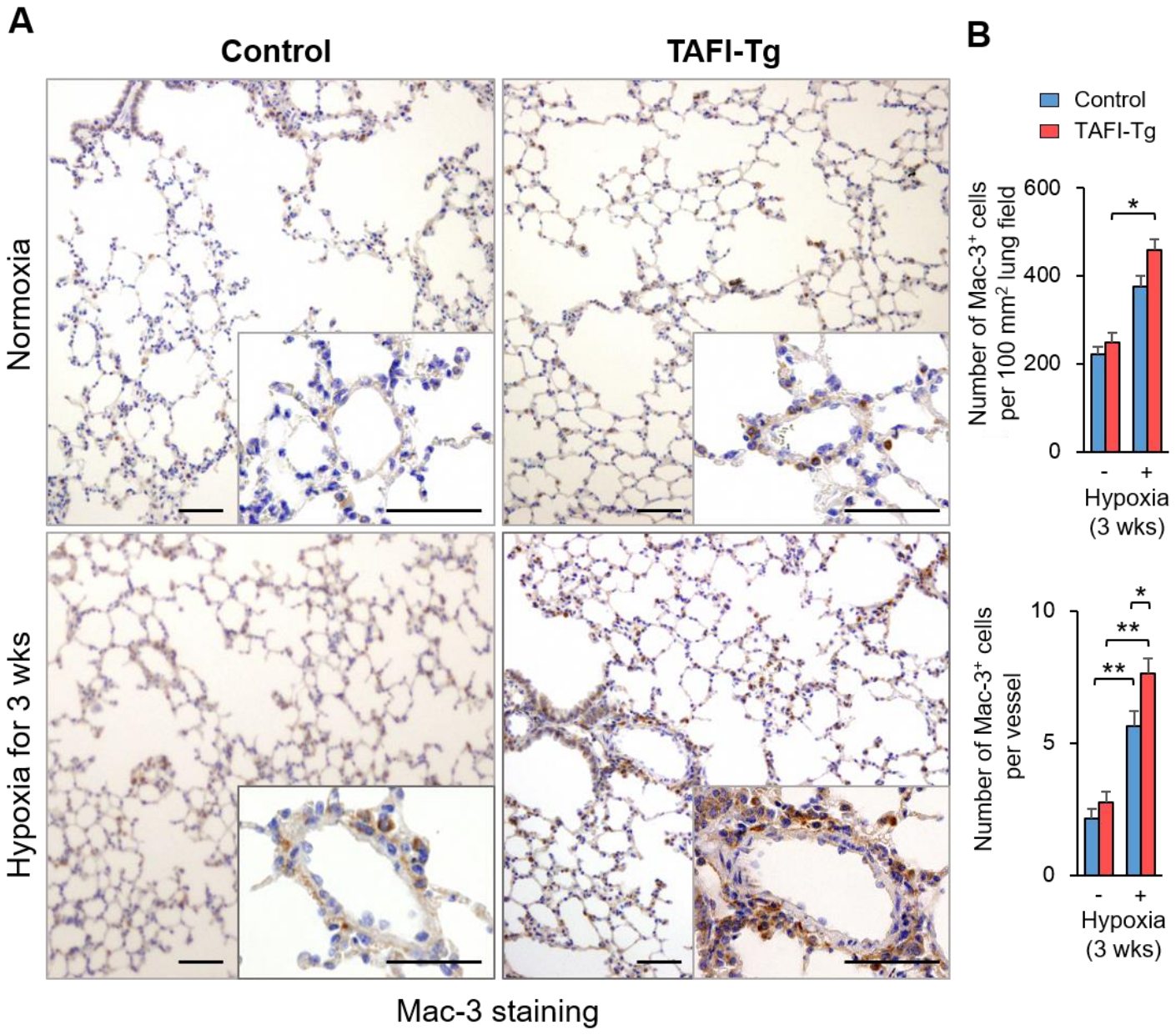

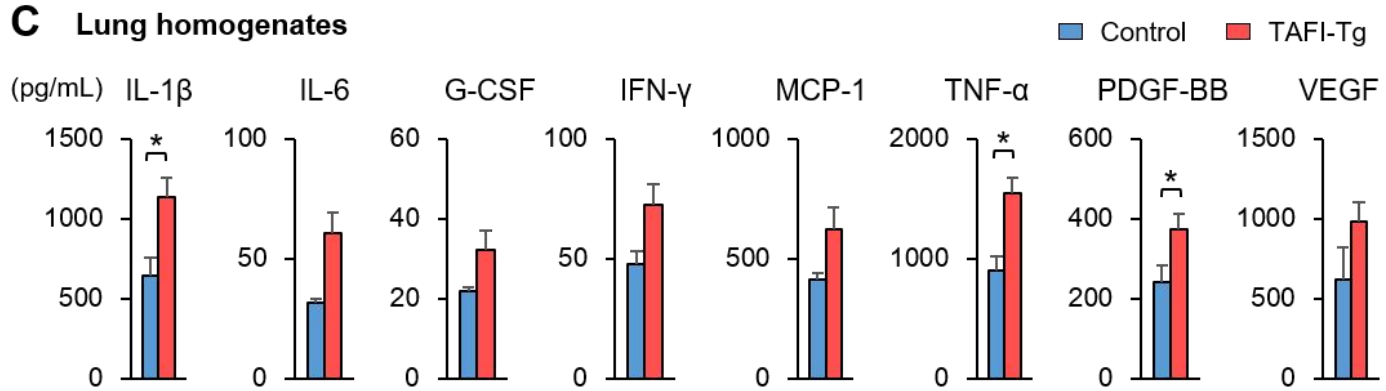

Supplementary Figure VII. TAFI Causes Inflammation in Mouse Lungs.

(**A**) Representative immunostaining for Mac-3 (CD107b) of the distal pulmonary arteries (PA) in TAFI-Tg and control mice exposed to normoxia or hypoxia (10% O_2) for 3 weeks. Scale bars, 50 μm. (**B**) Quantification of Mac-3^+ cells per 100 mm^2 lung field and vessel in TAFI-Tg and control mice exposed to normoxia (*n*=19 each) or hypoxia (10% O_2) for 3 weeks (TAFI-Tg, *n*=14; controls, n=21). (**C**) Quantification of protein levels of inflammatory cytokines (IL-1β, IL-6, MCP-1, TNF-α, G-CSF, IFN-γ, PDGF-BB, and VEGF) in lung homogenates of TAFI-Tg and control mice exposed to hypoxia (10% O_2) for 3 weeks (*n*=4 each). Results are expressed as mean±SEM. **P*<0.05, ***P*<0.01. Comparisons of parameters were performed with the unpaired Student's *t*-test or two-way ANOVA followed by Tukey's HSD test for multiple comparisons.

Supplementary Figure VIII

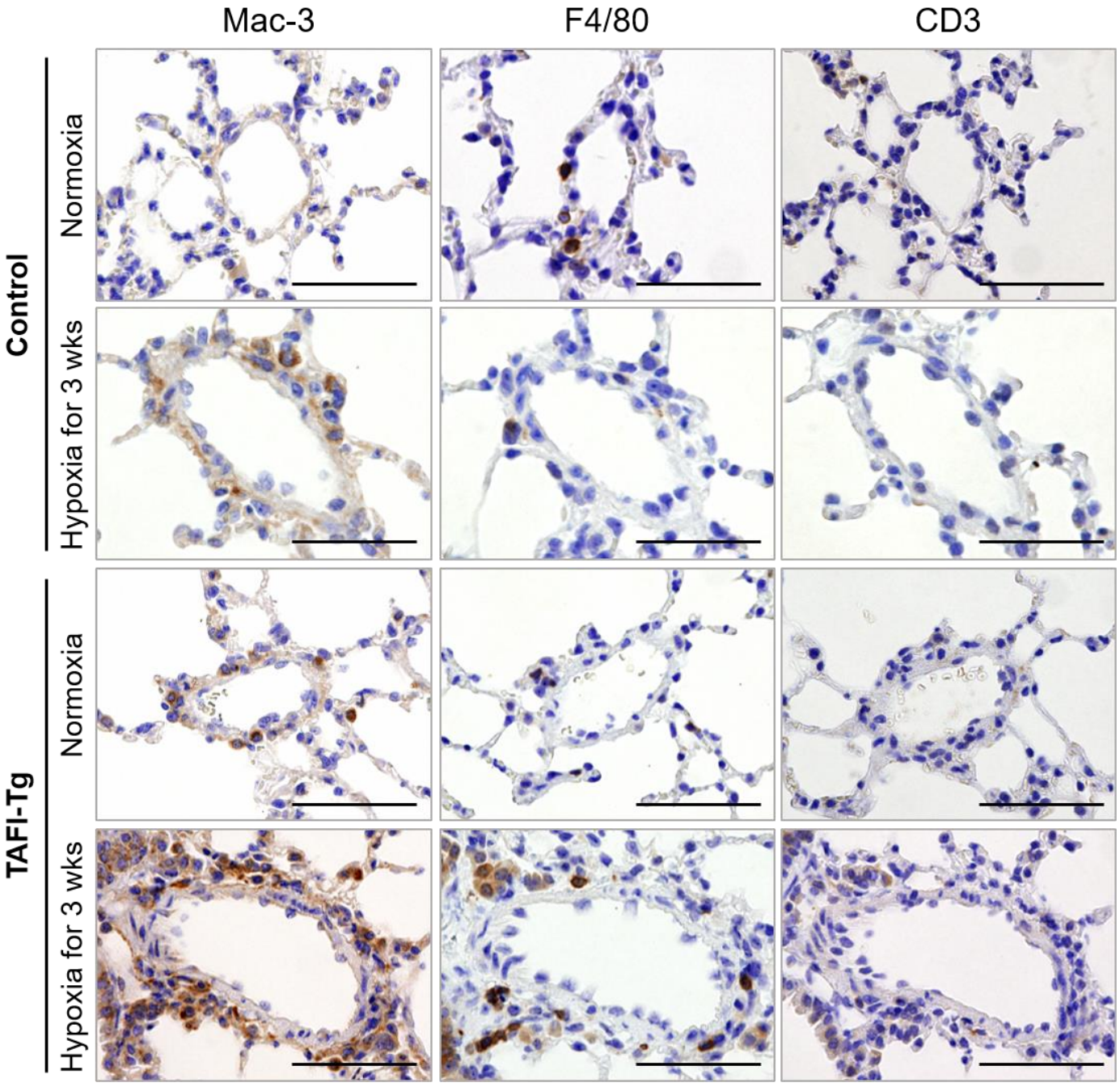

Supplementary Figure VIII. Perivascular Inflammatory Cells in Distal Pulmonary Arteries.
Representative images of Mac3, F4/80, and CD3 stainings of distal pulmonary arteries in TAFI-Tg and control mice exposed to normoxia or hypoxia for 3weeks. Scale bar 50 μm.

Supplementary Figure IX

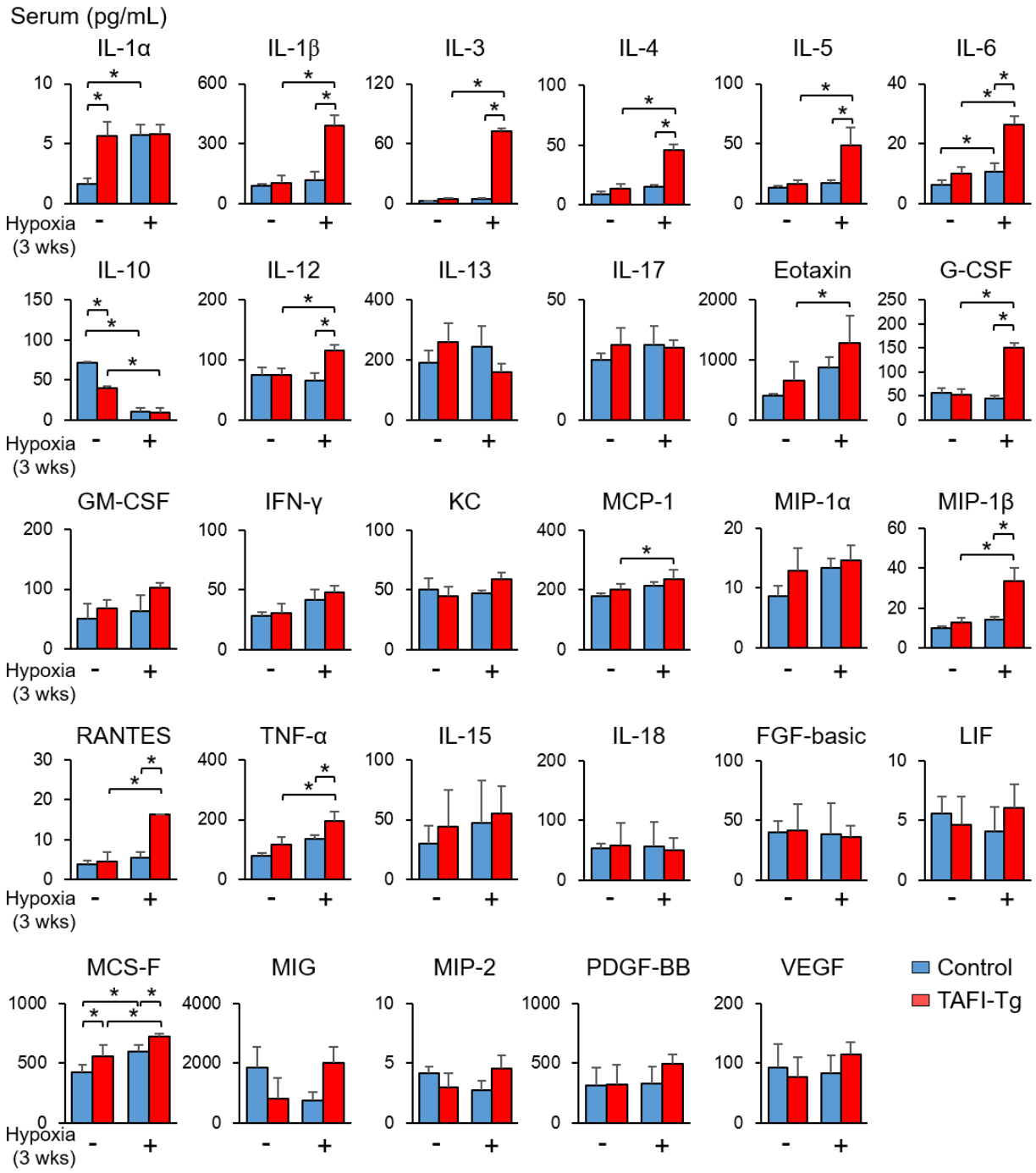

Supplementary Figure IX. Serum Levels of Cytokines/chemokines and Growth Factors in Mice. Serum levels of cytokines/chemokines and growth factors of TAFI-Tg and control mice exposed to normoxia or hypoxia (10% O_2) for 3 weeks (n=6 each). Results are expressed as mean±SEM. *P<0.05, **P<0.01.

Supplementary Figure X

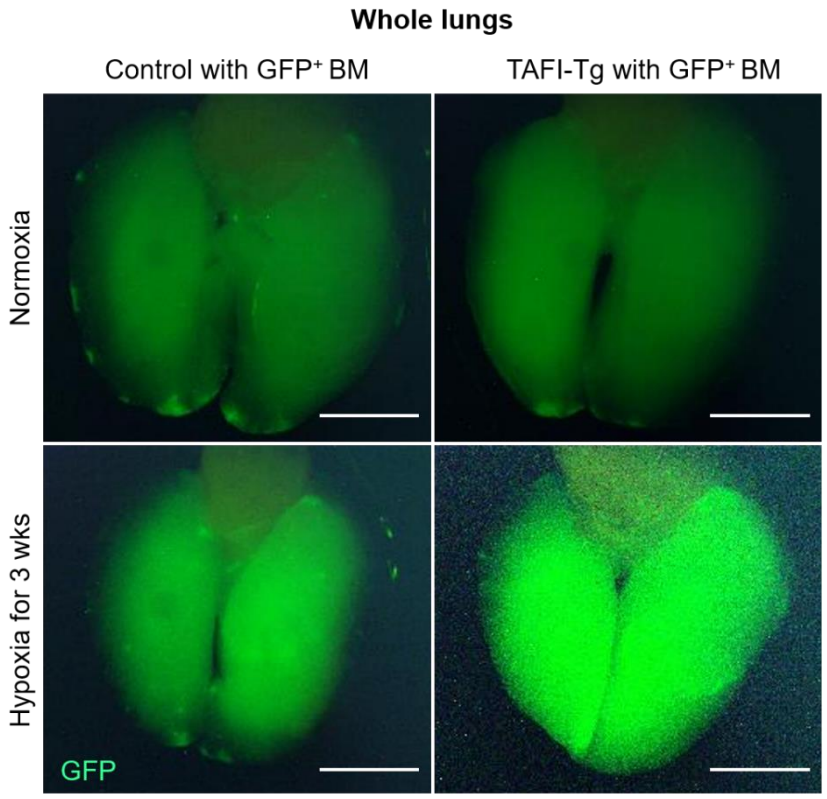

Supplementary Figure X. TAFI Recruits Bone Marrow-Derived Cells.

Representative pictures of the whole lung (GFP, green) from TAFI-Tg and WT recipient mice with GFP^+ bone marrow (BM) exposed to normoxia or hypoxia (10% O_2) for 3 weeks. Scale bars, 3 mm.

Supplementary Figure XI

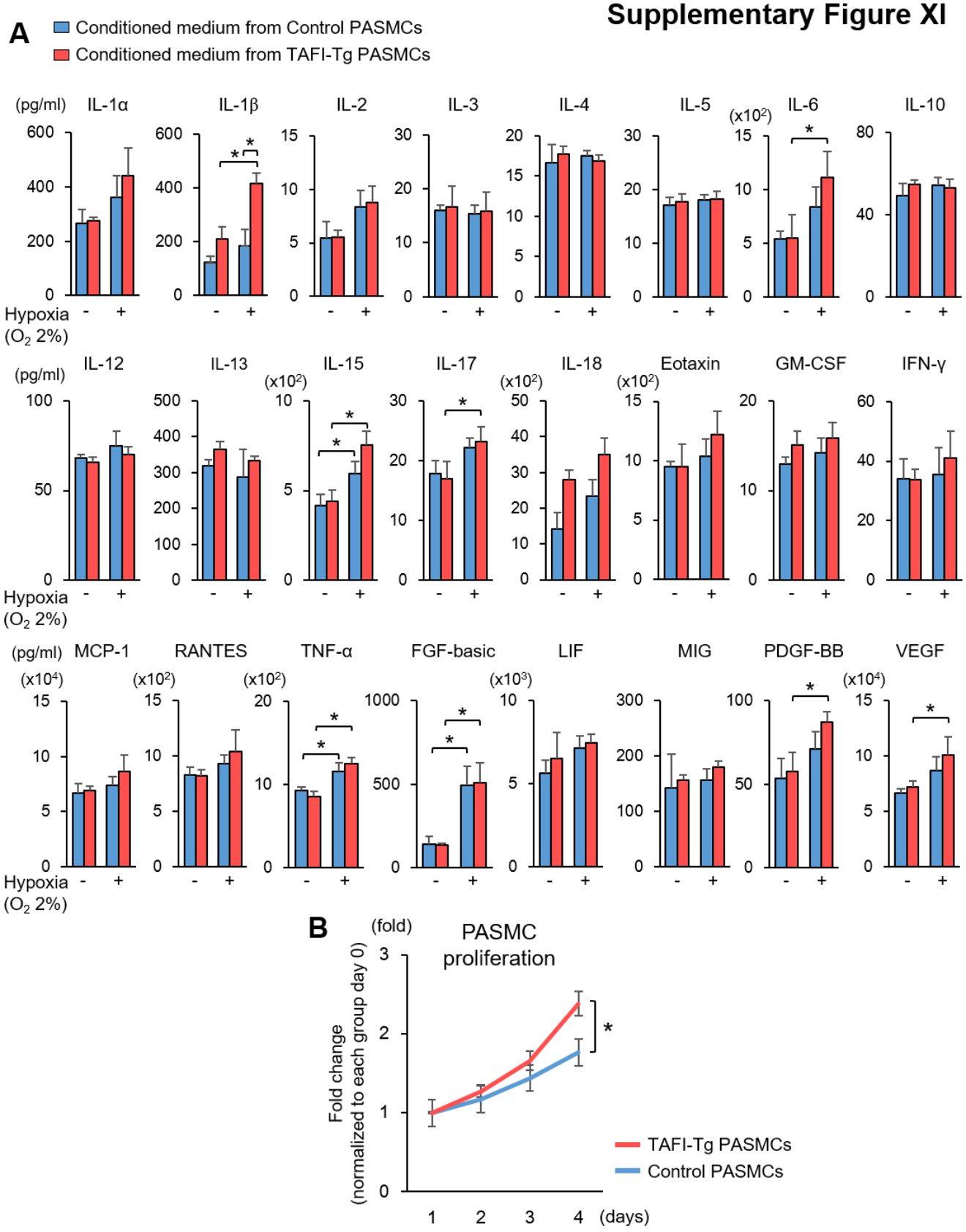

Supplementary Figure XI. TAFI Promotes Inflammation and PASMC Proliferation.
(**A**) Levels of cytokines/chemokines and growth factors in conditioned medium of pulmonary artery smooth muscle cells (PASMCs) exposed to normoxia or hypoxia (O_2 2%) for 24 h (*n*=4 each). (**B**) Proliferation assay (Cell Titer 96 MTT assay) of PASMCs harvested from TAFI-Tg and control mice cultured with 10% FBS for 4 days (*n*=8 each). Results are expressed as mean±SEM. **P*<0.05, ***P*<0.01.

Supplementary Figure XII

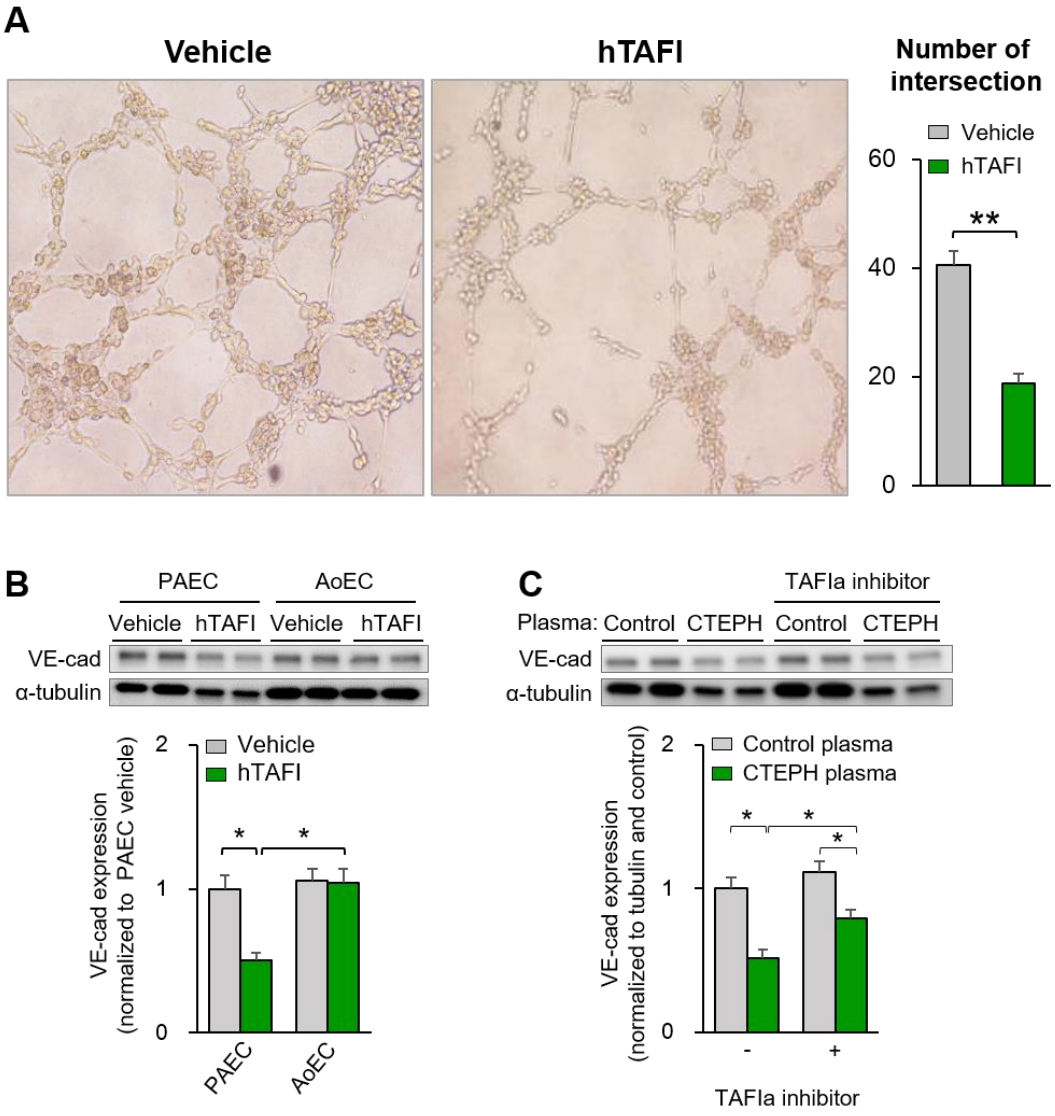

Supplementary Figure XII. TAFI Inhibits Angiogenesis.

(**A**) Representative images and quantification of tube formation assay in human pulmonary artery endothelial cells (PAECs) treated with human TAFI (300 μM) or vehicle for 12 h (*n*=8 samples per group). (**B**) Representative Western blot and quantification of VE-cadherin/α-tubulin in human PAECs and aortic endothelial cells (AoECs) treated with TAFI protein (300 nM) or vehicle for 24 h (*n*=4 samples per group). (**C**) Representative Western blot and quantification of VE-cadherin/α-tubulin in human PAECs treated with plasma from patients with CTEPH or controls with or without a TAFIa inhibitor (25 μg/mL) or vehicle (*n*=6 each). Results are expressed as mean±SEM. **P*<0.05, ***P*<0.01.

Supplementary Figure XIII

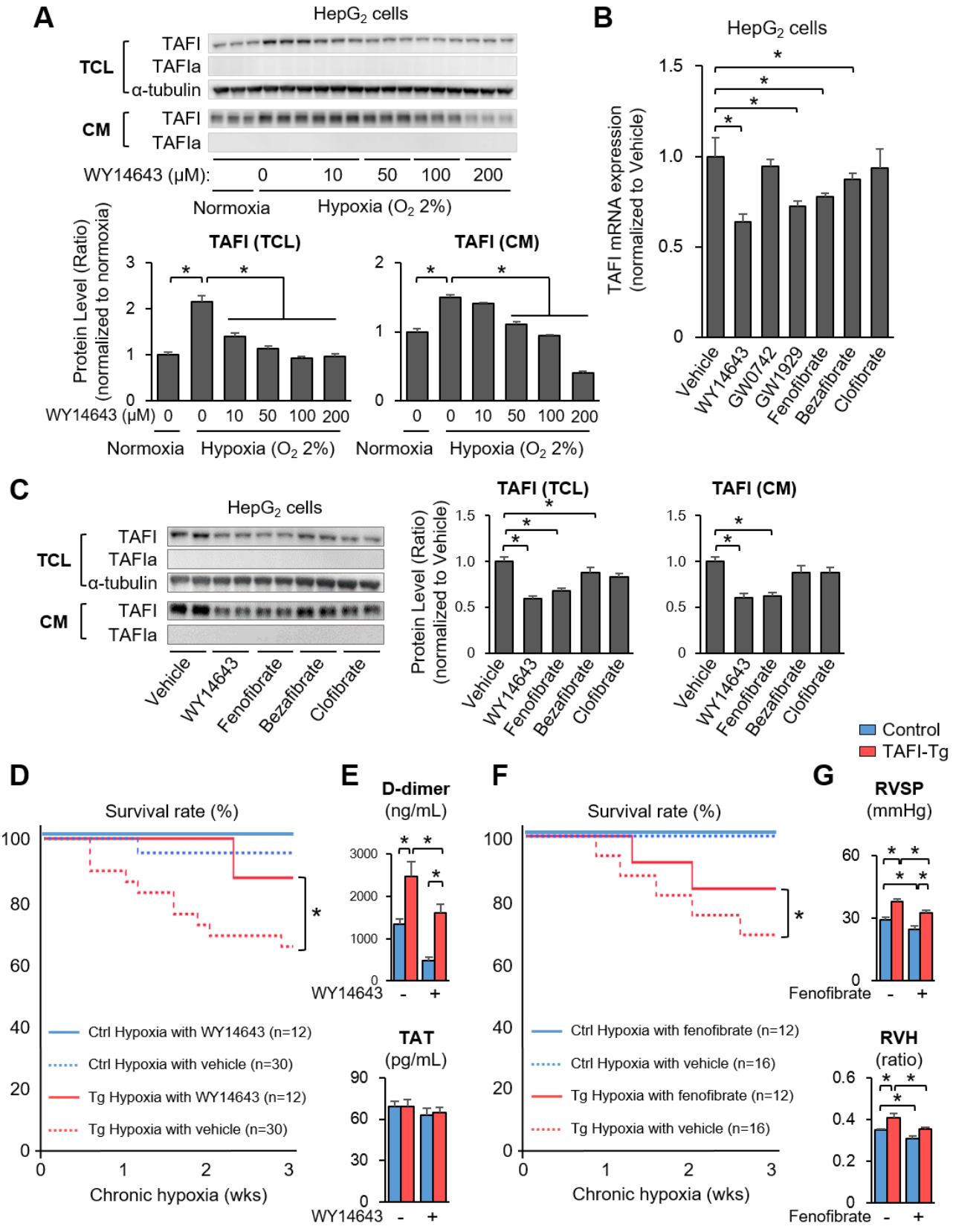

Supplementary Figure XIII. PPARα Agonists Ameliorate Hypoxia-induced PH in Mice.
(**A**) Representative Western blot and quantification of TAFI, TAFIa, and α-tubulin in total cell lysates (TCL) and conditioned medium (CM) of $HepG_2$ cells exposed to hypoxia (O_2 2%) with increasing concentrations of WY14643 (0, 10, 50, 100, and 200 μM) for 24 h (*n*=3 each). For the statistical analyses, unpaired Student's *t*-test was used. (**B**) Quantification of TAFI mRNA expression in $HepG_2$ cells treated with WY14643, GW0742, GW1929, fenofibrate, bezafibrate, clofibrate (10 μM each), or vehicle for 24 h. For statistical analysis, unpaired Student's *t*-test was used. (**C**) Representative Western blot and quantification of TAFI, TAFIa, and α-tubulin in TCL and CM of $HepG_2$ cells treated with WY14643, fenofibrate, bezafibrate, clofibrate (10 μM each), or vehicle for 24 h (*n*=4 each). (**D**) Survival rate of TAFI-Tg and control mice exposed to hypoxia (10% O_2) with WY14643 (3 mg/kg/day) or vehicle for 3 weeks. Results are expressed as log-rank test. (**E**) Quantification of plasma levels of D-dimer and thrombin-antithrombin complex (TAT) in TAFI-Tg and control mice exposed to hypoxia (10% O_2) with WY14643 (3 mg/kg/day) or vehicle (*n*=8 each) for 3 weeks. (**F**) Survival rate of systemic TAFI-overexpressing (TAFI-Tg) and control mice exposed to hypoxia (10% O_2) with fenofibrate (50 mg/kg/day) (*n*=12 each) or vehicle (*n*=16 each) for 3 weeks. Results are expressed as log-rank test. (**G**) Right ventricular systolic pressure (RVSP) and right ventricular hypertrophy (RVH) in TAFI-Tg and control mice exposed to hypoxia (10% O_2) with fenofibrate (50 mg/kg/day) (*n*=10 each) or vehicle (*n*=12 each) for 3 weeks. Results are expressed as mean±SEM. **P*<0.05, ***P*<0.01.

Supplementary Figure XIV

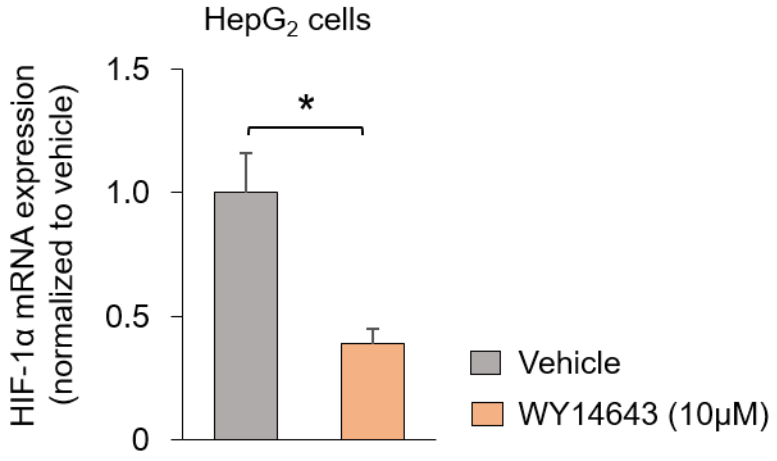

Supplementary Figure XIV. WY14643 Downregulates HIF-1α Expression in Hepatocytes.
Quantification of HIF-1α mRNA expression in $HepG_2$ cells treated with WY14643 (10 μM) or vehicle for 24 h. For statistical analysis, unpaired Student's *t*-test was used. Results are expressed as mean±SEM. **P*<0.05.

Supplementary Figure XV

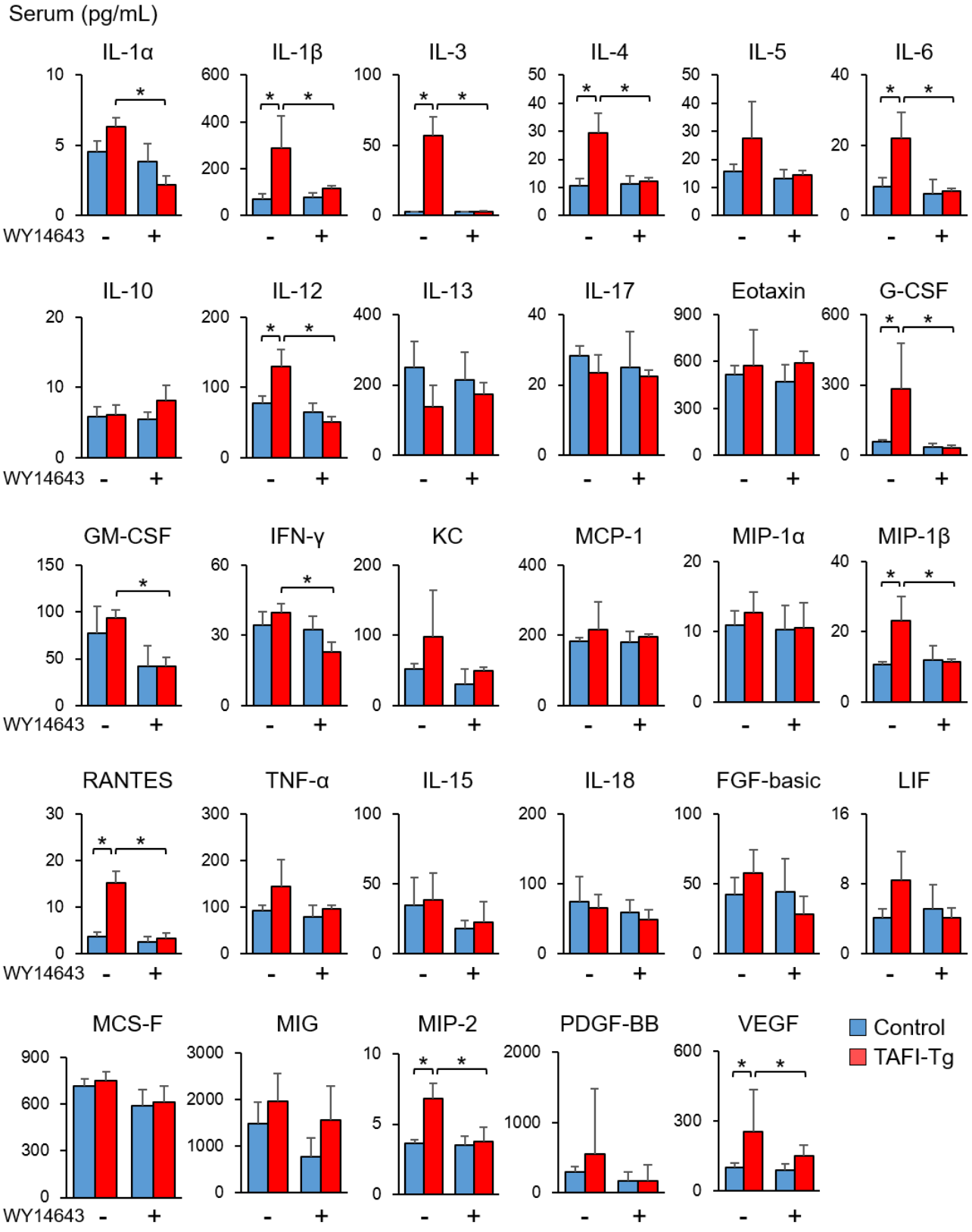

Supplementary Figure XV. Serum Levels of Cytokines/Chemokines and Growth Factors in Mice Treated with WY14643 or Vehicle.

Serum levels of cytokines/chemokines and growth factors in TAFI-Tg and control mice exposed to hypoxia (10% O_2) with WY14643 (3 mg/kg/day) or vehicle (n=6 each) for 3 weeks. Results are expressed as mean±SEM. *P<0.05, **P<0.01.